

ANALYSIS OF AN ENERGY-BASED ATOMISTIC/CONTINUUM COUPLING APPROXIMATION OF A VACANCY IN THE 2D TRIANGULAR LATTICE

C. ORTNER AND A. V. SHAPEEV

ABSTRACT. We present a comprehensive *a priori* error analysis of a practical energy based atomistic/continuum coupling method (Shapeev, arXiv:1010.0512) in two dimensions, for finite-range pair-potential interactions, in the presence of vacancy defects.

The majority of the work is devoted to the analysis of consistency and stability of the method. These yield *a priori* error estimates in the H^1 -norm and the energy, which depend on the mesh size and the “smoothness” of the atomistic solution in the continuum region. Based on these error estimates, we present heuristics for an optimal choice of the atomistic region and the finite element mesh, which yields convergence rates in terms of the number of degrees of freedom. The analytical predictions are supported by extensive numerical tests.

1. INTRODUCTION

The purpose of this work is a rigorous study of a new computational multiscale method coupling an atomistic description of a defect to a continuum model of the elastic far field.

The accurate computational modelling of crystal defects requires an atomistic description of the defect core, as well as an accurate resolution of the elastic far field. Using an atomistic model for the latter would be prohibitively expensive; hence, atomistic-to-continuum coupling methods (a/c methods) have been proposed to combine the accuracy of atomistic modelling with the efficiency of continuum mechanics (see [14, 20, 28, 30, 33] for selected references, and [18] for a recent overview).

Constructing accurate energy-based a/c methods has been proven particularly challenging, due to the so-called “ghost-forces” at the interface between the atomistic and continuum regions. This issue has been discussed at great length in [28, 4, 7, 19], and several interface corrections have been proposed to either remove or reduce the ghost forces [30, 7, 13, 33, 27, 12], however, the challenge of ghost-force removal still remains unsolved in general.

A growing body of literature exists on the rigorous analysis of a/c methods (we refer to [27, 22, 17] for recent overviews), which has been largely restricted to one-dimensional model problems. We are currently aware of only two rigorous analyses in more than one dimension: (1) In [22] it is shown that, in 2D, any a/c method that has no ghost forces is automatically first-order consistent. This work provides a general consistency analysis,

Date: March 8, 2022.

2000 Mathematics Subject Classification. 65N12, 65N15, 70C20.

Key words and phrases. atomistic models, atomistic-to-continuum coupling, coarse graining.

This work was supported by the EPSRC Critical Mass Programme “New Frontiers in the Mathematics of Solids” (OxMoS), by the EPSRC grant “Analysis of atomistic-to-continuum coupling methods”, and by the ANMC Chair at EPFL (Prof. Assyr Abdulle).

but does not discuss stability of a/c methods. (2) In [16], a force-based a/c method with an overlap region is analyzed in arbitrary dimension, in particular providing sharp stability conditions. The techniques used in [16] cannot accommodate defects, require a prohibitively large overlap region, and require that the continuum region is discretized with full atomistic resolution.

In the present work, we give a comprehensive *a priori* error analysis of a *practical* energy-based a/c method proposed by Shapeev [27], in the presence of simple defects. The formulation of the method (and its analysis) is restricted to pair interactions in two dimensions.

1.1. Outline. In §2 we formulate an atomistic model for the 2D triangular lattice, with periodic boundary conditions, and two-body interactions. We then introduce a convenient notation for bonds.

In §3, we formulate the a/c method studied in this paper: the ECC method introduced in [27], but with periodic boundary conditions. This section contains all necessary results and notation required for an implementation of the a/c method. In §3.3, we present a very brief sketch of the proof of the *a priori* error estimate, in order to motivate the analysis of §4–§6, which establishes the main results required.

The purpose of §4 is to collect auxiliary results, which are largely technical results for finite element spaces. In this section we also introduce a new idea to measure “smoothness” of discrete functions.

In §5 we prove consistency error estimates in discrete variants of the $W^{-1,p}$ -norm, $p \in [1, \infty]$. Our estimates are stronger and require fewer technical assumptions than the general result given in [22].

In §6 we develop the stability analysis. We define a “vacancy stability index”, which allows us to reduce the proof of stability of a lattice with vacancies to the proof of stability for a homogeneous lattice without defects. We provide numerical examples and one analytical computation of stability indices.

In §7 we assemble all our previous steps to obtain *a priori* error estimates in the H^1 -norm and for the energy. In §7.1 we translate these error estimates, which are stated in terms of the smoothness of the solution, into estimates in terms of degrees of freedom. This discussion also provides heuristics on how to choose the atomistic region and the finite element mesh in the continuum region in an optimal way.

Finally, in §8, we present extensive numerical examples to confirm our analytical results, and to provide further discussions of points where our rigorous analysis is not sharp.

1.2. Basic notational conventions. For $s, t \in \mathbb{R}$, we write $s \wedge t := \min\{s, t\}$.

The ℓ^p -norms in \mathbb{R}^k are denoted by $|\cdot|_p$. In addition, we define $|\cdot| := |\cdot|_2$. We do not normally distinguish between row and column vectors, but instead define the following three vector products: if $a, b \in \mathbb{R}^k$, then $a \cdot b := \sum_{j=1}^k a_j b_j$, and $a \otimes b := (a_i b_j)_{i,j=1}^k$, where i denotes the row index and j the column index. In addition, if $a, b \in \mathbb{R}^2$, then we define $a \times b := a_1 b_2 - a_2 b_1$.

Matrices are usually denoted by sans serif symbols, $\mathbf{A}, \mathbf{B}, \mathbf{F}, \mathbf{G}$, and so forth. The set of $k \times k$ matrices with positive determinant is denoted by $\mathbb{R}_+^{k \times k}$. The set of rotations of \mathbb{R}^2 is denoted by $\text{SO}(2)$. Throughout we will denote a rotation through angle $\pi/2$ by \mathbf{Q}_4 and a rotation through angle $\pi/3$ by \mathbf{Q}_6 . If $\mathbf{G} \in \mathbb{R}^{k \times k}$, then $\|\mathbf{G}\|$ denotes its ℓ^2 -operator

norm, and $|\mathbf{G}|_p$ the $\ell^p(\mathbb{R}^{k \times k})$ -norm. In particular, $|\mathbf{G}|$ is the Frobenius norm, with the associated inner product $\mathbf{F} : \mathbf{G}$. The symmetric component of a matrix $\mathbf{G} \in \mathbb{R}^{k \times k}$ is denoted by $\mathbf{G}^{\text{sym}} := \frac{1}{2}(\mathbf{G} + \mathbf{G}^\top)$.

If $A \subset \mathbb{R}^k$ is (Lebesgue-)measurable, then $|A|$ denotes its measure. If $A \subset \mathbb{R}^2$ has Hausdorff dimension one, then we will denote its length by $\text{length}(A)$. Volume integrals are denoted by dV , while surface (1D) integrals are denoted by ds . For bonds, which are specific one-dimensional objects, it will be convenient to introduce a slightly different notation (see §2.2.4 and §3.1.3).

The interior and closure of a set $A \subset \mathbb{R}^k$ are denoted, respectively, by $\text{int}(A)$ and $\text{clos}(A)$. If $A \subset \mathbb{R}^2$ is understood as a one-dimensional object, then we will also use $\text{int}(A)$ to denote its relative interior, but will normally specify this explicitly.

The Lebesgue norms $\|\cdot\|_{L^p(A)}$ for measurable sets A (either one- or two-dimensional) are defined in the usual way for scalar functions. If $w : A \rightarrow \mathbb{R}^k$ is measurable, then $\|w\|_{L^p(A)} := \||w|_2\|_{L^p(A)}$. If w is differentiable at a point x , then $\nabla w(x)$ denotes its Jacobi matrix. The symbol D is reserved for finite differences, and will be introduced in §2.2.

2. THE ATOMISTIC MODEL

In this section we define an atomistic model problem of a general two-body interaction energy in a 2D periodic domain. Although the model itself could be equally formulated in any space dimension, the presentation is restricted to 2D since the a/c method introduced in §3 is restricted to 2D.

2.1. Periodic deformations of a triangular lattice with vacancy defects.

2.1.1. *The triangular lattice.* The triangular lattice is the set

$$\mathbb{L}^\# := \mathbf{A}_6 \mathbb{Z}^2, \quad \text{where } \mathbf{A}_6 := [\mathbf{a}_1, \mathbf{a}_2] := \begin{bmatrix} 1 & 1/2 \\ 0 & \sqrt{3}/2 \end{bmatrix},$$

where \mathbf{a}_i , $i = 1, 2$, are called the *lattice vectors*. We furthermore set $\mathbf{a}_3 = (-1/2, \sqrt{3}/2)^\top$ and $\mathbf{a}_{i+3} = -\mathbf{a}_i$ for $i \in \mathbb{Z}$, so that the set of *nearest-neighbour directions* is given by

$$\mathbb{L}_{\text{nn}} := \{\mathbf{a}_j : j = 1, \dots, 6\} = \{\mathbf{Q}_6^{j-1} \mathbf{a}_1 : j = 1, \dots, 6\},$$

where $\mathbf{Q}_6 \in \text{SO}(2)$ denotes the rotation through $\pi/3$. Finally, we denote the set of all *lattice directions* by $\mathbb{L}_* := \mathbb{L}^\# \setminus \{0\}$.

The hexagonal symmetry of $\mathbb{L}^\#$ yields the following result, which decomposes the triangular lattice into lattice vectors of equal distance.

Lemma 2.1. *There exists a sequence $(r_n)_{n=1}^\infty \subset \mathbb{L}_*$ such that $\ell_n = |r_n|$ is monotonically increasing and the triangular lattice can be written as a union of disjoint sets*

$$\mathbb{L}_* = \bigcup_{n=1}^{\infty} \{\mathbf{Q}_6^j r_n : j = 1, \dots, 6\}.$$

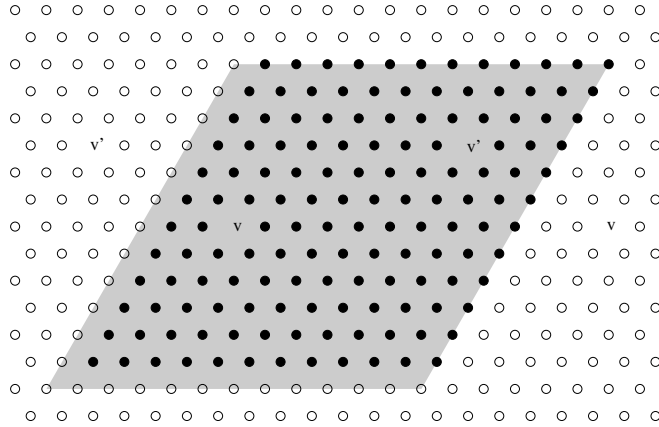


FIGURE 1. The lattice and the computational domain with $N = 12$ and two vacancies. The black disks denote the atoms belonging to the computational domain \mathcal{L} , the white disks denote the atoms belonging to $\mathcal{L}^\# \setminus \mathcal{L}$, and the vacancies are denoted by v and v' (periodic images of the same vacancy have the same symbol).

Lemma 2.1 motivates splitting certain lattice sums over hexagonally symmetric sets. In these calculations we will use the following two identities, which exploit the relation between hexagonal symmetry and isotropy. The proofs are given in Appendix A.

Lemma 2.2. *Let $\mathbf{G} \in \mathbb{R}^{2 \times 2}$, and $r \in \mathbb{R}^2$, $|r| = 1$; then*

$$\sum_{j=1}^6 |\mathbf{G} \mathbf{Q}_6^j r|^2 = 3|\mathbf{G}|^2, \quad \text{and} \quad (2.1)$$

$$\sum_{j=1}^6 [(\mathbf{Q}_6^j r)^\top \mathbf{G} (\mathbf{Q}_6^j r)]^2 = \frac{3}{2} |\mathbf{G}^{\text{sym}}|^2 + \frac{3}{4} |\text{tr} \mathbf{G}|^2. \quad (2.2)$$

2.1.2. *A periodic domain with defects.* Throughout the paper we fix a periodicity parameter $N \in \mathbb{N}$. We say that a set $A \subset \mathbb{R}^2$ is N -periodic if $A + N\mathbb{L}^\# = A$. For any set $A \subset \mathbb{R}^2$ we denote its periodic continuation by $A^\# = A + N\mathbb{L}^\#$. If \mathcal{A} is a family of sets, then we define $\mathcal{A}^\# = \{A^\# : A \in \mathcal{A}\}$.

Throughout our analysis we fix N -periodic continuous and discrete cells

$$\Omega := \mathbf{A}_6(0, N]^2 \quad \text{and} \quad \mathbb{L} := \mathbb{L}^\# \cap \Omega.$$

We fix a set of *vacancy sites* $\mathbb{V} \subset \mathbb{L}$ and define the *discrete computational domain* as

$$\mathcal{L} := \mathbb{L} \setminus \mathbb{V}.$$

The infinite perfect lattice $\mathbb{L}^\#$, the lattice with a periodic array of defects $\mathcal{L}^\#$, and the discrete computational domain \mathcal{L} are visualized in Figure 1.

2.1.3. *Periodic deformations of $\mathcal{L}^\#$.* A homogeneous deformation of $\mathcal{L}^\#$ is a map $y_B : \mathcal{L}^\# \rightarrow \mathbb{R}^2$ defined, for $B \in \mathbb{R}_+^{2 \times 2}$, as

$$y_B(x) := Bx \quad \text{for } x \in \mathcal{L}^\#,$$

The set of *periodic displacements* of $\mathcal{L}^\#$ is denoted by

$$\mathcal{U} = \{u : \mathcal{L}^\# \rightarrow \mathbb{R}^2 : u(x + Na_j) = u(x) \text{ for } x \in \mathcal{L}^\# \text{ and } j = 1, 2\}.$$

A map $y : \mathcal{L}^\# \rightarrow \mathbb{R}^2$ is said to be a *periodic deformation* with underlying macroscopic strain $B \in \mathbb{R}_+^{2 \times 2}$, if $y - y_B \in \mathcal{U}$ and if y is *invertible*. To quantify the invertibility condition we define

$$\mu_a(y) = \inf_{x \neq x' \in \mathcal{L}^\#} \frac{|y(x') - y(x)|}{|x - x'|}$$

and denote

$$\mathcal{Y}_B := \{y : \mathcal{L}^\# \rightarrow \mathbb{R}^2 : y - y_B \in \mathcal{U} \text{ and } \mu_a(y) > 0\}, \quad \text{and} \quad \mathcal{Y} := \bigcup_{B \in \mathbb{R}_+^{2 \times 2}} \mathcal{Y}_B.$$

2.2. The atomistic model.

2.2.1. *The atomistic energy.* We assume that there exists a potential $\varphi \in C^2(0, +\infty)$, such that the internal atomistic energy (per period) of a deformation $y \in \mathcal{Y}$ is given by

$$\mathcal{E}_a(y) := \sum_{x \in \mathcal{L}} \sum_{x' \in \mathcal{L}^\# \setminus \{x\}} \varphi(|y(x') - y(x)|).$$

The energy \mathcal{E}_a is twice continuously Gateaux differentiable at every point $y \in \mathcal{Y}$. We understand the first variation $\delta \mathcal{E}_a(y)$ as an element of \mathcal{U}^* , and the second variation $\delta^2 \mathcal{E}_a(y)$ as a linear operator from \mathcal{U} to \mathcal{U}^* , formally defined as

$$\begin{aligned} \langle \delta \mathcal{E}_a(y), u \rangle &= \frac{d}{dt} \mathcal{E}_a(y + tu)|_{t=0}, \quad \text{for } u \in \mathcal{U}, \text{ and} \\ \langle \delta^2 \mathcal{E}_a(y)u, v \rangle &= \frac{d}{dt} \langle \delta \mathcal{E}_a(y + tu), v \rangle|_{t=0}, \quad \text{for } u, v \in \mathcal{U}. \end{aligned}$$

For notational reasons it is convenient to also define a potential $\phi \in C^2(\mathbb{R}^2 \setminus \{0\})$, $\phi(r) := \varphi(|r|)$, so that \mathcal{E}_a can be rewritten as

$$\mathcal{E}_a(y) = \sum_{x \in \mathcal{L}} \sum_{x' \in \mathcal{L}^\# \setminus \{x\}} \phi(y(x') - y(x)). \quad (2.3)$$

Remark 2.1. The more general form of the interaction potential admitted by (2.3) is useful since it includes plane-strain models of 3D crystals [32]. Our results remain largely valid for this general form of the interaction potential. The consistency analysis never uses the fact that $\phi(r) = \varphi(|r|)$. We shall nevertheless use the potential ϕ mostly for notational convenience, since it renders our stability analysis more concrete. It would require some additional work to quantify our stability assumptions in the general case. \square

2.2.2. *The variational problem.* For some macroscopic strain $\mathbf{B} \in \mathbb{R}_+^{2 \times 2}$, which shall be fixed throughout, the atomistic problem is to find

$$y_a \in \operatorname{argmin} \mathcal{E}_a(\mathcal{Y}_{\mathbf{B}}), \quad (2.4)$$

where “argmin” denotes the set of *local* minimizers. If $y_a \in \mathcal{Y}_{\mathbf{B}}$ is a solution to (2.4), then it satisfies the first order necessary optimality condition

$$\langle \delta \mathcal{E}_a(y_a), u \rangle = 0 \quad \forall u \in \mathcal{U}. \quad (2.5)$$

2.2.3. *External forces.* External forces are often used to model, for example, a substrate or an indenter. In order avoid an additional level of complexity into our analysis we have decided against incorporating external forces. To obtain non-trivial solutions in our numerical experiments, we have instead allowed for defects in the atomistic lattice.

2.2.4. *Bonds.* A *bond* is an ordered pair $(x, x') \in \mathbb{L}^\# \times \mathbb{L}^\#, x \neq x'$. When convenient we identify the bond $b = (x, x')$ with the line segment $\operatorname{conv}\{x, x'\}$, for example, to integrate over the segment, and correspondingly define $|b| := |x - x'|$. The set of bonds between atoms in the computational domain \mathcal{L} and all other atoms is denoted by

$$\mathcal{B} := \{(x, x') \in \mathcal{L} \times \mathcal{L}^\# : x \neq x'\}.$$

The *direction* of a bond b will be denoted by r_b , that is $b = (x, x + r_b)$ for some $x \in \mathbb{L}^\#$.

For a map $v : \mathbb{L}^\# \rightarrow \mathbb{R}^k$ and a bond $b = (x, x + r)$, $r \in \mathbb{L}_*$, we define the finite difference operators

$$D_b v := D_r v(x) := v(x + r) - v(x). \quad (2.6)$$

With this notation the atomistic energy can be rewritten, once again, as

$$\mathcal{E}_a(y) = \sum_{b \in \mathcal{B}} \phi(D_b y). \quad (2.7)$$

We also remark that, with this notation, we have $\mu_a(y) = \min_{b \in \mathcal{B}} |D_b y| / |b|$.

Finally, we define the set of *all* bonds, including those involving vacancy sites, as

$$\mathbb{B} := \{(x, x + r) : x \in \mathbb{L}, r \in \mathbb{L}_*\}.$$

2.3. **Properties of the interaction potential.** A crucial assumption in our analysis is that $\phi(r)$ and its derivatives decay rapidly as $|r| \rightarrow +\infty$. For example, our analysis is invalid for the slowly decaying Coulomb interactions. To quantify this assumption, we define the monotonically decreasing functions $M_k : (0, +\infty) \rightarrow [0, +\infty)$, $k = 0, \dots, 3$,

$$M_k(s) = \sup_{\substack{r \in \mathbb{R}^2 \\ |r| \geq s}} \|\phi^{(k)}(r)\|, \quad (2.8)$$

where $\phi^{(k)}$ denotes the k th Frechet derivative of ϕ , e.g., $\phi^{(1)} = \phi' : \mathbb{R}^2 \setminus \{0\} \rightarrow \mathbb{R}^2$, $\phi^{(2)} = \phi'' : \mathbb{R}^2 \setminus \{0\} \rightarrow \mathbb{R}^{2 \times 2}$, and so forth, and $\|\cdot\|$ denotes the Euclidean norm of a vector, or the operator norm of a matrix or tensor. We remark that, in terms of φ ,

$$M_1(s) = \sup_{t \geq s} |\varphi'(t)| \quad \text{and} \quad M_2(s) = \sup_{t \geq s} \left(\left| \frac{\varphi''(t)}{t^2} \right|^2 + \left| \frac{\varphi'(t)}{t} \right|^2 \right)^{1/2}.$$

3. AN A/C COUPLING METHOD

In this section we formulate the a/c coupling method introduced in [27] for periodic boundary conditions.

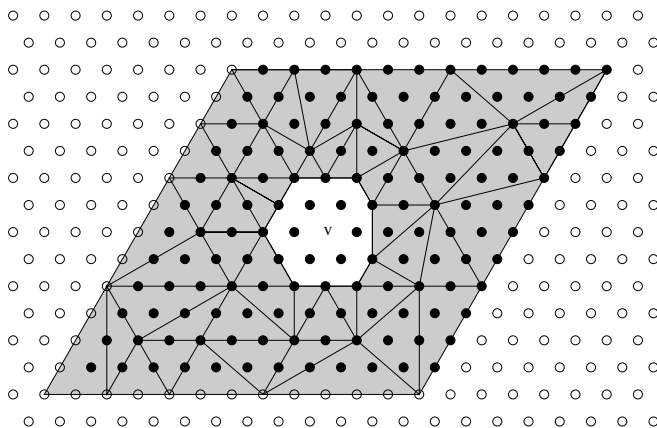


FIGURE 2. Example of a triangulation \mathcal{T}_h^c of the continuum region Ω_c (shaded area), with nodes on $\partial\Omega_c$ are such that the mesh can be extended periodically to a regular triangulation of $\Omega_c^\#$. Note that the boundary of the atomistic region need not be aligned with nearest-neighbour directions.

3.1. Preliminaries.

3.1.1. *The atomistic and continuum regions.* Let $\Omega_a \subset \text{int}(\Omega)$, the *atomistic region*, be a closed polygonal set with corners belonging to \mathcal{L} . We assume throughout that $\mathbb{V} \subset \text{int}(\Omega_a)$, that is, the interior of the atomistic region contains all vacancies in the lattice. The corresponding *continuum region* is defined as

$$\Omega_c := \text{clos}(\Omega \setminus \Omega_a) \cap \Omega.$$

3.1.2. *The finite element mesh.* Let $\mathcal{L}_{\text{rep}}^c \subset \mathcal{L} \cap \Omega_c$ be a set of finite element nodes, or, in the language of the quasicontinuum method [20], *representative atoms* or simply *repatoms*. We assume that the corners of the atomistic region belong to $\mathcal{L}_{\text{rep}}^c$. We also define $\mathcal{L}_{\text{rep}}^a = \mathcal{L} \cap \text{int}(\Omega_a)$, and $\mathcal{L}_{\text{rep}} = \mathcal{L}_{\text{rep}}^a \cup \mathcal{L}_{\text{rep}}^c$.

Let \mathcal{T}_h^c be a regular (and shape regular) triangulation of Ω_c with vertices belonging to $(\mathcal{L}_{\text{rep}}^c)^\#$, which can be extended periodically to a regular triangulation $(\mathcal{T}_h^c)^\#$ of $\Omega_c^\#$. An example of such a construction is displayed in Figure 2. We adopt the convention that lattice functions that are piecewise affine with respect to the triangulation $(\mathcal{T}_h^c)^\#$ are in fact understood as piecewise affine functions on *all of* $\Omega_c^\#$, that is, they may be evaluated at any point $x \in \Omega_c^\#$ and not only at lattice sites.

For each $T \in (\mathcal{T}_h^c)^\#$ we define $h_T := \text{diam}(T)$, and we define the mesh size function $h(x) := \max\{h_T : T \in (\mathcal{T}_h^c)^\#, x \in T\}$, for $x \in \Omega_c^\#$.

Whenever we refer to the *shape regularity of \mathcal{T}_h^c* (and later \mathcal{T}_h), we mean the ratio between the largest and smallest angle between any two adjacent edges in \mathcal{T}_h . We will assume throughout that this is moderate.

We define the set of admissible coarse-grained displacements and deformations, respectively, as

$$\begin{aligned} \mathcal{U}_h &= \{u_h \in \mathcal{U} : u_h \text{ is p.w. affine w.r.t. } \mathcal{T}_h^c\}, \\ \mathcal{B}_{B,h} &= \{y_h \in \mathcal{Y} : y_h - y_B \in \mathcal{U}_h \text{ and } \mu_c(y_h) > 0\}, \quad \text{and} \quad \mathcal{Y}_h = \bigcup_{B \in \mathbb{R}_+^{2 \times 2}} \mathcal{B}_{B,h}, \end{aligned}$$

where μ_c is defined as

$$\mu_c(y_h) := \inf_{\substack{x, x' \in \Omega_c \\ x \neq x'}} \frac{|y_h(x) - y_h(x')|}{|x - x'|} \leq \operatorname{ess\,inf}_{x \in \Omega_c} \min_{\substack{r \in \mathbb{R}^2 \\ |r|=1}} |\nabla y_h(x)r|. \quad (3.1)$$

Note that we are requiring a more stringent invertibility condition on coarse-grained deformations y_h . This is due to the fact that a continuous interpolant of an invertible atomistic deformation need not necessarily be invertible.

Finally, we define the nodal interpolation operator $I_h : \mathcal{U} \rightarrow \mathcal{U}_h$ by

$$I_h u(x) = u(x) \quad \forall x \in \mathcal{L}_{\text{rep}},$$

and extend its definition to deformations by $I_h y - y_B = I_h(y - y_B)$, for all $y \in \mathcal{Y}_B$, $B \in \mathbb{R}_+^{2 \times 2}$.

3.1.3. Bond integrals. There are two crucial steps in the construction of the a/c method we are about to present. In a first step, all bonds b that are entirely contained within the continuum region are replaced by line integrals. We collect these bonds into the set

$$\mathcal{B}_c = \{b \in \mathcal{B} : b \subset \operatorname{int}(\Omega_c^\#)\},$$

and we define the complement to be the set of atomistic bonds $\mathcal{B}_a = \mathcal{B} \setminus \mathcal{B}_c$. We recall that we identify b with the line segment spanned by its endpoints whenever convenient. Next we define, for any function v that is measurable on the segment $b = (x, x + r_b)$, the *bond integral*

$$\int_b v \, db = \int_x^{x+r_b} v \, db = \int_0^1 v(x + tr_b) \, dt.$$

3.2. The a/c method.

3.2.1. Formulation in terms of bond integrals. Let $b = (x, x + r) \in \mathcal{B}_c$ then for any function $v_h \in \mathcal{U}_h \cup \mathcal{Y}_h$ the following one-sided directional derivatives are well-defined at almost every point of b :

$$\nabla_b v_h(x) = \nabla_r v_h(x) = \lim_{t \searrow 0} \frac{v_h(x + tr) - v_h(x)}{t}.$$

We remark that, if x lies in the interior of an element T then v_h is differentiable at x and hence $\nabla_r v_h(x) = \nabla v_h(x)r$. Moreover, even if x lies on an edge or a vertex of the triangulation, the one-sided directional derivative of a continuous piecewise affine function is always well-defined. The directional derivative $\nabla_r v_h(x)$ is only undefined at points $x \in \partial\Omega_a$ if r points to the interior of Ω_a . For future reference we note the following useful identity:

$$D_r y_h(x) = \int_x^{x+r} \nabla_r y_h \, db, \quad \text{for } y \in \mathcal{Y}, x \in \mathbb{L}^\#, r \in \mathbb{L}_*. \quad (3.2)$$

We use this notation to define the following *continuum bond energies* to approximate the atomistic bond energies

$$\phi(D_b y_h) \approx \int_b \phi(\nabla_b y_h) \, db. \quad (3.3)$$

The motivation behind this idea is that, if ∇y_h does not vary too much along the bond b , then $D_b y_h \approx \nabla_b y_h(x)$ for all $x \in \operatorname{int}(b)$.

This leads to the following definition of an a/c coupling method, which is labelled the ECC method in [27]:

$$\mathcal{E}_{\text{ac}}(y_h) = \sum_{b \in \mathcal{B}_a} \phi(D_b y_h) + \sum_{b \in \mathcal{B}_c} \int_b \phi(\nabla_b y_h) \, \text{db}. \quad (3.4)$$

We will use this formulation of the a/c method heavily in our analysis, however, it does not yet reduce the complexity of the energy evaluation. This will be achieved in the next paragraph, where we will show that bond integrals can be transformed into volume integrals.

It is again easy to see that \mathcal{E}_{ac} is twice continuously Gateaux differentiable in $\mathcal{Y}_{\mathbf{B},h}$, for all $\mathbf{B} \in \mathbb{R}_+^{2 \times 2}$, and we define the first and second variations $\delta \mathcal{E}_{\text{ac}}$ and $\delta^2 \mathcal{E}_{\text{ac}}$ analogously to $\delta \mathcal{E}_a$ and $\delta^2 \mathcal{E}_a$ in §2.2.

Remark 3.1. The origin of the approximation (3.3) lies in the quasinonlocal QC method proposed by Shimokawa *et al* [30] and the geometrically consistent coupling method [7]. Their approximation of second neighbour bonds, although much more general, reduces for 1D pair interaction models to

$$\phi(y(x+1) - y(x-1)) \approx \frac{1}{2} \phi(2D_{-1}y(x)) + \frac{1}{2} \phi(2D_1y(x)),$$

which was also the starting point for recent analyses of the quasinonlocal QC method [21, 25]; a similar observation was also used in [19]. (By contrast, [4] worked directly with absence of a ghost force.)

Generalisations beyond second neighbour interactions were proposed in [15, 27]; the formulation in terms of bond integrals is due to Shapeev [27]. \square

3.2.2. The bond-density lemma. The second crucial step in the formulation of the a/c method (3.4) is to rewrite the energy in terms of volume integrals over the Cauchy–Born stored energy density. The main tool in achieving this is the following lemma established in [27], which requires the definition of a pointwise *characteristic function*. For any polygonal set $U \subset \mathbb{R}^2$ we define

$$\chi_U(x) = \lim_{t \rightarrow 0} \frac{|U \cap B_t(x)|}{|B_t(x)|} \quad \text{for } x \in \mathbb{R}^2, \quad (3.5)$$

where $B_t(x)$ denotes the closed ball in \mathbb{R}^2 with radius t and centre x . The characteristic functions are additive in the following sense: if $U_1, U_2 \subset \mathbb{R}^2$ are polygonal sets with $|\text{int}(U_1) \cap \text{int}(U_2)| = 0$, then $\chi_{U_1 \cup U_2} = \chi_{U_1} + \chi_{U_2}$. This follows immediately from the definition of the characteristic function.

We remark that the following result is false for general tetrahedra in three dimensions, which is the main reason the method has not been extended to that case.

Lemma 3.1 (Bond-Density Lemma [27, Lemma 4.4]). *Let $T \subset \mathbb{R}^2$ be a triangle with vertices belonging to $\mathbb{L}^\#$ and let $r \in \mathbb{L}_*$, then*

$$\sum_{x \in \mathbb{L}^\#} \int_x^{x+r} \chi_T \, \text{db} = \frac{1}{\det \mathbf{A}_6} |T|,$$

that is, $\frac{1}{\det \mathbf{A}_6}$ is the effective density of bonds in T .

Next, we formulate a variant that is more suitable in the context of periodic boundary conditions. Recall that $T^\# = T + N\mathbb{L}^\#$.

Lemma 3.2 (Periodic Bond-Density Lemma). *Let $T \subset \text{clos}(\Omega)$ be a non-degenerate triangle with vertices belonging to $\mathbb{L}^\#$, and $r \in \mathbb{L}_*^\#$, then*

$$\sum_{x \in \mathbb{L}} \int_x^{x+r} \chi_{T^\#} \, db = \frac{1}{\det \mathbf{A}_6} |T|.$$

Proof. According to Lemma 3.1 we have

$$\frac{1}{\det \mathbf{A}_6} |T| = \sum_{x \in \mathbb{L}^\#} \int_x^{x+r} \chi_T \, db = \sum_{x \in \mathbb{L}} \sum_{z \in N\mathbb{L}^\#} \int_{x+z}^{x+z+r} \chi_T \, db.$$

Upon shifting the integration variable by $-z$, we can rewrite this as

$$\frac{1}{\det \mathbf{A}_6} |T| = \sum_{x \in \mathbb{L}} \int_x^{x+r} \sum_{z \in N\mathbb{L}^\#} \chi_{T-z} \, db = \sum_{x \in \mathbb{L}} \int_x^{x+r} \chi_{T^\#} \, db. \quad \square$$

3.2.3. Practical reformulation of \mathcal{E}_{ac} . Equipped with the bond-density lemma, we can now derive a practical formulation of the a/c method (3.4). The proof of this result for Dirichlet boundary conditions is contained in [27]. With the modification of the bond-density lemma for periodic boundary conditions the necessary changes to the proof, detailed in Appendix A, are straightforward.

Theorem 3.3. *The a/c energy \mathcal{E}_{ac} defined in (3.4) can be rewritten as*

$$\begin{aligned} \mathcal{E}_{ac}(y_h) &= \sum_{b \in \mathcal{B}_a} \phi(D_b y_h) + \int_{\Omega_c} W(\nabla y_h) \, dV + \Phi_i(y_h), \quad \text{where} \quad (3.6) \\ \Phi_i(y_h) &:= - \sum_{b \in \mathbb{B} \setminus \mathcal{B}_c} \int_b \chi_{\Omega^\#} \phi(\nabla_b y_h) \, db, \end{aligned}$$

and where $W : \mathbb{R}^{2 \times 2} \rightarrow \mathbb{R} \cup \{+\infty\}$ is the Cauchy–Born stored energy function,

$$W(\mathbf{F}) := \frac{1}{\det \mathbf{A}_6} \sum_{r \in \mathbb{L}_*^\#} \phi(\mathbf{F}r).$$

Remark 3.2. While the bond-integral formulation (3.4) is easily extended to higher dimensions and to higher order finite element spaces, Theorem 3.3 holds only for piecewise affine trial functions in 2D. \square

3.2.4. *The coarse grained variational problem.* In the a/c method we wish to compute

$$y_{ac} \in \operatorname{argmin} \mathcal{E}_{ac}(\mathcal{Y}_{\mathbb{B},h}). \quad (3.7)$$

If $y_{ac} \in \mathcal{Y}_{\mathbb{B},h}$ is a solution to (3.7), then it satisfies the *first order necessary optimality condition*

$$\langle \delta \mathcal{E}_{ac}(y_{ac}), u_h \rangle = 0 \quad \forall u_h \in \mathcal{U}_h, \quad (3.8)$$

as well as the *second order necessary optimality condition*

$$\langle \delta^2 \mathcal{E}_{ac}(y_{ac}) u_h, u_h \rangle \geq 0 \quad \forall u_h \in \mathcal{U}_h. \quad (3.9)$$

Condition (3.9) is insufficient for error estimates; hence we will aim to prove the stronger *second order sufficient optimality condition*

$$\langle \delta^2 \mathcal{E}_{ac}(y_{ac}) u_h, u_h \rangle \geq \gamma \|\nabla u_h\|_{L^2(\Omega)}^2 \quad \forall u_h \in \mathcal{U}_h. \quad (3.10)$$

for some $\gamma > 0$, where the norm $\|\nabla u_h\|_{L^2(\Omega)}^2$ is yet to be defined for $u_h \in \mathcal{U}_h$. The choice of norm on the right-hand side of (3.10) is motivated by the fact that the equations (3.8) have a similar structure as finite element discretisations of second order elliptic equations.

3.3. Brief outline of the error analysis. We give a brief sketch of the main result, Theorem 7.1, in order to motivate the subsequent technical details that we provide in §5–§7. The following discussion is merely schematic, and some steps are not properly defined at this point.

Let y_a be a solution of (2.4), and y_{ac} a solution of (3.7), and assume that y_a, y_{ac} , and $I_h y_a$ are “close” in a sense to be made precise. Suppose, moreover, that (3.10) holds. Let $e_h := I_h y_a - y_{ac}$, then we can estimate

$$\begin{aligned} \gamma \|\nabla e_h\|_{L^2(\Omega)}^2 &\leq \langle \delta^2 \mathcal{E}_{ac}(y_{ac}) e_h, e_h \rangle \\ &\approx \langle \delta \mathcal{E}_{ac}(I_h y_a) - \delta \mathcal{E}_{ac}(y_{ac}), e_h \rangle = \langle \delta \mathcal{E}_{ac}(I_h y_a), e_h \rangle. \end{aligned}$$

The first inequality in the above estimate is the focus of the stability analysis in §6. The purpose of the consistency analysis §5 is to estimate

$$\langle \delta \mathcal{E}_{ac}(I_h y_a), e_h \rangle \leq \mathcal{E}^{\text{cons}} \|\nabla e_h\|_{L^2(\Omega)},$$

which immediately yields an *a priori* error estimate:

$$\|\nabla I_h y_a - \nabla y_h\|_{L^2(\Omega)} \lesssim \gamma^{-1} \mathcal{E}^{\text{cons}}.$$

In §4 we will give an interpretation to ∇y_a , and establish interpolation error estimates, so that we can also estimate $\|\nabla y_a - \nabla y_{ac}\|_{L^2(\Omega)}$. In §7, we will make the above arguments rigorous, and in addition establish an error estimate for the energy.

4. AUXILIARY RESULTS

4.1. Extension to the vacancy set. A substantial simplification of the subsequent analysis and notation can be achieved if we extend all function values to the vacancy set \mathbb{V} . We have also considered other approaches, but have found that they are significantly more technical and would yield only minor quantitative improvements over our results. (The reason for this is that some non-nearest neighbour bonds “cross” into the vacancy neighbourhoods, and therefore cannot be easily controlled by nearest-neighbour bonds.) A different approach might be required, however, if one were to extend the analysis to more general classes of defects.

We define the extension operator as the solution of a variational problem. Let

$$\mathcal{U}_E := \{v : \mathbb{L}^\# \rightarrow \mathbb{R}^2 : v(x + Na_j) = v(x) \text{ for } x \in \mathbb{L}^\#, j = 1, 2\};$$

then, for $u \in \mathcal{U}$, we define

$$Eu := \operatorname{argmin}_{\substack{v \in \mathcal{U}_E \\ v = u \text{ on } \mathcal{L}}} \Phi_{\mathbb{B}_{\text{nn}}}(v), \quad \text{where} \quad \Phi_{\mathbb{B}_{\text{nn}}}(v) := \sum_{b \in \mathbb{B}_{\text{nn}}} |r_b \cdot D_b v|^2. \quad (4.1)$$

This definition is motivated by the stability analysis, more precisely the definition of the *vacancy stability index* in §6.1.2.

Proposition 4.1. *The extension operator E is well-defined, that is, the variational problem (4.1) has a unique solution. Moreover, $E : \mathcal{U} \rightarrow \mathcal{U}_E$ is linear.*

Proof. To prove that (4.1) has a unique solution it is sufficient to show that $\Phi_{\mathbb{B}_{\text{nn}}}$ is a positive definite quadratic form on the affine subspace of \mathcal{U}_E defined through the constraint $v = u$ on \mathcal{L} . The linearity is a straightforward consequence.

To establish this, we need to employ notation that will be properly defined in §4.2: let \mathcal{T}_a denote the canonical triangulation of $\mathbb{L}^\#$, and, for each $v \in \mathcal{U}_E$, let \bar{v} denote the corresponding continuous piecewise affine interpolant. In particular, we then have $D_b v = \nabla_b \bar{v}$ for all bonds $b \in \mathbb{B}_{\text{nn}}$.

Moreover, applying the bond density lemma, and Lemma 2.2, (2.2), we obtain

$$\Phi_{\mathbb{B}_{\text{nn}}}(v) = \int_{\Omega} \sum_{r \in \mathbb{L}_{\text{nn}}} |r \cdot \nabla \bar{v}|^2 dV = \int_{\Omega} \left\{ \frac{3}{2} |(\nabla \bar{v})^{\text{sym}}|^2 + \frac{3}{4} |\operatorname{tr}(\nabla \bar{v})|^2 \right\} dV.$$

Since \bar{v} is fixed in the continuum region, Korn's inequality shows that $\Phi_{\mathbb{B}_{\text{nn}}}$ is indeed coercive.

This proof shows that, in fact, E is defined through the solution of an isotropic linear elasticity problem, with boundary data provided on the edge of a suitably defined neighbourhood of the vacancy set. \square

We extend the definition of E to include deformations $y \in \mathcal{Y}$, via $E(y_{\mathbb{B}} + u) = y_{\mathbb{B}} + Eu$ for all $\mathbb{B} \in \mathbb{R}_+^{2 \times 2}$. We stress, however, that none of our results depend (explicitly or implicitly) on the extension of deformations. By contrast, the extension of displacements enters our analysis heavily.

For the sake of simplicity of notation, we will henceforth identify $Ew \equiv w$, except where we need to strictly distinguish the original function w and its extension.

4.2. Micro-triangulation and extension of \mathcal{T}_h^c . The triangular lattice $\mathbb{L}^\#$ has a ‘‘canonical’’ triangulation $\mathcal{T}_a^\#$, which is defined so that every nearest-neighbour bond is the edge of a triangle; see Figure 3. The subset of triangles $\tau \in \mathcal{T}_a^\#$ that are contained in $\operatorname{clos}(\Omega)$ is denoted by \mathcal{T}_a . We will assume throughout that the following assumption holds, but only cite it explicitly in the main results.

Assumption A. *The boundary of Ω_a is aligned with edges of \mathcal{T}_a and the mesh size on $\partial\Omega_a$ is equal to the lattice spacing.*

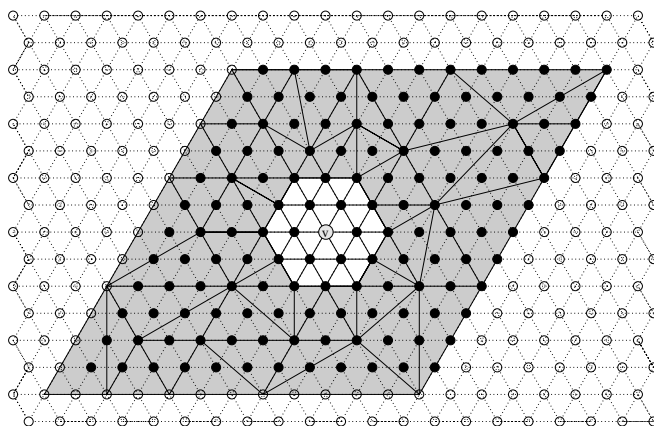


FIGURE 3. The micro-triangulation \mathcal{T}_a (dotted lines) and the extension \mathcal{T}_h of the macro-triangulation to the atomistic domain. Note that in Ω_a , \mathcal{T}_h coincides with \mathcal{T}_a and has no hanging nodes.

Assumption A implies that any microelement $\tau \in \mathcal{T}_a$ must belong either entirely to Ω_a or to Ω_c . This yields a natural extension \mathcal{T}_h of \mathcal{T}_h^c , which is obtained by adding all micro-elements $\tau \in \mathcal{T}_a$, $\tau \subset \Omega_a$, so that \mathcal{T}_h and \mathcal{T}_a coincide in Ω_a . The requirement that the mesh size on $\partial\Omega_a$ is equal to the lattice spacing implies that the extended mesh \mathcal{T}_h has no hanging nodes, which requires that the mesh size on $\partial\Omega_a$ is equal to the lattice spacing.

The definitions of the element size h_T , the mesh size function $h(x)$, and the shape regularity, from §3.1.2, are extended to \mathcal{T}_h and $\mathcal{T}_h^\#$.

For any lattice function $w : \mathbb{L}^\# \rightarrow \mathbb{R}^k$ we define the P1 micro-interpolant \bar{w} , that is, $\bar{w} \in W_{\text{loc}}^{1,\infty}(\mathbb{R}^2)^k$ and $\bar{w}(x) = w(x)$ on the lattice sites $x \in \mathbb{L}^\#$. In particular, the gradient $\nabla\bar{w}$, which is a piecewise constant function, is also well-defined.

Note that, if $y_h \in \mathcal{Y}_h$, then y_h is interpreted as the continuous P1 interpolant with respect to the mesh \mathcal{T}_h (the *macro-interpolant*), while \bar{y}_h is understood as the P1 interpolant with respect to the mesh \mathcal{T}_a (the *micro-interpolant*). In our analysis we will require some technical results to compare \bar{y}_h and y_h . The following Lemma gives a global comparison result, while a local variant is established in Lemma 4.5 below. The proof is given in Appendix A.

Lemma 4.2. *Let $y_h \in \mathcal{Y}_h$, and $p \in [1, \infty]$; then*

$$\|\nabla\bar{y}_h\|_{L^p(\Omega)} \leq \bar{C}_\Omega \|\nabla y_h\|_{L^p(\Omega)}, \quad (4.2)$$

where $\bar{C}_\Omega = \max(3^{(p-2)/(2p)}, 3^{(2-p)/(2p)}) \leq \sqrt{3}$.

4.3. $W^{2,\infty}$ -conforming interpolants. Smoothness of the atomistic solution in the continuum region is one of the key requirements for error estimates in a/c methods [6, 21]. In previous 1D analyses of a/c methods smoothness was measured via second and third order finite differences. Although this is in principle still possible in 2D, it is more convenient in the analysis to make use of the smoothness of interpolants that belong to $W_{\text{loc}}^{2,\infty}(\mathbb{R}^2)$. One possible approach is to choose one of the $W^{2,\infty}$ -conforming finite elements (see Remark 4.1), however, it turns out that our analysis requires no explicit construction and

it is therefore more convenient to define the class of all $W^{2,\infty}$ -conforming interpolants of deformations $y \in \mathcal{Y}_B$:

$$\begin{aligned} \Pi_2(y) := \{ \tilde{y} \in W^{2,\infty}(\mathbb{R}^2)^2 : \tilde{y}(x) = y(x) \text{ for all } x \in \mathbb{L}^\#, \text{ and} \\ \tilde{y}(x + Na_j) = B(Na_j) + \tilde{y}(x) \text{ for all } x \in \mathbb{R}^2, j = 1, 2 \}. \end{aligned}$$

We immediately obtain the following results.

Lemma 4.3 (Interpolation Error Estimates). *Let $p \in [1, \infty]$, then there exists a constant \tilde{C}_h that depends only on p and on the shape regularity of \mathcal{T}_h , such that, for all $y \in \mathcal{Y}$,*

$$\| \nabla \tilde{y} - \nabla I_h y \|_{L^p(T)} \leq \tilde{C}_h h_T \| \nabla^2 \tilde{y} \|_{L^p(T)} \quad \forall T \in \mathcal{T}_h \quad \forall \tilde{y} \in \Pi_2(y). \quad (4.3)$$

Moreover, there exists a constant \tilde{C}_a , which depends only on p , such that

$$\| \nabla \tilde{y} - \nabla \bar{y} \|_{L^p(\tau)} \leq \tilde{C}_a \| \nabla^2 \tilde{y} \|_{L^p(\tau)} \quad \forall \tau \in \mathcal{T}_a \quad \forall \tilde{y} \in \Pi_2(y). \quad (4.4)$$

Proof. The estimate (4.3) is a standard interpolation error estimate [1]. The estimate (4.4) follows from the fact that \bar{y} is the P1-interpolant of \tilde{y} on the micro-triangulation. The constant \tilde{C}_a is independent of the mesh quality since \mathcal{T}_a contains only a single element shape. \square

We conclude this section with a remark on a specific choice of interpolant $\tilde{y} \in \Pi_2(y)$, which can be used to establish an equivalence between $\nabla^2 \tilde{y}$, for some $\tilde{y} \in \Pi_2(y)$, and jumps of $\nabla \bar{y}$ across micro-element edges. Measuring smoothness of y in terms of these jumps would in fact be a natural extension of second order finite differences to 2D. To this end, we define $\mathcal{F}_a^\#$ to be the set of edges of $\mathcal{T}_a^\#$. The set of edges $f \in \mathcal{F}_a^\#$ such that $\text{int}(f) \subset \Omega$ is denoted by \mathcal{F}_a , where $\text{int}(f)$ denotes the relative interior.

Remark 4.1 (The HCT interpolant). The Hsieh–Clough–Tocher (HCT) element is a C^1 -conforming element for which the degrees of freedom are point values, gradient values, and normal derivatives; see Figure 4. We refer to [1, Sec. 6.1] for a detailed discussion and further references.

For each micro-element $\tau \in \mathcal{T}_a^\#$, let $Q_\tau \subset \mathbb{L}^\#$ denote the set of vertices, $F_\tau \subset \mathcal{F}_a^\#$ the set of edges, and q_f the edge midpoint of an edge $f \in \mathcal{F}_a$. We denote the basis function associated with the nodal value at a vertex q by ψ_q , the basis function associated with the partial derivatives $\partial_\alpha, \alpha = 1, 2$, at a vertex q by $\Psi_{q,\alpha}$, and the basis function associated with the normal derivative at an edge midpoint $q_f, f \in \mathcal{F}_a$, by ψ_f .

For each $q \in \mathbb{L}^\#$ and $f \in \mathcal{F}_a^\#$ we define the patches

$$\omega_q := \bigcup \{ \tau \in \mathcal{T}_a^\# : q \in \tau \}, \quad \text{and} \quad \omega_f := \bigcup \{ \tau \in \mathcal{T}_a^\# : f \subset \tau \}.$$

We define the HCT interpolant \tilde{w} of a lattice function $w : \mathbb{L}^\# \rightarrow \mathbb{R}$ by

$$\tilde{w}_{\text{hct}} := \sum_{q \in \mathbb{L}^\#} \psi_q w(q) + \sum_{q \in \mathbb{L}^\#} \sum_{\alpha=1}^2 \Psi_{q,\alpha} \int_{\omega_q} \partial_\alpha \bar{w} \, dV + \sum_{f \in \mathcal{F}_a^\#} \psi_f \int_{\omega_f} \partial_{\nu_f} \bar{w} \, dV.$$

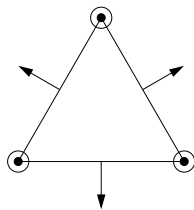


FIGURE 4. Illustration of the degrees of freedom in the C^1 -conforming Hsieh–Clough–Tocher element: black dots denote point values, circles denote gradient values, arrows denote directional derivatives.

According to [1, Thm. 6.1.2], the HCT interpolant \tilde{w}_{hct} admits one classical and two weak derivatives. For vector valued functions the HCT interpolant is defined componentwise.

With these definitions it is fairly straightforward to prove the following chain of inequalities:

$$c_1 \|\nabla^2 \tilde{w}_{\text{hct}}\|_{L^p(\tau)} \leq \|[\nabla \bar{w}]\|_{L^p(\Gamma_\tau)} \leq c_2 \|\nabla^2 \tilde{w}_{\text{hct}}\|_{L^p(\omega_\tau)}, \quad (4.5)$$

for all micro-elements $\tau \in \mathcal{T}_a^\#$ and lattice functions w ; where $c_1, c_2 > 0$,

$$\Gamma_\tau = \bigcup \{f \in \mathcal{F}_a^\# : f \cap \tau \neq \emptyset\}, \quad \text{and} \quad \omega_\tau = \bigcup \{\tau' \in \mathcal{T}_a^\# : \tau' \cap \tau \neq \emptyset\},$$

and where $[\nabla \bar{w}]$ denotes the jump of $\nabla \bar{w}$ across the element edges.

In particular, the inequalities in (4.5) show a local equivalence between second derivatives of “good” $W^{2,\infty}$ -conforming interpolants and jumps of $\nabla \bar{w}$. \square

4.4. Notation for edges. Several of our estimates will be phrased in terms of the jumps of ∇y_h , $y_h \in \mathcal{Y}_h$, across element edges, for which we now introduce some notation: let $\mathcal{F}_h^\#$ denote the set of (closed) edges of the triangulation $\mathcal{T}_h^\#$, and let

$$\mathcal{F}_h = \{f \in \mathcal{F}_h^\# : \text{int}(f) \subset \Omega\}, \quad \text{and} \quad \mathcal{F}_h^c = \{f \in \mathcal{F}_h : f \not\subset \Omega_a\},$$

where $\text{int}(f)$ denotes the relative interior of f . That is, the set \mathcal{F}_h includes one periodic copy of all element edges contained in Ω , and \mathcal{F}_h^c excludes all edges that are subsets of Ω_a .

Let $f \in \mathcal{F}_h^\#$, $f = T_+ \cap T_-$, $T_\pm \in \mathcal{T}_h$, and suppose that $w : \text{int}(T_+) \cup \text{int}(T_-) \rightarrow \mathbb{R}^k$ has well-defined traces w^\pm from T^\pm , then we define the jump $[w](x) := w_+(x) - w_-(x)$ for all $x \in \text{int}(f)$.

Whenever we write $\int_{\mathcal{F}_h^c}$, $L^p(\mathcal{F}_h^c)$, etc., we identify \mathcal{F}_h^c with the union of its elements.

4.5. Further auxiliary results. Our next lemma provides a tool to estimate jumps across edges. The proof is given in Appendix A.

Lemma 4.4. *Let $y \in \mathcal{Y}$ and let $f \in \mathcal{F}_h^\#$, $f = T_+ \cap T_-$ for $T_\pm \in \mathcal{T}_h$; then*

$$\|[\nabla I_h y]\|_{L^p(f)} \leq C_f \|h^{1/p'} \nabla^2 \tilde{y}\|_{L^p(T_+ \cup T_-)} \quad \forall \tilde{y} \in \Pi_2(y), \quad (4.6)$$

where C_f depends only on the shape regularity of \mathcal{T}_h . In particular, we also have

$$\|[\nabla I_h y]\|_{L^p(\mathcal{F}_h^c)} \leq C_f 3^{1/p} \|h^{1/p'} \nabla^2 \tilde{y}\|_{L^p(\Omega_c)} \quad \forall \tilde{y} \in \Pi_2(y). \quad (4.7)$$

The previous lemma shows that we can admit jumps in our estimates, and subsequently bound them in terms of the smooth interpolants. The following local version of Lemma 4.2 and its corollary, Lemma 4.6, are motivated by this observation. The proof of Lemma 4.5 is again given in Appendix A. We remark that the constant \bar{C}_a is fairly moderate as the discussion at the end of the proof shows.

Lemma 4.5. *Let $y_h \in \mathcal{Y}_h$, $\tau \in \mathcal{T}_a$, and $p \in [1, \infty]$; then*

$$\|\nabla \bar{y}_h\|_{L^p(\tau)} \leq \bar{C}_a \left(\|\nabla y_h\|_{L^p(\tau)}^p + \|[\nabla y_h]\|_{L^p(\mathcal{F}_h^\# \cap \text{int}(\tau))}^p \right)^{1/p}, \quad (4.8)$$

where \bar{C}_a depends only on the shape regularity of \mathcal{T}_h .

Combining Lemma 4.5 and Lemma 4.3, we obtain the following corollary. Since this is such a central tool in our analysis we give its complete proof in the present section.

Lemma 4.6. *Let $y \in \mathcal{Y}$, $y_h \in \mathcal{Y}_h$, and $p \in [1, \infty]$; then*

$$\|\nabla \bar{y} - \nabla \overline{I_h y}\|_{L^p(\Omega_c)} \leq \bar{C}_{I_h} \|h \nabla^2 \tilde{y}\|_{L^p(\Omega_c)} \quad \forall \tilde{y} \in \Pi_2(y), \quad (4.9)$$

where \bar{C}_{I_h} depends only on the shape regularity of \mathcal{T}_h .

Proof. We cannot immediately use the interpolation error estimates (4.3) and (4.4) to estimate the term $\|\nabla(\bar{y} - \overline{I_h y})\|_{L^p(\Omega)}$, due to the occurrence of $\overline{I_h y}$. Instead, we first fix a micro-element $\tau \subset \Omega_c$, define $z(x) := (\nabla \bar{y}|_\tau)x$ for all $x \in \mathbb{R}^2$, and use (4.8) to estimate

$$\begin{aligned} \|\nabla(\bar{y} - \overline{I_h y})\|_{L^p(\tau)}^p &= \|\nabla \overline{I_h(y - z)}\|_{L^p(\tau)}^p \\ &\leq \bar{C}_a^p \left[\|\nabla I_h(y - z)\|_{L^p(\tau)}^p + \|[\nabla I_h(y - z)]\|_{L^p(\mathcal{F}_h^c \cap \text{int}(\tau))}^p \right] \\ &= \bar{C}_a^p \left[\|\nabla(I_h y - \bar{y})\|_{L^p(\tau)}^p + \|[\nabla I_h y]\|_{L^p(\mathcal{F}_h^c \cap \text{int}(\tau))}^p \right]. \end{aligned}$$

We will next sum this estimate for all $\tau \in \mathcal{T}_a$. Using the fact that $\bar{y} = I_h y$ in Ω_a , as well as the interpolation error estimates (4.3) and (4.4), and the jump estimate (4.7), we obtain, for any $\tilde{y} \in \Pi_2(y)$,

$$\begin{aligned} \|\nabla(\bar{y} - \overline{I_h y})\|_{L^p(\Omega)} &\leq \bar{C}_a \left[\|\nabla(I_h y - \bar{y})\|_{L^p(\Omega_c)} + \|[\nabla I_h y]\|_{L^p(\mathcal{F}_h^c)} \right] \\ &\leq \bar{C}_a \left[\|\nabla(I_h y - \tilde{y})\|_{L^p(\Omega_c)} + \|\nabla(\tilde{y} - \bar{y})\|_{L^p(\Omega_c)} + \|[\nabla I_h y]\|_{L^p(\mathcal{F}_h^c)} \right] \\ &\leq \bar{C}_a \left[\tilde{C}_h \|h \nabla^2 \tilde{y}\|_{L^p(\Omega_c)} + \tilde{C}_a \|\nabla^2 \tilde{y}\|_{L^p(\Omega_c)} + C_f 3^{1/p} \|h^{1/p'} \nabla^2 \tilde{y}\|_{L^p(\Omega_c)} \right]. \end{aligned}$$

Since $h \geq 1$, the stated result follows. \square

5. CONSISTENCY

Recall from our preliminary discussion in §3.3 that the *total consistency error* associated with the atomistic solution y^a is

$$\|\delta \mathcal{E}_{\text{ac}}(I_h y^a)\|_{W_h^{-1,p}} = \|\delta \mathcal{E}_{\text{ac}}(I_h y^a) - \delta \mathcal{E}_a(y^a)\|_{W_h^{-1,p}} =: \mathcal{E}_p^{\text{cons}}(y^a),$$

where, for a functional $\Psi \in \mathcal{U}_h^*$, the negative Sobolev norm is defined as

$$\|\Psi\|_{W_h^{-1,p}} := \sup_{\substack{u_h \in \mathcal{U}_h \\ \|\nabla u_h\|_{L^{p'}(\Omega)}=1}} \langle \Psi, u_h \rangle.$$

The purpose of the present section is to prove the following estimate on $\mathcal{E}_p^{\text{cons}}$.

Theorem 5.1 (Consistency). *Suppose that Assumption A holds. Let $y \in \mathcal{Y}$ such that $\mu_a(y) > 0$ and $\mu_c(I_h y) > 0$. Then, for each $p \in [1, \infty]$, we have*

$$\mathcal{E}_p^{\text{cons}}(y) \leq C^{\text{cons}} \inf_{\tilde{y} \in \Pi_2(y)} \|h \nabla^2 \tilde{y}\|_{L^p(\Omega_c)}, \quad (5.1)$$

where C^{cons} depends on $\mu_a(y_a)$, on $\mu_c(I_h y)$, and on the shape regularity of \mathcal{T}_h .

Proof. To prove this result, we first split the consistency error into a *coarsening error* and a *modelling error*:

$$\begin{aligned} \mathcal{E}_p^{\text{cons}}(y) &= \left\| \delta \mathcal{E}_{\text{ac}}(I_h y) - \delta \mathcal{E}_a(y) \right\|_{W_h^{-1,p}} \\ &\leq \left\| \delta \mathcal{E}_{\text{ac}}(I_h y) - \delta \mathcal{E}_a(I_h y) \right\|_{W_h^{-1,p}} + \left\| \delta \mathcal{E}_a(I_h y) - \delta \mathcal{E}_a(y) \right\|_{W_h^{-1,p}}, \\ &=: \mathcal{E}_p^{\text{model}}(y) + \mathcal{E}_p^{\text{coarse}}(y). \end{aligned}$$

We note, however, that due to the fact that we estimate the modelling error at the interpolant $I_h y$, the mesh dependence is not entirely removed from $\mathcal{E}^{\text{model}}$.

The estimate for the coarsening error is given in Lemma 5.4, and the estimate for the modelling error in Lemma 5.9, which together yield (5.1) with $C^{\text{cons}} = C^{\text{coarse}} + C^{\text{model}}$. Note that we have ignored the improved mesh size dependence of the modelling error and estimated $1 \leq h$ to obtain $\mathcal{E}_p^{\text{model}}(y) \leq C^{\text{model}} \|h \nabla^2 \tilde{y}\|_{L^p(\Omega_c)}$ for all $\tilde{y} \in \Pi_2(y)$. \square

Remark 5.1. The proof of Theorem 5.1 is fairly involved. This is due to the relatively weak assumptions that we made on the mesh \mathcal{T}_h , as well as the fact that we insisted to estimate the consistency error in terms of $\|h \nabla^2 \tilde{y}\|_{L^p(\Omega_c)}$ only. Simpler arguments can be given if weaker estimates are sufficient; see Appendix B. \square

5.1. Coarsening error. In this section, we establish the coarsening error estimate. The two main ingredients are a local Lipschitz bound on $\delta \mathcal{E}_a$, and the interpolation error estimate established in Lemma 4.6. We begin by stating a useful auxiliary lemma.

Lemma 5.2. *Let $r \in \mathbb{L}_*$ and $q \in [1, \infty)$, then*

$$\sum_{x \in \mathbb{L}} |D_r u_h(x)|^q \leq \sum_{x \in \mathbb{L}} \int_x^{x+r} |\nabla_r u_h|^q \, \text{db} = \|\nabla_r u_h\|_{L^q(\Omega)}^q \quad \forall u_h \in \mathcal{U}_h, \quad \text{and} \quad (5.2)$$

$$\sum_{x \in \mathbb{L}} |D_r u(x)|^q \leq \sum_{x \in \mathbb{L}} \int_x^{x+r} |\nabla_r \bar{u}|^q \, \text{db} = \|\nabla_r \bar{u}\|_{L^q(\Omega)}^q \quad \forall u \in \mathcal{U}. \quad (5.3)$$

Proof. The result is a straightforward application of the periodic bond density lemma. We give the proof for (5.2), since (5.3) is a particular case.

First, we use Jensen's inequality to establish the inequality in (5.2):

$$|D_r u_h(x)|^q = \left| \int_x^{x+r} \nabla_r u_h \, \text{db} \right|^q \leq \int_x^{x+r} |\nabla_r u_h|^q \, \text{db}.$$

Using (i) the fact that $\{\chi_T^\# : T \in \mathcal{T}_h\}$ is a partition of unity; (ii) continuity of $\nabla_r u_h$ across faces that have direction r ; and (iii) Lemma 3.2, we have

$$\begin{aligned} \sum_{x \in \mathbb{L}} \int_x^{x+r} |\nabla_r u_h|^q \, db &= \sum_{T \in \mathcal{T}_h} \sum_{x \in \mathbb{L}} \int_x^{x+r} \chi_{T^\#} |\nabla_r u_h|^q \, db \\ &= \sum_{T \in \mathcal{T}_h} |\nabla_r u_h|_T^q \sum_{x \in \mathbb{L}} \int_x^{x+r} \chi_{T^\#} \, db \\ &= \sum_{T \in \mathcal{T}_h} |T| |\nabla_r u_h|_T^q. \end{aligned} \quad \square$$

The next auxiliary result is a Lipschitz bound on $\delta \mathcal{E}_a$.

Lemma 5.3. *Let $y^{(i)} \in \mathcal{Y}$, $i = 1, 2$, and let $\mu := \min\{\mu_a(y^{(1)}), \mu_a(y^{(2)})\} > 0$; then*

$$|\langle \delta \mathcal{E}_a(y^{(1)}) - \delta \mathcal{E}_a(y^{(2)}), u_h \rangle| \leq C_L \|\nabla \bar{y}^{(1)} - \nabla \bar{y}^{(2)}\|_{L^p(\Omega)} \|\nabla u_h\|_{L^{p'}(\Omega)} \quad \forall u_h \in \mathcal{U}_h, \quad (5.4)$$

where $C_L = C_L(\mu) := \sum_{r \in \mathbb{L}_*} |r|^2 M_2(\mu|r|)$.

Proof. Fix $u \in \mathcal{U}$, $y^{(i)} \in \mathcal{Y}$, $i = 1, 2$, and $p \in (1, \infty)$; then

$$\begin{aligned} |\langle \delta \mathcal{E}_a(y^{(1)}) - \delta \mathcal{E}_a(y^{(2)}), u_h \rangle| &\leq \sum_{b \in \mathcal{B}} |\phi'(D_b y^{(1)}) - \phi'(D_b y^{(2)})| |D_b u_h| \\ &\leq \sum_{b \in \mathcal{B}} M'_{|b|} \left| \frac{D_b y^{(1)} - D_b y^{(2)}}{|b|} \right| \left| \frac{D_b u_h}{|b|} \right|, \end{aligned}$$

where $M'_\rho = M_2(\mu\rho)\rho^2$. Let $w = y^{(1)} - y^{(2)}$, then, applying a Hölder inequality, we obtain that

$$|\langle \delta \mathcal{E}_a(y^{(1)}) - \delta \mathcal{E}_a(y^{(2)}), u_h \rangle| \leq \left(\sum_{b \in \mathcal{B}} M'_{|b|} \left| \frac{D_b w}{|b|} \right|^p \right)^{1/p} \left(\sum_{b \in \mathcal{B}} M'_{|b|} \left| \frac{D_b u_h}{|b|} \right|^{p'} \right)^{1/p'}.$$

Each of the two groups can be estimated using Lemma 5.2, for example,

$$\begin{aligned} \sum_{b \in \mathcal{B}} M'_{|b|} \left| \frac{D_b w}{|b|} \right|^p &\leq \sum_{b \in \mathbb{B}} M'_{|b|} \left| \frac{D_b w}{|b|} \right|^p = \sum_{r \in \mathbb{L}_*} M'_{|r|} |r|^{-p} \sum_{x \in \mathbb{L}} |D_r w(x)|^p \\ &\leq \sum_{r \in \mathbb{L}_*} M'_{|r|} |r|^{-p} \|\nabla_r \bar{w}\|_{L^p(\Omega)}^p = \|\nabla \bar{w}\|_{L^p(\Omega)}^p \sum_{r \in \mathbb{L}_*} M'_{|r|}. \end{aligned}$$

By the same argument, using (5.2) instead of (5.3), we obtain

$$\sum_{b \in \mathcal{B}} M'_{|b|} \left| \frac{D_b u_h}{|b|} \right|^{p'} \leq \sum_{r \in \mathbb{L}_*} M'_{|r|} \|\nabla u_h\|_{L^{p'}(\Omega)}^{p'}.$$

This establishes (5.4) for $p \in (1, \infty)$. The cases $p \in \{1, \infty\}$ are obtained by taking the corresponding limits as $p \rightarrow 1$, or as $p \rightarrow \infty$, or with minor modifications of the above argument. \square

We can now formulate the coarsening error estimate.

Lemma 5.4. *Let $y \in \mathcal{Y}$ and suppose that $\mu := \min(\mu_a(y), \mu_a(I_h y)) > 0$; then,*

$$\mathcal{E}_p^{\text{coarse}}(y) \leq C^{\text{coarse}} \|h \nabla^2 \tilde{y}\|_{L^p(\Omega_c)}, \quad (5.5)$$

for all $p \in [1, \infty]$ and for all $\tilde{y} \in \Pi_2(y)$, where $C^{\text{coarse}} = C_L(\mu)\bar{C}_{I_h}$.

Proof. According to Lemma 5.3 we have

$$\langle \delta \mathcal{E}_a(y) - \delta \mathcal{E}_a(I_h y), u_h \rangle \leq C_L \|\nabla(\bar{y} - \overline{I_h y})\|_{L^p(\Omega)} \|\nabla u_h\|_{L^{p'}(\Omega)}.$$

From Lemma 4.6 we obtain that

$$\|\nabla(\bar{y} - \overline{I_h y})\|_{L^p(\Omega)} \leq \bar{C}_{I_h} \|h \nabla^2 \tilde{y}\|_{L^p(\Omega_c)} \quad \forall \tilde{y} \in \Pi_2(y),$$

which yields (5.5) with $C^{\text{coarse}} = C_L \bar{C}_{I_h}$. \square

Remark 5.2. We are now in a position to comment on our choice of splitting the consistency error. If we had estimated the coarsening on the level of \mathcal{E}_{ac} , then we would have needed a Lipschitz estimate on $\delta \mathcal{E}_{ac}$. Defining $\mathcal{E}_{ac}(\bar{y})$ in a canonical way, our proof above is easily modified to yield

$$\begin{aligned} |\langle \delta \mathcal{E}_{ac}(I_h y) - \delta \mathcal{E}_{ac}(\bar{y}), u_h \rangle| &\leq \left\{ \sum_{b \in \mathcal{B}_a} M'_{|b|} \int_b |\nabla_b \overline{I_h y} - \nabla_b \bar{y}|^p \, db \right. \\ &\quad \left. + \sum_{b \in \mathcal{B}_c} M'_{|b|} \int_b |\nabla_b y_h - \nabla_b \bar{y}|^p \, db \right\}^{1/p} C_L^{1/p'} \|\nabla u_h\|_{L^{p'}}. \end{aligned}$$

The first group we can again convert into volume integrals and estimate using Lemma 4.6. However, the second group contains integrals over both macro- and micro-interpolants, and therefore cannot be converted into volume integrals using the bond density lemma.

However, as we demonstrate in Appendix B, weaker (though technically less demanding) estimates can be obtained in this way. \square

5.2. Modelling error. In §5.1 we estimated the coarsening error $\mathcal{E}^{\text{coarse}}$. We will now analyze the second contribution to the consistency error: the modelling error $\mathcal{E}^{\text{model}}$.

For the majority of this analysis we can replace $I_h y$ by an arbitrary discrete deformation $y_h \in \mathcal{Y}_h$. Hence, we fix $y_h \in \mathcal{Y}_h$ such that $\mu := \min(\mu_a(y_h), \mu_c(y_h)) > 0$. Moreover, we fix constants $a_r > 0$, $r \in \mathbb{L}_*$, which will be determined later, $a_b := a_{r_b}$ for all bonds $b \in \mathbb{B}$, and $M'_\rho := M_2(\mu\rho)\rho^2$ for $\rho > 0$.

With this notation, and using (3.2), we have

$$\begin{aligned} \langle \delta \mathcal{E}_{ac}(y_h) - \delta \mathcal{E}_a(y_h), u_h \rangle &= \sum_{b \in \mathcal{B}_c} \int_b \phi'(\nabla_b y_h) \cdot \nabla_b u_h \, db - \sum_{b \in \mathcal{B}_c} \phi'(D_b y_h) D_b u_h \\ &= \sum_{b \in \mathcal{B}_c} \int_b [\phi'(\nabla_b y_h) - \phi'(D_b y_h)] \cdot \nabla_b u_h \, db \\ &\leq \sum_{b \in \mathcal{B}_c} M_2(\mu|b|) \int_b |\nabla_b y_h - D_b y_h| |\nabla_b u_h| \, db \\ &= \sum_{b \in \mathcal{B}_c} M'_{|b|} \int_b (a_b^{-1} |b|^{-1} |\nabla_b y_h - D_b y_h|) (a_b |b|^{-1} |\nabla_b u_h|) \, db. \end{aligned}$$

Following a similar procedure as in the proof of Lemma 5.3 (applying a Hölder inequality and Lemma 5.2), we obtain

$$\begin{aligned} \langle \delta \mathcal{E}_{ac}(y_h) - \delta \mathcal{E}_a(y_h), u_h \rangle &\leq \left(\sum_{b \in \mathcal{B}_c} M'_{|b|} |b|^{-p} a_b^{-p} \int_b |\nabla_b y_h - D_b y_h|^p db \right)^{1/p} C_1^{1/p'} \|\nabla u_h\|_{L^{p'}(\Omega)} \\ &=: C_1^{1/p'} E(y_h) \|\nabla u_h\|_{L^{p'}(\Omega)}, \end{aligned} \quad (5.6)$$

where $C_1 = \sum_{r \in \mathbb{L}_*} M'_{|r|} a_r^{p'}$, and where

$$E(y_h)^p := \sum_{b \in \mathcal{B}_c} M'_{|b|} |b|^{-p} a_b^{-p} E_b(y_h)^p, \quad E_b(y_h)^p := \int_b |\nabla_b y_h - D_b y_h|^p db. \quad (5.7)$$

Next, we investigate a single bond $b \in \mathcal{B}_c$. We will estimate the term $E_b(y_h)^p$ in terms of the jumps of ∇y_h across element faces. To that end, we define the jump sets

$$J(b) := \{f \in \mathcal{F}_h : \#(f \cap \text{int}(b)) = 1\}, \quad (5.8)$$

where $\text{int}(b)$ denotes the *relative interior* of b . Faces parallel to b are ignored since the directional derivative $\nabla_{r_b} y_h$ is continuous across these faces. For each $f \in J(b)$ we define weights $w_{b,f}$,

$$w_{b,f} = \begin{cases} 1, & \text{if } f \cap \text{int}(b) \subset \text{int}(f), \\ 1/2, & \text{otherwise;} \end{cases}$$

that is, $w_{b,f} = 1$ if b crosses f in its relative interior, and $w_{b,f} = 1/2$ if b crosses f at one of its endpoints. Finally we define the quantities

$$N_j(b) := \sum_{f \in J(b)} w_{b,f}, \quad \text{and} \quad N_j(r) := \max_{\substack{b \in \mathcal{B}_c \\ r_b = r}} N_j(b). \quad (5.9)$$

With these definitions we obtain the following lemma.

Lemma 5.5. *Let $b \in \mathcal{B}_c$, then*

$$E_b(y_h)^p \leq N_j(b)^{p-1} \sum_{f \in J(b)} w_{b,f} |[\nabla_b y_h]_f|^p. \quad (5.10)$$

Proof. Define $\psi(t) = \nabla_b y_h(x + t r_b)$ and let $J_\psi \subset (0, 1)$ be the set of jumps of ψ , then

$$E_b(y_h)^p = \int_0^1 \left| \psi(t) - \int_0^1 \psi(s) ds \right|^p dt. \quad (5.11)$$

For any point $t \in (0, 1) \setminus J_\psi$ we can estimate

$$\begin{aligned} \left| \psi(t) - \int_0^1 \psi(s) ds \right| &\leq \int_0^1 |\psi(t) - \psi(s)| ds \\ &\leq \int_0^1 \int_{r \in (t,s)} |\psi'(r)| dr ds \\ &\leq \int_0^1 |\psi'(r)| dr = \sum_{r \in J_\psi} |\psi(r+) - \psi(r-)|, \end{aligned}$$

where $|\psi'| dr$ is understood as the measure that represents the distributional derivative of ψ . Inserting this estimate into (5.11), yields

$$E_b(y_h)^p \leq \left| \sum_{r \in J_\psi} |\psi(r+) - \psi(r-)| \right|^p \leq (\#J_\psi)^{p-1} \sum_{r \in J_\psi} |\psi(r+) - \psi(r-)|^p,$$

which translates directly into (5.10), in the case that b does not intersect any faces in their endpoints.

If b does intersect certain faces in endpoints then one replaces the path $\{x + tr_b : t \in (0, 1)\}$ by two paths that “circle” around the endpoints, each weighted with a factor $1/2$. \square

Recall the detail of the definition of \mathcal{F}_h^c from §4.4. Since only bonds $b \in \mathcal{B}_c$ contribute to the consistency error, it follows that only jumps across faces $f \in \mathcal{F}_h^c$ occur in the following estimate. Interchanging the order of summation, we obtain

$$\begin{aligned} E(y_h)^p &\leq \sum_{b \in \mathcal{B}_c} M'_{|b|} |b|^{-p} a_b^{-p} N_j(b)^{p-1} \sum_{f \in J(b)} w_{b,f} |\nabla_b y_h|_f|^p \\ &\leq \sum_{r \in \mathbb{L}_*} M'_{|r|} |r|^{-p} a_r^{-p} N_j(r)^{p-1} \sum_{\substack{b \in \mathcal{B}_c \\ r_b=r}} \sum_{f \in J(b)} w_{b,f} |\nabla_b y_h|_f|^p \\ &= \sum_{r \in \mathbb{L}_*} M'_{|r|} |r|^{-p} a_r^{-p} N_j(r)^{p-1} \sum_{f \in \mathcal{F}_h^c} N_{\text{cross}}(f, r) |\nabla_r y_h|_f|^p, \end{aligned} \quad (5.12)$$

where $N_{\text{cross}}(f, r)$ is the (weighted) number of bonds b with direction r_b and crossing the face f ; more precisely,

$$N_{\text{cross}}(f, r) := \sum_{\substack{b \in \mathcal{B}_c, r_b=r \\ f \in J(b)}} w_{b,f}.$$

In the next lemma, we estimate N_{cross} .

Lemma 5.6. *Let $f \in \mathcal{F}_h^c$, $r \in \mathbb{L}_*$ such that the angle between the face f and the vector r is θ ; then*

$$N_{\text{cross}}(f, r) \leq 2|r|h_f |\sin(\theta)|, \quad (5.13)$$

where $h_f = \text{length}(f)$.

Proof. Suppose that the face f is given by $f = \{z + ts : t \in [0, 1]\}$, and define the parallelogram

$$P = \{z + t_1 s + t_2 r : t_1 \in [0, 1], t_2 \in (-1, 1)\},$$

Then we have

$$N_{\text{cross}}(f, r) = \sum_{\substack{b \in \mathcal{B}_c, r_b=r \\ f \in J(b)}} \int_b \chi_P db \leq \sum_{x \in \mathbb{L}^\#} \int_x^{x+r} \chi_P db = |P|,$$

where, in the last equality, we have used the fact that P is the union of two triangles, which implies that the bond density lemma holds for P as well. To obtain the result we simply note that $|P| = 2|r|h_f \sin(\theta)$. \square

If we crudely estimate $|\sin(\theta)| \leq 1$ and $|\llbracket \nabla_r y_h \rrbracket_f| \leq |r| |\llbracket \nabla y_h \rrbracket_f|$ then we arrive at the following estimate:

$$E(y_h)^p \leq C_2 \left(\sum_{f \in \mathcal{F}_h^c} h_f |\llbracket \nabla y_h \rrbracket_f|^p \right), \quad (5.14)$$

where $C_2 = \sum_{r \in \mathbb{L}_*} 2M'_{|r|} |r| a_r^{-p} N_j(r)^{p-1}$.

We choose the constants a_r such that C_1 and C_2 are proportional, for example, as

$$2|r| a_r^{-p} N_j(r)^{p-1} = a_r^{p'} = (2|r|)^{1/p} N_j(r)^{1/p'}.$$

This choice yields

$$C_1 = C_2 = 2^{1/p} \sum_{r \in \mathbb{L}_*} M_2(\mu|r|) |r|^{2+1/p} N_j(r)^{1/p'}. \quad (5.15)$$

To obtain a more explicit constant, we estimate $N_j(r)$ next.

Lemma 5.7. *There exists a constant C_{N_j} , which depends only on the shape regularity of \mathcal{T}_h , such that*

$$N_j(b) \leq C_{N_j} (|b| + 1) \quad \forall b \in \mathcal{B}_c. \quad (5.16)$$

Proof. We will in fact prove a stronger statement: that (5.16) is true for any segment $b = (x, x+r)$ with arbitrary $x, r \in \mathbb{R}^2$. We hence extend the definitions of $J(b)$ and $N_j(b)$ canonically to all such segments b .

Throughout this proof, we denote the set of vertices of \mathcal{T}_h by \mathcal{V}_h . An inequality \lesssim denotes a bound up to a constant that may only depend on the mesh regularity.

The idea of the proof is the following: we will first reduce the statement to the case $\text{int}(b) \cap \mathcal{V}_h = \emptyset$ (recall that $\text{int}(b)$ denotes the relative interior of b) and $N_j(b) \neq 0$, and then estimate the lengths between points of intersections of b with $f \in J(b)$ and compare these lengths to $|b|$.

Case 1. ($\text{int}(b) \cap \mathcal{V}_h \neq \emptyset$) Denote $x_0 = x$, $x_n = x+r$ and let $\text{int}(b) \cap \mathcal{V}_h = \{x_1, \dots, x_{n-1}\}$, $n > 1$, where x_1, \dots, x_n are sorted by increasing distance to x . Since any two points in \mathcal{V}_h have at least distance 1, $n \leq |b|$.

If (5.16) holds for all $b_i = (x_{i-1}, x_i)$ ($i = 1, \dots, n$) then we can estimate $N_j(b)$ by respective contributions of b_i and contributions of those $f \in \mathcal{F}_h$ that contain any of points x_i . We will show that $N_j(b_i) \lesssim |b_i| + 1$ (it falls under Case 2), and hence we can estimate

$$N_j(b) \lesssim n + \sum_{i=1}^n N_j(b_i) \lesssim n + \sum_{i=1}^n (|b_i| + 1) = 2n + |b| \leq 3|b| + 2,$$

which proves (5.16) for b .

Case 2.1. ($\text{int}(b) \cap \mathcal{V}_h = \emptyset$ and $N_j(b) = 0$) The estimate (5.16) is trivial in this case.

Case 2.2. ($\text{int}(b) \cap \mathcal{V}_h = \emptyset$ and $N_j(b) \neq 0$) In this case, $N_j := N_j(b)$ is simply the number of faces that cross b . Let $J(b) = \{f_1, \dots, f_m\}$, where f_i are sorted by increasing distance of $f_i \cap b$ to x . We need to prove that $N_j \lesssim |b| + 1$. Any two faces, f_i and f_{i+1} , share exactly one common vertex $v_i \in \mathcal{V}_h$, $i = 1, \dots, N_j - 1$. We also denote by v_0 the vertex of f_1 other than v_1 , and by v_{N_j} the vertex of f_{N_j} other than v_{N_j-1} .

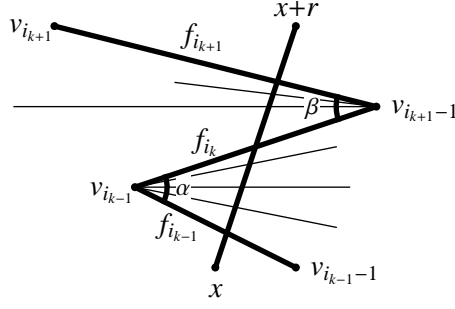


FIGURE 5. Illustration of counting the number of faces crossing a bond $b = (x, x+r)$. The bond b and the faces $f_{i_{k-1}}$, f_{i_k} and $f_{i_{k+1}}$ are bold lines. The rest of the faces $f \in J(b)$ are normal lines.

It is of course possible that v_i coincides with v_{i+1} for some $i = 1, \dots, N_j - 2$. Hence, denote the indices i of unique vertices v_i as

$$\mathcal{I} = \{i \in \{1, \dots, N_j - 2\} : v_i \neq v_{i+1}\} \cup \{0, N_j - 1, N_j\},$$

and let $\mathcal{I} = \{i_1, \dots, i_K\}$, where i_k is an increasing sequence.

If $K = 2$, then $N_j = 1$. If $K = 3$ then N_j is bounded by the number of faces touching the vertex v_{i_2} , which is bounded by a constant depending only on the shape regularity of \mathcal{T}_h . Hence, assume in the following that $K \geq 4$.

Split all faces in $J(b)$ into groups of faces between $f_{i_{k-1}}$ and $f_{i_{k+1}}$ ($k = 2, 4, \dots, 2\lfloor \frac{K}{2} \rfloor$) and, if K is odd, the faces between $f_{i_{K-1}}$ and f_{i_K} . The number of faces in each group is bounded by a finite number that depends only on the shape regularity of \mathcal{T}_h . To estimate the number of groups, notice that the distance between $b \cap f_{i_{k-1}}$ and $b \cap f_{i_{k+1}}$ can be bounded below in the following way (see illustration on Figure 5):

$$\begin{aligned} \text{dist}(b \cap f_{i_{k-1}}, b \cap f_{i_{k+1}}) &\geq \text{dist}(f_{i_{k-1}}, f_{i_{k+1}}) \\ &= \min\{\text{dist}(v_{i_{k-1}-1}, f_{i_{k+1}}), \text{dist}(v_{i_{k-1}}, f_{i_{k+1}})\} \\ &\geq \min\{\text{dist}(v_{i_{k-1}-1}, f_{i_k}), \text{dist}(v_{i_{k-1}}, f_{i_{k+1}})\}, \end{aligned}$$

Denote α and β to be angles formed by, respectively, the vertices $v_{i_{k-1}-1}, v_{i_{k-1}}, v_{i_{k+1}-1}$ and $v_{i_{k-1}}, v_{i_{k+1}-1}, v_{i_{k+1}}$ (cf. Figure 5). Then we obtain

$$\text{dist}(b \cap f_{i_{k-1}}, b \cap f_{i_{k+1}}) \geq \min\{|f_{i_{k-1}}| \sin \alpha, |f_{i_k}| \sin \beta\} \geq \min\{\sin \alpha, \sin \beta\},$$

which is bounded below by a positive number that depends only on the shape regularity of \mathcal{T}_h . Thus, the number of such groups, $\lfloor \frac{K}{2} \rfloor$, is bounded by a constant multiple of $|b|$.

This finally establishes the estimate $N_j(b) = \#(J(b)) \lesssim |b| + 1$. \square

Combining (5.14), (5.15), and (5.16), we deduce the following intermediate result, which is interesting in its own right, since it could serve as a basis for *a posteriori* error estimates.

Lemma 5.8. *Let $y_h \in \mathcal{Y}_h$ such that $\mu := \min(\mu_a(y_h), \mu_c(y_h)) > 0$; then*

$$\langle \delta \mathcal{E}_{ac}(y_h) - \delta \mathcal{E}_a(y_h), u_h \rangle \leq C_1^{\text{model}} \left\| [\nabla y_h] \right\|_{L^p(\mathcal{F}_h^c)} \|\nabla u_h\|_{L^{p'}(\Omega)} \quad \forall u_h \in \mathcal{U}_h, \quad (5.17)$$

where $C_1^{\text{model}} = C' \sum_{r \in \mathbb{L}_*} M_r(\mu|r|)|r|^3$ and C' depends only on the shape regularity of \mathcal{T}_h .

Applying Lemma 4.4 to estimate $\|[\nabla y_h]\|_{L^p(\mathcal{F}_h^c)}$ in (5.17), we obtain the final modelling error estimate.

Lemma 5.9 (Modelling Error). *Let $y \in \mathcal{Y}$ such that $\mu := \min(\mu_a(I_h y), \mu_c(I_h y)) > 0$; then*

$$\mathcal{E}_p^{\text{model}}(y) \leq C^{\text{model}} \|h^{1/p'} \nabla^2 \tilde{y}\|_{L^p(\Omega_c)}, \quad (5.18)$$

where $C^{\text{model}} = C \sum_{r \in \mathbb{L}_*} M_2(\mu|r|)|r|^3$ and C depends only on the shape regularity of \mathcal{T}_h .

Remark 5.3. At first glance it may seem that the terms $\|[\nabla y_h]\|_{L^p(\mathcal{F}_h^c)}$ in (5.17) and $\|h^{1/p'} \nabla^2 \tilde{y}\|_{L^p(\Omega_c)}$ in (5.9) are not scale invariant. This is, however, deceiving. In our case, the mesh size h is in fact replaced by the atomic scale 1, and one should read

$$\|[\nabla y_h]\|_{L^p(\mathcal{F}_h^c)} = \|1^{1/p} [\nabla y_h]\|_{L^p(\mathcal{F}_h^c)}, \quad \text{and} \quad \|h^{1/p'} \nabla^2 \tilde{y}\|_{L^p(\Omega_c)} = \|1^{1/p} h^{1/p'} \nabla^2 \tilde{y}\|_{L^p(\Omega_c)},$$

which is again scale invariant if 1 scales in the same way as h . Indeed, it can be checked that, had we formulated the entire analysis with scaled quantities $x \rightarrow \varepsilon x$, $y \rightarrow \varepsilon y$, and $\Sigma \rightarrow \varepsilon^2 \Sigma$, then we would have obtained $\|\varepsilon^{1/p} [\nabla y_h]\|_{L^p(\mathcal{F}_h^c)}$ and $\|\varepsilon^{1/p} h^{1/p'} \nabla^2 \tilde{y}\|_{L^p(\Omega_c)}$. \square

6. STABILITY

6.1. Main result. The most natural notion of stability for variational problems is positivity of the second variation (at certain deformations of interest). We will establish such a result for homogeneous lattices without defects, and use a perturbation argument to extend it to nonlinear deformations. The effect of the vacancy sites will be controlled by defining a “stability index”. We give a rigorous estimate on the stability index of separated single vacancies, and numerical estimates for divacancies.

6.1.1. Stability estimate for a Bravais lattice. We first state the main stability result for the case of a homogeneous deformation and $\mathbb{V} = \emptyset$. This serves as reference point and motivation for the general stability result below, which has a more involved formulation. To formulate the first result, for $0 < m \leq M$, we define the constants $c_n = c_n(m, M)$ and $c_n^\perp = c_n^\perp(m, M)$ by

$$\begin{aligned} c_n &:= \begin{cases} \min_{s \in [m, M]} \frac{\varphi''(s)}{s^2}, & n = 1, \\ 0 \wedge \min_{s \in [m, M]} \frac{\ell_n^2 \varphi''(s \ell_n)}{s^2}, & n > 1, \end{cases} & \text{and} \\ c_n^\perp &:= \begin{cases} \min_{s \in [m, M]} \frac{\varphi'(s)}{s}, & n = 1, \\ 0 \wedge \min_{s \in [m, M]} \frac{\ell_n \varphi'(s \ell_n)}{s^3}, & n > 1, \end{cases} \end{aligned} \quad (6.1)$$

as well as $c = c(m, M) := \sum_{n=1}^{\infty} c_n$, and $c^\perp = c^\perp(m, M) := \sum_{n=1}^{\infty} c_n^\perp$.

Theorem 6.1. *Suppose that Assumption A holds, and that $\mathbb{V} = \emptyset$. Let $\mathbf{B} \in \mathbb{R}_+^{2 \times 2}$ with singular values $0 < m \leq M$; then*

$$\langle \delta^2 \mathcal{E}_{\text{ac}}(y_{\mathbf{B}}) u_h, u_h \rangle \geq \gamma_{\text{hom}} \|\mathbf{B}^\top \nabla u_h\|_{L^2(\Omega)}^2 \quad \forall u_h \in \mathcal{U}_h,$$

where $\gamma_{\text{hom}} = \gamma_{\text{hom}}(m, M) := \min(\frac{3}{4}c + \frac{9}{4}c^\perp, \frac{9}{4}c + \frac{3}{4}c^\perp)$.

Theorem 6.1 is a special case of Theorem 6.2 below. A direct proof can be given by first specializing the definition of $\mathcal{H}(y_h)$ in (6.12) to $y_h = y_{\mathbf{B}}$ and $\mathbb{V} = \emptyset$, and then applying Lemma 6.5, with $\overline{\mathcal{H}}$ replaced with $\mathcal{H}(y_{\mathbf{B}})$.

Separation distance	4	8	12
$\mathbb{V} = \emptyset$	1		
Vacancies	0.28	0.39	0.41
Divacancies	0.16	0.26	0.29

TABLE 1. Numerically determined vacancy stability indices when \mathbb{V} consists of either single vacancies, or divacancies separated by “separation distance” (measured in Euclidean norm).

6.1.2. *The vacancy stability index.* The generalisation of Theorem 6.1 requires the following concept. Recall that in §4.1 we have defined the extension operator $E : \mathcal{U} \rightarrow \mathcal{U}_E$. We define the *vacancy stability index* as

$$\kappa(\mathbb{V}) := \max \left\{ k > 0 : \sum_{b \in \mathbb{B}_{\text{nn}}} |r_b \cdot D_b u_h|^2 \geq k \sum_{b \in \mathbb{B}_{\text{nn}}} |r_b \cdot D_b E u|^2 \text{ for all } u \in \mathcal{U} \right\}. \quad (6.2)$$

In Table 1, we present numerically estimated values on $\kappa(\mathbb{V})$ for a few simple situations. In §6.5 we rigorously prove the bound $\kappa(\mathbb{V}) \geq 2/7$ for separated single vacancies.

Remark 6.1 (Optimality of the extension operator). Recall the definition of $\Phi_{\mathbb{B}_{\text{nn}}}$ from §4.1, and let $\Phi_{\mathcal{B}_{\text{nn}}}$ be defined analogously (replacing \mathbb{B}_{nn} with \mathcal{B}_{nn} in its definition), then (6.2) can be rewritten as

$$\kappa(\mathbb{V}) = \max \left\{ k > 0 : \Phi_{\mathcal{B}_{\text{nn}}}(u) \geq k \Phi_{\mathcal{B}_{\text{nn}}}(Eu) \text{ for all } u \in \mathcal{U} \right\}.$$

Since, for fixed u , $\Phi_{\mathcal{B}_{\text{nn}}}(u)$ is also fixed, and Eu is chosen to minimize the value of $\Phi_{\mathcal{B}_{\text{nn}}}(Eu)$, it follows that among all possible extensions of u , Eu gives the largest possible stability index.

Moreover, we can characterise $\kappa(\mathbb{V})$ in terms of an operator norm of E . Let \mathcal{U} be equipped with the norm $\sqrt{\Phi_{\mathcal{B}_{\text{nn}}}}$ and \mathcal{U}_E with the norm $\sqrt{\Phi_{\mathbb{B}_{\text{nn}}}}$, then

$$\kappa(\mathbb{V}) = \inf_{u \in \mathcal{U} \setminus \{0\}} \frac{\Phi_{\mathcal{B}_{\text{nn}}}(u)}{\Phi_{\mathbb{B}_{\text{nn}}}(Eu)} = \frac{1}{\|E\|_{L(\mathcal{U}, \mathcal{U}_E)}^2}. \quad \square$$

6.1.3. *The main stability result.* Before we state the result, we introduce some additional notation. We define a family of regions in the space of deformations: for $0 < m \leq M$ and $\Delta > 0$ let

$$\begin{aligned} \mathcal{S}_{\mathcal{B},h}(m, M, \Delta) := & \left\{ y_h \in \mathcal{Y}_{\mathcal{B},h} : \mu_a(y_h) \geq m \text{ and } \mu_c(y_h) \geq m; \right. \\ & |D_b y_h| \leq M|b| \ \forall b \in \mathcal{B}_a \text{ and } \|\nabla y_h|_T\| \leq M \ \forall T \in \mathcal{T}_h^c; \\ & |\mathbb{B}^{-1} D_b y_h - r_b| \leq \Delta|b| \ \forall b \in \mathcal{B}_a \text{ and } \|\mathbb{B}^{-1} \nabla y_h|_T - \mathbb{1}\| \leq \Delta \ \forall T \in \mathcal{T}_h^c \left. \right\}. \end{aligned}$$

Next, for parameters m, M, Δ , and for $\kappa := \kappa(\mathbb{V})$, we define

$$\begin{aligned}\gamma_1 &:= \min \left\{ \left(\frac{3}{4}\kappa - 3\sqrt{\kappa}\Delta - 3\Delta^2 \right) c_1, \left(\frac{3}{4} + 3\Delta + 3\Delta^2 \right) c_1 \right\} + \sum_{n=2}^{\infty} \left(\frac{3}{4} + 3\Delta + 3\Delta^2 \right) c_n, \\ \gamma_1^\perp &:= \min \left\{ \left(\frac{9}{4}\kappa - 3\sqrt{3\kappa}\Delta - 3\Delta^2 \right) c_1^\perp, \left(\frac{9}{4} + 3\sqrt{3}\Delta + 3\Delta^2 \right) c_1^\perp \right\} + \sum_{n=2}^{\infty} \left(\frac{9}{4} + 3\sqrt{3}\Delta + 3\Delta^2 \right) c_n^\perp, \\ \gamma_2 &:= \min \left\{ \left(\frac{9}{4}\kappa - 6\sqrt{\kappa}\Delta - 3\Delta^2 \right) c_1, \left(\frac{9}{4} + 6\Delta + 3\Delta^2 \right) c_1 \right\} + \sum_{n=2}^{\infty} \left(\frac{9}{4} + 6\Delta + 3\Delta^2 \right) c_n, \text{ and} \\ \gamma_2^\perp &:= \min \left\{ \left(\frac{3}{4}\kappa - 2\sqrt{3\kappa}\Delta - 3\Delta^2 \right) c_1^\perp, \left(\frac{3}{4} + 2\sqrt{3}\Delta + 3\Delta^2 \right) c_1^\perp \right\} + \sum_{n=2}^{\infty} \left(\frac{3}{4} + 2\sqrt{3}\Delta + 3\Delta^2 \right) c_n^\perp.\end{aligned}$$

Finally, we define the coercivity constant $\gamma = \gamma(m, M, \Delta, \kappa(\mathbb{V}))$ as

$$\gamma := \min(\gamma_1 + \gamma_1^\perp, \gamma_2 + \gamma_2^\perp). \quad (6.3)$$

We will investigate the parameter region where γ is positive in §6.6.

With the notation just introduced we can now formulate the main stability result. The proof of Theorem 6.2 is given in §6.2–6.4 and is finalized in §6.4.2.

Theorem 6.2. *Suppose that Assumption A holds. Let $y_h \in \mathcal{S}_{\mathbb{B},h}(m, M, \Delta)$ for constants $0 < m \leq M$ and $0 \leq \Delta \leq \sqrt{\kappa(\mathbb{V})}/2$. Then \mathcal{E}_{ac} is twice Gateaux-differentiable at y_h , and*

$$\langle \delta^2 \mathcal{E}_{ac}(y_h) u_h, u_h \rangle \geq \gamma \| \mathbf{B}^\top \nabla u_h \|_{L^2(\Omega)}^2 \quad \text{for all } u_h \in \mathcal{U}_h,$$

where the coercivity constant $\gamma = \gamma(m, M, \Delta, \kappa(\mathbb{V}))$ is defined in (6.3).

By choosing $\Omega_c = \emptyset$, we obtain the following stability result for the atomistic energy as an immediate corollary.

Corollary 6.3. *Let $y \in \mathcal{Y}$, and define*

$$m := \mu_a(y), \quad M := \max_{b \in \mathcal{B}} \frac{|D_b y|}{|b|}, \quad \text{and} \quad \Delta := \max_{b \in \mathcal{B}} \frac{|\mathbf{B}^{-1} D_b y_h - r_b|}{|b|}.$$

If $\Delta \leq \sqrt{\kappa(\mathbb{V})}/2$, then \mathcal{E}_a is twice Gateaux-differentiable at y , and

$$\langle \delta^2 \mathcal{E}_a(y) u, u \rangle \geq \gamma \| \mathbf{B}^\top \nabla \bar{u} \|_{L^2(\Omega)}^2 \quad \text{for all } u \in \mathcal{U},$$

where $\gamma = \gamma(m, M, \Delta, \kappa(\mathbb{V}))$ is defined in (6.3).

Remark 6.2. The restriction $\Delta \leq \sqrt{\kappa}/2$ is imposed since our proof does not guarantee that γ is a lower bound on the coercivity constant in this case. As a matter of fact, modifying our strategy of proof to include $\Delta > \sqrt{\kappa}/2$ would not in fact give a positive constant γ . This can be seen from the proof of Lemma 6.7. \square

6.2. Proof of the stability result I: reduction to the Bravais lattice case.

6.2.1. *Representation of $\delta^2 \mathcal{E}_{ac}$.* In view of our assumptions on the potential φ , and since $y_h \in \mathcal{S}_{\mathbb{B},h}(m, M, \Delta)$, $m > 0$, it is clear that \mathcal{E}_{ac} is twice differentiable at y_h . The representation (3.4) of the a/c energy \mathcal{E}_{ac} yields the following expression for the second variation $\delta^2 \mathcal{E}_{ac}$:

$$\langle \delta^2 \mathcal{E}_{ac}(y_h) u_h, u_h \rangle = \sum_{b \in \mathcal{B}_a} D_b u_h^\top \phi''(D_b y_h) D_b u_h + \sum_{b \in \mathcal{B}_c} \int_b \nabla_b u_h^\top \phi''(\nabla_b y_h) \nabla_b u_h \, db, \quad (6.4)$$

for all $u_h \in \mathcal{U}_h$, where we recall that $\phi''(r)$ is understood as the Hessian matrix of ϕ . A straightforward calculation shows that ϕ'' can be written, in terms of φ' and φ'' , as

$$\phi''(r) = \varphi''(|r|) \frac{r}{|r|} \otimes \frac{r}{|r|} + \frac{\varphi'(|r|)}{|r|} \left(\mathbb{1} - \frac{r}{|r|} \otimes \frac{r}{|r|} \right). \quad (6.5)$$

We use the fact that $\frac{r}{|r|} \otimes \frac{r}{|r|}$ is the orthogonal projection onto the space $\text{span}\{r\}$ and that $(\mathbb{1} - \frac{r}{|r|} \otimes \frac{r}{|r|})$ is the orthogonal projection onto $\text{span}\{r\}^\perp$, to derive a convenient alternative representation. Note that, using the notation

$$a \times b = (\mathbf{Q}_4 a) \cdot b \quad \text{for } a, b \in \mathbb{R}^2,$$

where \mathbf{Q}_4 denotes a rotation through angle $\pi/2$, we have

$$h^\top (r \otimes r) h = |h \cdot r|^2, \quad \text{while} \quad h^\top (\mathbb{1} - r \otimes r) h = |h|^2 - |r \cdot h|^2 = |h \times r|^2.$$

Hence, we rewrite (6.4) as

$$\begin{aligned} \langle \delta^2 \mathcal{E}_{\text{ac}}(y_h) u_h, u_h \rangle &= \sum_{b \in \mathcal{B}_a} \left\{ \frac{\varphi''(|D_b y_h|)}{|D_b y_h|^2} |D_b y_h \cdot D_b u_h|^2 + \frac{\varphi'(|D_b y_h|)}{|D_b y_h|^3} |D_b y_h \times D_b u_h|^2 \right\} \\ &\quad + \sum_{b \in \mathcal{B}_c} \int_b \left\{ \frac{\varphi''(|\nabla_b y_h|)}{|\nabla_b y_h|^2} |\nabla_b y_h \cdot \nabla_b u_h|^2 + \frac{\varphi'(|\nabla_b y_h|)}{|\nabla_b y_h|^3} |\nabla_b y_h \times \nabla_b u_h|^2 \right\} \text{db}. \end{aligned} \quad (6.6)$$

6.2.2. A general lower bound. Next, we construct a relatively crude lower bound on the Hessian $\delta^2 \mathcal{E}_{\text{ac}}$, which will nevertheless be sufficient to obtain stability estimates in a range of interesting deformations. Our goal is to “localise” the finite differences $D_b u_h$ occurring in the Hessian representation (6.6), and to render the scalar coefficients hexagonally symmetric.

Since $y_h \in \mathcal{S}_{\mathbf{B},h}(m, M, \Delta)$, we can estimate the coefficients in (6.6) by

$$\frac{\varphi''(|D_b y_h|)}{|D_b y_h|^2} \geq C_{|b|} \quad \text{and} \quad \frac{\varphi'(|D_b y_h|)}{|D_b y_h|^3} \geq C_{|b|}^\perp,$$

with similar estimates for $b \in \mathcal{B}_c$, where

$$\begin{aligned} C_\rho &:= \begin{cases} \min_{s \in [m, M]} \frac{\varphi''(\rho s)}{(\rho s)^2}, & \rho = 1, \\ 0 \wedge \min_{s \in [m, M]} \frac{\varphi''(\rho s)}{(\rho s)^2}, & \rho > 1, \end{cases} \quad \text{and} \\ C_\rho^\perp &:= \begin{cases} \min_{s \in [m, M]} \frac{\varphi'(\rho s)}{(\rho s)^3}, & \rho = 1, \\ 0 \wedge \min_{s \in [m, M]} \frac{\varphi'(\rho s)}{(\rho s)^3}, & \rho > 1. \end{cases} \end{aligned} \quad (6.7)$$

We note that these lower bounds do not depend anymore on y_h , and moreover, they were constructed so that all coefficients for non-nearest neighbour bonds are non-positive.

With this notation, we obtain from (6.6) that

$$\begin{aligned} \langle \delta^2 \mathcal{E}_{\text{ac}}(y_h) u_h, u_h \rangle &\geq \sum_{b \in \mathcal{B}_a} \left\{ C_{|b|} |D_b y_h \cdot D_b u_h|^2 + C_{|b|}^\perp |D_b y_h \times D_b u_h|^2 \right\} \\ &\quad + \sum_{b \in \mathcal{B}_c} \int_b \left\{ C_{|b|} |\nabla_b y_h \cdot \nabla_b u_h|^2 + C_{|b|}^\perp |\nabla_b y_h \times \nabla_b u_h|^2 \right\} \text{db}. \end{aligned} \quad (6.8)$$

We now observe that we have constructed the extended mesh \mathcal{T}_h in such a way that in the atomistic region every nearest-neighbour bond $b \in \mathcal{B}_{\text{nn}}$ lies on the edge of a triangle.

As a result we have the identity

$$D_b u_h = \nabla_b u_h(x) \quad \text{for all } x \in \text{int}(b), \text{ for all } b \in \mathcal{B}_a \cap \mathcal{B}_{\text{nn}}, \quad (6.9)$$

which we will use heavily throughout. In particular, this implies that

$$\begin{aligned} & \sum_{b \in \mathcal{B}_{\text{nn}} \cap \mathcal{B}_a} \left\{ C_1 |D_b y_h \cdot D_b u_h|^2 + C_1^\perp |D_b y_h \times D_b u_h|^2 \right\} \\ &= \sum_{b \in \mathcal{B}_{\text{nn}} \cap \mathcal{B}_a} \int_b \left\{ C_1 |D_b y_h \cdot \nabla_b u_h|^2 + C_1^\perp |D_b y_h \times \nabla_b u_h|^2 \right\} \text{db}. \end{aligned} \quad (6.10)$$

Our second observation is that, for $b \in \mathcal{B}_a \setminus \mathcal{B}_{\text{nn}}$ we have $C_{|b|}, C_{|b|}^\perp \leq 0$, and hence we can use (3.2) and Jensen's inequality to estimate

$$\begin{aligned} & \sum_{b \in \mathcal{B}_a \setminus \mathcal{B}_{\text{nn}}} \left\{ C_{|b|} |D_b y_h \cdot D_b u_h|^2 + C_{|b|}^\perp |D_b y_h \times D_b u_h|^2 \right\} \\ &= \sum_{b \in \mathcal{B}_a \setminus \mathcal{B}_{\text{nn}}} \left\{ C_{|b|} |D_b y_h \cdot \int_b \nabla_b u_h \text{db}|^2 + C_{|b|}^\perp |D_b y_h \times \int_b \nabla_b u_h \text{db}|^2 \right\} \\ &\geq \sum_{b \in \mathcal{B}_a \setminus \mathcal{B}_{\text{nn}}} \int_b \left\{ C_{|b|} |D_b y_h \cdot \nabla_b u_h|^2 + C_{|b|}^\perp |D_b y_h \times \nabla_b u_h|^2 \right\} \text{db}. \end{aligned} \quad (6.11)$$

Inserting (6.10) and (6.11) into (6.8) we obtain the following estimate:

$$\begin{aligned} \langle \delta^2 \mathcal{E}_{\text{ac}}(y_h) u_h, u_h \rangle &\geq \sum_{b \in \mathcal{B}_c} \int_b \left\{ C_{|b|} |\nabla_b y_h \cdot \nabla_b u_h|^2 + C_{|b|}^\perp |\nabla_b y_h \times \nabla_b u_h|^2 \right\} \text{db} \\ &\quad + \sum_{b \in \mathcal{B}_a} \int_b \left\{ C_{|b|} |D_b y_h \cdot \nabla_b u_h|^2 + C_{|b|}^\perp |D_b y_h \times \nabla_b u_h|^2 \right\} \text{db} \\ &=: \langle \mathcal{H}(y_h) u_h, u_h \rangle, \end{aligned} \quad (6.12)$$

where $C_{|b|}, C_{|b|}^\perp$ are defined in (6.7).

6.2.3. The perturbation argument. In the next step, we will estimate the effect of replacing $D_r y_h$ and $\nabla_r y_h$ with Br . To that end, the following Lemma will be helpful.

Lemma 6.4. *Suppose that $y_h \in \mathcal{S}_{\mathcal{B},h}(m, M, \Delta)$; then, for all $g \in \mathbb{R}^2, x \in \Omega, r \in \mathbb{R}^2$, and for all possible choices of $\alpha > 0$,*

$$| |\nabla_r y_h(x) \cdot g|^2 - |\text{Br} \cdot g|^2 | \leq \alpha |\text{Br} \cdot g|^2 + (1 + \frac{1}{\alpha}) \Delta^2 |r|^2 |\mathbf{B}^\top g|^2, \quad (6.13)$$

Similarly, for all $g \in \mathbb{R}^2, x \in \mathcal{L}, r \in \mathbb{L}_*$, and $\alpha > 0$, we have

$$| |D_r y_h(x) \cdot g|^2 - |\text{Br} \cdot g|^2 | \leq \alpha |\text{Br} \cdot g|^2 + (1 + \frac{1}{\alpha}) \Delta^2 |r|^2 |\mathbf{B}^\top g|^2. \quad (6.14)$$

The same inequalities remain true if “ \cdot ” is replaced with “ \times ”.

Proof. We verify the bound (6.13) by a straightforward algebraic manipulation (suppressing the argument x), using the fact that $\|\mathbf{B}^{-1}\nabla y_h - \mathbb{1}\| \leq \Delta$:

$$\begin{aligned} \left| |\nabla_r y_h \cdot g|^2 - |\mathbf{B}r \cdot g|^2 \right| &= \left| (|\nabla_r y_h \cdot g| + |\mathbf{B}r \cdot g|) (|\nabla_r y_h \cdot g| - |\mathbf{B}r \cdot g|) \right| \\ &\leq (|\nabla_r y_h - \mathbf{B}r| \cdot |g| + 2|\mathbf{B}r \cdot g|) |\nabla_r y_h - \mathbf{B}r| \cdot |g| \\ &\leq 2|\mathbf{B}r \cdot g| \Delta |r| |\mathbf{B}^\top g| + \Delta^2 |r|^2 |\mathbf{B}^\top g|^2. \end{aligned}$$

Applying a weighted Cauchy inequality $2ab \leq \alpha a^2 + \alpha^{-1}b^2$ we obtain (6.13). The proofs of (6.14), and of the inequalities where “ \cdot ” is replaced with “ \times ” are analogous. \square

Employing Lemma 6.4 to the operator $\mathcal{H}(y_h)$ defined in (6.12), we obtain

$$\begin{aligned} \langle \mathcal{H}(y_h)u_h, u_h \rangle &\geq \langle \mathcal{H}(y_{\mathbf{B}})u_h, u_h \rangle \\ &\quad - \sum_{b \in \mathcal{B}} \int_b \left\{ \alpha_{|b|} |C_{|b|}| |\mathbf{B}r_b \cdot \nabla_b u_h|^2 + \alpha_{|b|}^\perp |C_{|b|}^\perp| |\mathbf{B}r_b \times \nabla_b u_h|^2 \right\} db \quad (6.15) \\ &\quad - \Delta^2 \sum_{b \in \mathbb{B}} |b|^2 \left\{ \left(1 + \frac{1}{\alpha_{|b|}}\right) |C_{|b|}| + \left(1 + \frac{1}{\alpha_{|b|}^\perp}\right) |C_{|b|}^\perp| \right\} \int_b |\mathbf{B}^\top \nabla_b u_h|^2 db, \end{aligned}$$

for all $y_h \in \mathcal{S}_{\mathbf{B},h}(m, M, \Delta)$ and $u_h \in \mathcal{U}_h$. Note that, in the third term, we have estimated the sum over \mathcal{B} below by the sum over \mathbb{B} . We also remark that, for the time being, we retain maximal flexibility in the our choice of the constants $\alpha_{|b|}$ and $\alpha_{|b|}^\perp$. We will (partially) optimize over all possible choices in the last step of our proof.

From here on, to simplify the notation, we define the transformed displacement

$$v_h := \mathbf{B}^\top u_h.$$

This means that we can replace $(\mathbf{B}r_b \cdot \nabla_b u_h)$ by $(r_b \cdot \nabla_b v_h)$, and so forth.

Since the algebraic structure of the first and second term in (6.15) is identical it is natural to combine them. Hence, we define $\tilde{C}_\rho^{(\perp)} := C_\rho^{(\perp)} - \alpha_\rho^{(\perp)} |C_\rho^{(\perp)}|$, and

$$\begin{aligned} \langle \tilde{\mathcal{H}}u_h, u_h \rangle &:= \sum_{b \in \mathcal{B}} \int_b \left\{ \tilde{C}_{|b|} |r_b \cdot \nabla_b v_h|^2 + \tilde{C}_{|b|}^\perp |r_b \times \nabla_b v_h|^2 \right\} db, \quad \text{and} \quad (6.16) \\ \langle \tilde{\mathcal{L}}u_h, u_h \rangle &:= \sum_{b \in \mathbb{B}} |b|^2 \left\{ \left(1 + \frac{1}{\alpha_{|b|}}\right) |C_{|b|}| + \left(1 + \frac{1}{\alpha_{|b|}^\perp}\right) |C_{|b|}^\perp| \right\} \int_b |\nabla_b v_h|^2 db. \end{aligned}$$

Here and throughout the superscript (\perp) , e.g., in $C_\rho^{(\perp)}$, refers to both C_ρ or C_ρ^\perp . Employing the periodic bond-density lemma, the decomposition of the triangular lattice described in Lemma 2.1, and the definition of the constants $c_n^{(\perp)} := \ell_n^4 C_{\ell_n}^{(\perp)}$, the operator $\tilde{\mathcal{L}}$ can be rewritten as follows:

$$\langle \tilde{\mathcal{L}}u_h, u_h \rangle = (\tilde{L} + \tilde{L}^\perp) \|\nabla v_h\|_{L^2(\Omega)}^2, \quad \text{where} \quad \begin{cases} \tilde{L} = 3 \sum_{n=1}^{\infty} \left(1 + \frac{1}{\alpha_{\ell_n}}\right) |c_n|, & \text{and} \\ \tilde{L}^\perp = 3 \sum_{n=1}^{\infty} \left(1 + \frac{1}{\alpha_{\ell_n}^\perp}\right) |c_n^\perp|. \end{cases} \quad (6.17)$$

In summary so far, we have obtained that, if $y_h \in \mathcal{S}_{\mathbf{B},h}(m, M, \Delta)$, then

$$\langle \delta^2 \mathcal{E}_{\text{ac}}(y_h)u_h, u_h \rangle \geq \langle \tilde{\mathcal{H}}u_h, u_h \rangle - \Delta^2 (\tilde{L} + \tilde{L}^\perp) \|\nabla v_h\|_{L^2}^2 \quad \forall u_h \in \mathcal{U}_h, \quad (6.18)$$

where $\tilde{\mathcal{H}}$ and \tilde{L} are defined in (6.17).

6.2.4. *Extension to \mathbb{B} .* In the next step, we use of the extension operator (see §4.1) and the definition of the stability index $\kappa := \kappa(\mathbb{V})$ (see §6.1.2).

Distinguishing whether \tilde{C}_1 is positive or negative, using the definition of κ in the first case, we obtain

$$\begin{aligned} \sum_{b \in \mathcal{B}_{\text{nn}}} \tilde{C}_1 |r_b \cdot D_b v_h|^2 &\geq \kappa \sum_{b \in \mathbb{B}_{\text{nn}}} \tilde{C}_1 |r_b \cdot D_b v_h|^2, & \text{if } \tilde{C}_1 \geq 0, \quad \text{and} \\ \sum_{b \in \mathcal{B}_{\text{nn}}} \tilde{C}_1 |r_b \cdot D_b v_h|^2 &\geq \sum_{b \in \mathbb{B}_{\text{nn}}} \tilde{C}_1 |r_b \cdot D_b v_h|^2, & \text{if } \tilde{C}_1 \leq 0, \end{aligned}$$

which, combined, can be written as

$$\sum_{b \in \mathcal{B}_{\text{nn}}} C_1 \int_b |r_b \cdot \nabla_b v_h|^2 \, \text{db} \geq \min(\tilde{C}_1, \kappa \tilde{C}_1) \sum_{b \in \mathbb{B}_{\text{nn}}} \int_b |r_b \cdot \nabla_b v_h|^2 \, \text{db}, \quad (6.19)$$

For the ‘‘perpendicular’’ nearest-neighbour terms the same argument (we now need to use (6.2) with $u = \mathbf{Q}_4^\top \mathbf{B}^\top u_h = \mathbf{Q}_4^\top v_h$), yields

$$\sum_{b \in \mathcal{B}_{\text{nn}}} C_1^\perp \int_b |r_b \times \nabla_b v_h|^2 \, \text{db} \geq \min(\tilde{C}_1^\perp, \kappa \tilde{C}_1^\perp) \sum_{b \in \mathbb{B}_{\text{nn}}} \int_b |r_b \times \nabla_b v_h|^2 \, \text{db}, \quad (6.20)$$

Since all contributions from non-nearest-neighbours to the operator $\tilde{\mathcal{H}}$ are non-positive, we can estimate

$$\begin{aligned} \sum_{b \in \mathcal{B} \setminus \mathcal{B}_{\text{nn}}} \int_b C_{|b|} |r_b \cdot \nabla_b v_h|^2 \, \text{db} &\geq \sum_{b \in \mathbb{B} \setminus \mathbb{B}_{\text{nn}}} \int_b C_{|b|} |r_b \cdot \nabla_b v_h|^2 \, \text{db}, \quad \text{and} \\ \sum_{b \in \mathcal{B} \setminus \mathcal{B}_{\text{nn}}} \int_b C_{|b|}^\perp |r_b \times \nabla_b v_h|^2 \, \text{db} &\geq \sum_{b \in \mathbb{B} \setminus \mathbb{B}_{\text{nn}}} \int_b C_{|b|}^\perp |r_b \times \nabla_b v_h|^2 \, \text{db}. \end{aligned}$$

Hence, defining the constants (recall that $\tilde{C}_\rho^{(\perp)} = C_\rho^{(\perp)} - \alpha_\rho^{(\perp)} |C_\rho^{(\perp)}|$)

$$\bar{C}_\rho^{(\perp)} := \begin{cases} \min(\tilde{C}_\rho^{(\perp)}, \kappa \tilde{C}_\rho^{(\perp)}), & \rho = 1, \\ \tilde{C}_\rho^{(\perp)}, & \rho > 1, \end{cases} \quad (6.21)$$

we arrive at (recall that $v_h = \mathbf{B}^\top u_h$)

$$\begin{aligned} \langle \tilde{\mathcal{H}} u_h, u_h \rangle &\geq \sum_{b \in \mathbb{B}} \int_b \left\{ \bar{C}_{|b|} |r_b \cdot \nabla_b v_h|^2 + \bar{C}_{|b|}^\perp |r_b \times \nabla_b v_h|^2 \right\} \, \text{db} \\ &=: \langle \bar{\mathcal{H}} u_h, u_h \rangle \quad \forall u_h \in \mathcal{U}_h. \end{aligned} \quad (6.22)$$

6.3. Proof of the stability result II: stability of the homogeneous lattice. Combining (6.22) and (6.18), we have shown so that that, for $y_h \in \mathcal{S}_{\mathbb{B},h}(m, M, \Delta)$,

$$\langle \delta^2 \mathcal{E}_{\text{ac}}(y_h) u_h, u_h \rangle \geq \langle \bar{\mathcal{H}} u_h, u_h \rangle - \Delta^2 (\tilde{L} + \tilde{L}^\perp) \|\mathbf{B}^\top \nabla u_h\|_{L^2(\Omega)}^2 \quad \forall u_h \in \mathcal{U}_h, \quad (6.23)$$

where the operator $\bar{\mathcal{H}}$ depends only on the parameters m, M, Δ , and $\kappa(\mathbb{V})$ (and, strictly speaking, also on \mathbb{B} through the identification $v_h = \mathbf{B}^\top u_h$). In the present section, we will prove the following estimate for the operator $\bar{\mathcal{H}}$.

Lemma 6.5. *The operator $\bar{\mathcal{H}}$ satisfies the lower bound*

$$\langle \bar{\mathcal{H}} u_h, u_h \rangle \geq \bar{\gamma} \|\mathbf{B}^\top \nabla u_h\|_{L^2(\Omega)}^2 \quad \forall u_h \in \mathcal{U}_h, \quad (6.24)$$

where $\bar{\gamma} := \min(\frac{3}{4}\bar{c} + \frac{9}{4}\bar{c}^\perp, \frac{3}{4}\bar{c} + \frac{9}{4}\bar{c}^\perp)$ and where $\bar{c}^{(\perp)} := \sum_{n=1}^{\infty} \ell_n^4 \bar{C}_{\ell_n}^{(\perp)}$.

Remark 6.3. The estimate (6.24) is sharp in the sense that, if $\mathcal{T}_h = \mathcal{T}_a$, then

$$\lim_{N \rightarrow \infty} \inf_{u \in \mathcal{U}} \frac{\langle \bar{\mathcal{H}}_B u, u \rangle}{\|\mathbf{B}^\top \nabla \bar{u}\|^2} = \bar{\gamma}. \quad (6.25)$$

This statement follows immediately from the proof of Lemma 6.5. \square

6.3.1. *Rewriting $\bar{\mathcal{H}}$.* Application of the bond-density lemma to the definition of $\bar{\mathcal{H}}$ in (6.22) yields

$$\begin{aligned} \langle \bar{\mathcal{H}} u_h, u_h \rangle &= \sum_{T \in \mathcal{T}_h} |T| \left\{ \sum_{r \in \mathbb{L}_*} \bar{C}_{|r|} |r \cdot \nabla_r v_h|_T|^2 + \sum_{r \in \mathbb{L}_*} \bar{C}_{|r|}^\perp |r \times \nabla_r v_h|_T|^2 \right\} \\ &=: \sum_{T \in \mathcal{T}_h} |T| \{ H_T[v_h] + H_T^\perp[v_h] \}. \end{aligned} \quad (6.26)$$

6.3.2. *Computation of $H_T[v_h]$ and $H_T^\perp[v_h]$.* Let $\mathbf{G} := \nabla v_h = \mathbf{B}^\top \nabla u_h$, and $\mathbf{G}_T := \nabla v_h|_T$, then we can rewrite $H_T[v_h]$, using Lemma 2.1, in the form

$$H_T[u_h] = \sum_{r \in \mathbb{L}_*} \bar{C}_{|r|} [r^\top \mathbf{G}_T r]^2 = \sum_{n=1}^{\infty} \bar{C}_{\ell_n} \sum_{j=1}^6 [(\mathbf{Q}_4^j r_n)^\top \mathbf{G}_T (\mathbf{Q}_4^j r_n)]^2. \quad (6.27)$$

Exploiting the hexagonal symmetry of the inner sum, using Lemma 2.2, (2.2), and recalling the definition of \bar{c} from Lemma 6.5, we obtain

$$H_T[v_h] = \{ \sum_{n=1}^{\infty} \ell_n^4 \bar{C}_{\ell_n} \} |\mathbf{G}_T|_{\text{el}}^2 = \bar{c} |\mathbf{G}_T|_{\text{el}}^2, \quad (6.28)$$

where $|\mathbf{G}|_{\text{el}} := \frac{3}{2} |\mathbf{G}^{\text{sym}}|^2 + \frac{3}{4} |\text{tr} \mathbf{G}|^2$ (cf. (2.2)).

Replacing r with $\mathbf{Q}_4 r$ in the above computations, we obtain, moreover, that

$$H_T^\perp[v_h] = \{ \sum_{n=1}^{\infty} \ell_n^4 \bar{C}_{\ell_n}^\perp \} |\mathbf{Q}_4 \mathbf{G}_T|_{\text{el}}^2 = \bar{c}^\perp |\mathbf{Q}_4 \mathbf{G}_T|_{\text{el}}^2. \quad (6.29)$$

6.3.3. *Proof of Lemma 6.5.* Combining (6.26), (6.28), and (6.29), we obtain

$$\langle \bar{\mathcal{H}} u_h, u_h \rangle = \sum_{T \in \mathcal{T}_h} |T| \left\{ \bar{c} |\mathbf{G}_T|_{\text{el}}^2 + \bar{c}^\perp |\mathbf{Q}_4 \mathbf{G}_T|_{\text{el}}^2 \right\} =: \int_{\Omega} \mathbb{C}_{i\alpha}^{j\beta} \mathbf{G}_{i\alpha} \mathbf{G}_{j\beta} \, dV, \quad (6.30)$$

using summation convention, for some fourth order tensor \mathbb{C} , implicitly defined through this relation. Note, in particular, that (6.30) extends the definition of $\bar{\mathcal{H}}$ to all of $\mathbf{H}_{\#}^1(\Omega)^2$. In the following lemma we compute a more explicit representation of \mathbb{C} .

Lemma 6.6. *Let $|\cdot|_{\text{el}}$ be defined as in (2.2), and let $\mathbf{G} \in \mathbb{R}^{2 \times 2}$, then*

$$\begin{aligned} |\mathbf{G}|_{\text{el}}^2 &= \frac{3}{4} |\mathbf{G}|^2 + \frac{3}{2} (\mathbf{G}_{11} + \mathbf{G}_{22})^2 - \frac{3}{2} \det \mathbf{G}, \quad \text{and} \\ |\mathbf{Q}_4 \mathbf{G}|_{\text{el}}^2 &= \frac{3}{4} |\mathbf{G}|^2 + \frac{3}{2} (\mathbf{G}_{12} - \mathbf{G}_{21})^2 - \frac{3}{2} \det \mathbf{G}. \end{aligned}$$

In particular, we have, for $d = \frac{3}{2}(\bar{c} + \bar{c}^\perp)$

$$\mathbb{C}_{i\alpha}^{j\beta} \mathbf{G}_{i\alpha} \mathbf{G}_{j\beta} = \frac{3}{4} (\bar{c} + \bar{c}^\perp) |\mathbf{G}|^2 + \frac{3}{2} \bar{c} |\mathbf{G}_{11} + \mathbf{G}_{22}|^2 + \frac{3}{2} \bar{c}^\perp |\mathbf{G}_{12} - \mathbf{G}_{21}|^2 - d \det \mathbf{G}. \quad (6.31)$$

Proof. The first identity can be verified by a straightforward algebraic manipulation. The second identity is an immediate consequence of the first. The third identity follows by combining the first two. \square

Using identity (6.31) we can now prove Lemma 6.5.

Proof of Lemma 6.5. The Legendre–Hadamard condition (see, e.g., [10]) states that

$$\inf_{\substack{v \in \mathbf{H}_{\#}^1(\Omega)^2 \\ \|\nabla v\|_{L^2} = 1}} \int_{\Omega} \mathbb{C}_{i\alpha}^{j\beta} (\nabla v)_{i\alpha} (\nabla v)_{j\beta} \, dV = \min_{\substack{w, k \in \mathbb{R}^2 \\ |w|=|k|=1}} \mathbb{C}_{i\alpha}^{j\beta} w_i w_j k_\alpha k_\beta =: \bar{\gamma}.$$

Thus, we have reduced the task to testing \mathbb{C} with rank-1 matrices $w \otimes k$. Using the definition of \mathbb{C} , identity (6.31), and noting that $\det(w \otimes k) = 0$, we obtain

$$\mathbb{C}_{i\alpha}^{j\beta} w_i w_j k_\alpha k_\beta = \frac{3}{4}(\bar{c} + \bar{c}^\perp) |w|^2 |k|^2 + \frac{3}{2} \bar{c} (w \cdot k)^2 + \frac{3}{2} \bar{c}^\perp (w \times k)^2. \quad (6.32)$$

If $\bar{c} \geq \bar{c}^\perp$ then (6.32) is minimised for $w \perp k$, and hence

$$\bar{\gamma} = \frac{3}{4}(\bar{c} + \bar{c}^\perp) + \frac{3}{2} \bar{c}^\perp = \frac{3}{4} \bar{c} + \frac{9}{4} \bar{c}^\perp.$$

If $\bar{c} \leq \bar{c}^\perp$ then (6.32) is minimised for $w = k$, and hence

$$\bar{\gamma} = \frac{3}{4}(\bar{c} + \bar{c}^\perp) + \frac{3}{2} \bar{c} = \frac{9}{4} \bar{c} + \frac{3}{4} \bar{c}^\perp.$$

Combining the two cases gives the stated result. \square

6.4. Proof of the stability result III: optimizing the parameters. Combining Lemma 6.5 with (6.23), we obtain the stability estimate

$$\langle \delta^2 \mathcal{E}_{\text{ac}}(y_h) u_h, u_h \rangle \geq \gamma \|\mathbf{B}^\top \nabla u_h\|_{L^2}^2, \quad \text{where } \gamma = \bar{\gamma} - \Delta^2(\tilde{L} + \tilde{L}^\perp), \quad (6.33)$$

for all $y_h \in \mathcal{S}_{\mathbf{B},h}(m, M, \Delta)$ and $u_h \in \mathcal{U}_h$. The lower bound γ still depends on the free parameters $\alpha_{\ell_n}, \alpha_{\ell_n}^\perp > 0$. Ideally, we would like to optimize γ over all possible choices, however, the double-minimization problem in the definition of γ makes this impractical. We will choose the parameters so that they are optimal in the case, which is the most important in our numerical computations. A more detailed analysis would reveal, in fact, that our choice fairly close to optimal.

For the following discussion, recall the definition of c_n, c_n^\perp from (6.1) and, with some abuse of notation, let $\alpha_n^{(\perp)} := \alpha_{\ell_n}^{(\perp)}$.

6.4.1. Optimising for a special case. We begin by noting that γ can be rewritten in the form (cf. (6.3))

$$\gamma = \min(\gamma_1 + \gamma_1^\perp, \gamma_2 + \gamma_2^\perp), \quad \text{where} \quad \begin{cases} \gamma_1 = \frac{3}{4} \bar{c} - \Delta^2 \tilde{L}, \\ \gamma_1^\perp = \frac{9}{4} \bar{c}^\perp - \Delta^2 \tilde{L}^\perp, \\ \gamma_2 = \frac{9}{4} \bar{c} - \Delta^2 \tilde{L}, \text{ and} \\ \gamma_2^\perp = \frac{3}{4} \bar{c}^\perp - \Delta^2 \tilde{L}^\perp. \end{cases} \quad (6.34)$$

Near global minima of \mathcal{E}_{ac} (over Bravais lattices) we expect that $c_1 > 0$ and $c_1^\perp \approx 0$, which suggests to optimise the parameters $\alpha_n^{(\perp)}$ for the case $\gamma = \gamma_1 + \gamma_1^\perp$.

Recalling from (6.17) the definition of \tilde{L} , and recalling that $c_n \leq 0$ for $n \geq 2$, we can rewrite γ_1 in the form

$$\begin{aligned} \gamma_1 &= \left(\min \left\{ \frac{3}{4}(c_1 - \alpha_1|c_1|), \frac{3}{4}\kappa(c_1 - \alpha_1|c_1|) \right\} - 3\left(1 + \frac{1}{\alpha_1}\right)\Delta^2|c_1| \right) \\ &\quad + \sum_{n=2}^{\infty} \left(\frac{3}{4} + \frac{3}{4}\alpha_n + 3\left(1 + \frac{1}{\alpha_n}\right)\Delta^2 \right) c_n \\ &=: \psi_1(\alpha_1) + \sum_{n=2}^{\infty} \left(\frac{3}{4} + \frac{3}{4}\alpha_n + 3\left(1 + \frac{1}{\alpha_n}\right)\Delta^2 \right) c_n. \end{aligned} \quad (6.35)$$

We see immediately that $\alpha_n = 2\Delta$ is optimal for $n \geq 2$. For $n = 1$, the situation is more complicated and we treat it separately in the following lemma.

Lemma 6.7. *Suppose that $\Delta \leq \sqrt{\kappa}/2$; then*

$$\max_{\alpha_1 > 0} \psi_1(\alpha_1) = \min \left\{ \left(\frac{3}{4}\kappa - 3\sqrt{\kappa}\Delta - 3\Delta^2 \right) c_1, \left(\frac{3}{4} + 3\Delta + 3\Delta^2 \right) c_1 \right\}, \quad (6.36)$$

which is attained for $\alpha_1 = 2\Delta/\sqrt{\kappa}$ if $c_1 > 0$ and for $\alpha_1 = 2\Delta$ if $c_1 \leq 0$.

Proof. Case 1: $c_1 \leq 0$. Assume, first, that $c_1 \leq 0$. In this case it is easy to see that

$$\psi_1(\alpha_1) = \left[\frac{3}{4}(1 + \alpha_1) + 3\left(1 + \frac{1}{\alpha_1}\right)\Delta^2 \right] c_1.$$

Hence, $\alpha_1 = 2\Delta$ is optimal, and $\psi_1(2\Delta) = \left[\frac{3}{4} + 3\Delta + 3\Delta^2 \right] c_1$.

Case 2: $c_1 > 0$. We minimize ψ_1 separately over the intervals $(1, \infty)$ and $(0, 1]$. Suppose, first, that $\alpha_1 > 1$, then

$$\psi_1(\alpha_1) = \left[\frac{3}{4}(1 - \alpha_1) - 3\left(1 + \frac{1}{\alpha_1}\right)\Delta^2 \right] c_1.$$

This is a strictly concave expression, which is maximised on $[1, \infty)$ at $\alpha_1 = \max(1, 2\Delta) = 1$, due to the assumption that $\Delta \leq \sqrt{\kappa}/2 \leq 1/2$, and hence reduces to the next case.

On the interval $(0, 1]$ we have

$$\psi_1(\alpha_1) = \left[\frac{3}{4}\kappa(1 - \alpha_1) - 3\left(1 + \frac{1}{\alpha_1}\right)\Delta^2 \right] c_1,$$

which is maximised on $(0, 1]$ for $\alpha_1 = \min(1, 2\Delta/\sqrt{\kappa}) = 2\Delta/\kappa$, and we have

$$\psi_1(2\Delta/\sqrt{\kappa}) = \left[\frac{3}{4}\kappa - 3\sqrt{\kappa}\Delta - 3\Delta^2 \right] c_1.$$

To see that (6.36) holds, it suffices to note that the first argument is automatically selected if $c_1 > 0$ and the second argument if $c_1 \leq 0$. \square

If we insert $\alpha_n = 2\Delta$ for $n \geq 2$, and the value for α_1 for which (6.36) is attained, into (6.35), then we obtain

$$\begin{aligned} \gamma_1 &= \min \left\{ \left(\frac{3}{4}\kappa - 3\sqrt{\kappa}\Delta - 3\Delta^2 \right) c_1, \left(\frac{3}{4} + 3\Delta + 3\Delta^2 \right) c_1 \right\} \\ &\quad + \sum_{n=2}^{\infty} \left(\frac{3}{4} + 3\Delta + 3\Delta^2 \right) c_n. \end{aligned} \quad (6.37)$$

Using analogous arguments, we choose $\alpha_n^\perp = 2\Delta/\sqrt{3}$ for $n \geq 2$ and for $n = 1$ if $c_1^\perp \leq 0$; and $\alpha_1^\perp = 2\Delta/\sqrt{3\kappa}$ if $c_1^\perp > 0$ (note that under the assumption $\Delta \leq \sqrt{\kappa}/2$ we also get $\alpha_1^\perp \leq 1$). Inserting these values into γ_1^\perp , we obtain

$$\begin{aligned} \gamma_1^\perp &= \min \left\{ \left(\frac{9}{4}\kappa - 3\sqrt{3\kappa}\Delta - 3\Delta^2 \right) c_1^\perp, \left(\frac{9}{4} + 3\sqrt{3}\Delta + 3\Delta^2 \right) c_1^\perp \right\} \\ &\quad + \sum_{n=2}^{\infty} \left(\frac{9}{4} + 3\sqrt{3}\Delta + 3\Delta^2 \right) c_n^\perp. \end{aligned} \quad (6.38)$$

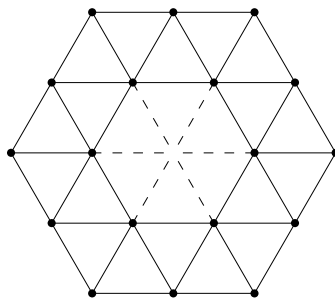


FIGURE 6. Neighbourhood of a void to illustrate the proof of Theorem 6.8. The bonds \mathcal{B}_1 are dashed, the bonds \mathcal{B}_2 are solid.

We observe that (6.37) and (6.38) agree with the definitions given in §6.1.3.

6.4.2. *Concluding the proof of Theorem 6.2.* In the previous paragraph we have fixed the values for $\alpha_n^{(\perp)}$, and we have seen that the resulting values for γ_1 and γ_1^\perp agree with the definitions in §6.1.3. A tedious but straightforward computation, for which we skip the details, shows that, if γ_2, γ_2^\perp are defined by (6.34), then the above choices for $\alpha_n^{(\perp)}$ yield precisely the formulae given in §6.1.3 again. Combining these observations with (6.33) and (6.34), we obtain the statement of Theorem 6.2.

6.5. **Stability index of separated vacancies.** In Table 1 we have provided numerical (i.e., non-rigorous) estimates for vacancy stability indices. In this section, we prove that the extension operator E can be defined in such a way that $\kappa(\mathbb{V}) \geq 2/7$ if \mathbb{V} consists only of single vacancy sites, which are separated by a short distance. More precisely, we will assume in this section that \mathbb{V} satisfies the separation condition

$$x_1 \in \mathbb{V}, x_2 \in \mathbb{V}^\# \setminus \{x_1\} \quad \Rightarrow \quad |x_1 - x_2| \geq 4. \quad (6.39)$$

Theorem 6.8. *Suppose that \mathbb{V} satisfies the separation condition (6.39), then $\kappa(\mathbb{V}) \geq \frac{2}{7}$.*

Proof. We define an alternative extension operator \tilde{E} as follows (cf. Figure 6):

$$(\tilde{E}w)(x) := \frac{1}{6} \sum_{r \in \mathbb{L}_{\text{nn}}} w(x+r) \quad \forall x \in \mathbb{V}^\#. \quad (6.40)$$

Using the notation introduced in Figure 6 we aim to prove that

$$\sum_{b \in \mathcal{B}_2} |r_b \cdot D_b u|^2 \geq \kappa \sum_{b \in \mathcal{B}_1 \cup \mathcal{B}_2} |r_b \cdot D_b \tilde{E}u|^2 \quad \forall u \in \mathcal{U}, \quad (6.41)$$

for $\kappa = \frac{2}{7}$.

Before we prove (6.41), let us discuss why this establishes the result. Firstly, (6.41) and the separation condition (6.39) imply immediately that

$$\sum_{b \in \mathcal{B}} |r_b \cdot D_b u|^2 \geq \kappa \sum_{b \in \mathbb{B}} |r_b \cdot D_b \tilde{E}u|^2 \quad \forall u \in \mathcal{U}.$$

Since the actual extension operator minimizes the right-hand side, we can replace \tilde{E} with E , and hence obtain the result.

To prove (6.41), we begin by noting that 18 vertices of \mathcal{T}_h are involved in (6.41), which correspond to 36 degrees of freedom for a transformed displacement u . We construct a basis of the space of these degrees of freedom $\{w^{(k,j)} : -2 \leq k \leq 3, 1 \leq j \leq 6\}$ as follows: Firstly, we require that all basis functions satisfy the symmetry

$$w^{(k,j)}(\mathbf{Q}_6\xi) = e^{ik \arg(\xi)} \mathbf{Q}_6 w^{(k,j)}(\xi). \quad (6.42)$$

Secondly, we specify the nodal values

$$\begin{aligned} w^{(k,1)}(1,0) &= (-\sqrt{3}, 0), \\ w^{(k,2)}(1,0) &= (0, 3i), \\ w^{(k,3)}\left(\frac{3}{2}, \frac{\sqrt{3}}{2}\right) &= 3 e^{ik \frac{\pi}{6}} \left(\cos \frac{\pi}{6}, -\sin \frac{\pi}{6}\right), \\ w^{(k,4)}\left(\frac{3}{2}, \frac{\sqrt{3}}{2}\right) &= -\sqrt{3}i e^{ik \frac{\pi}{6}} \left(\sin \frac{\pi}{6}, \cos \frac{\pi}{6}\right), \\ w^{(k,5)}(2,0) &= (\sqrt{3}, 0), \\ w^{(k,6)}(2,0) &= (0, 3i). \end{aligned}$$

Finally, for all vertices ξ where $w^{(k,j)}(\xi)$ is still undefined we set $w^{(k,j)}(\xi) = (0, 0)$.

Consider the two quadratic forms

$$a[u] = \sum_{b \in \mathcal{B}_2} |r_b \cdot D_b u|^2, \quad \text{and} \quad b[u] = \sum_{b \in \mathcal{B}_1 \cup \mathcal{B}_2} |r_b \cdot D_b u|^2.$$

It turns out that the corresponding ‘‘stiffness matrices’’ with respect to the basis defined above have a block-diagonal structure, that is, if $u = \sum_{k=-2}^3 \sum_{j=1}^6 U_{k,j} w^{(k,j)}$ then

$$a[u] = \sum_{k=-2}^3 \sum_{j,j'=1}^6 A_{j,j'}^{(k)} U_{k,j} U_{k,j'} \quad \text{and} \quad b[u] = \sum_{k=-2}^3 \sum_{j,j'=1}^6 B_{j,j'}^{(k)} U_{k,j} U_{k,j'}$$

with the blocks

$$A^{(k)} = \begin{pmatrix} 3 + (1 + \cos(\frac{k\pi}{3})) & \sin(\frac{k\pi}{3}) & \cos(\frac{k\pi}{6}) & \sin(\frac{k\pi}{6}) & 2 & 0 \\ \sin(\frac{k\pi}{3}) & 3 - (1 + \cos(\frac{k\pi}{3})) & -\sin(\frac{k\pi}{6}) & \cos(\frac{k\pi}{6}) & 0 & 0 \\ \cos(\frac{k\pi}{6}) & -\sin(\frac{k\pi}{6}) & 1 & 0 & 0 & 0 \\ \sin(\frac{k\pi}{6}) & \cos(\frac{k\pi}{6}) & 0 & 5 & 2 \sin(\frac{k\pi}{6}) & 2 \cos(\frac{k\pi}{6}) \\ 2 & 0 & 0 & 2 \sin(\frac{k\pi}{6}) & 3 & 0 \\ 0 & 0 & 0 & 2 \cos(\frac{k\pi}{6}) & 0 & 1 \end{pmatrix}$$

and

$$B^{(k)} = A^{(k)} + \begin{pmatrix} 2 - \frac{1}{2}(1 - (-1)^k)(1 + \cos(\frac{k\pi}{3})) & \frac{1}{6}(1 - (-1)^k) \sin(\frac{k\pi}{3}) & 0 & 0 & 0 & 0 \\ \frac{1}{6}(1 - (-1)^k) \sin(\frac{k\pi}{3}) & \frac{1}{18}(1 - (-1)^k)(1 + \cos(\frac{k\pi}{3})) & 0 & 0 & 0 & 0 \\ 0 & 0 & 0 & 0 & 0 & 0 \\ 0 & 0 & 0 & 0 & 0 & 0 \\ 0 & 0 & 0 & 0 & 0 & 0 \\ 0 & 0 & 0 & 0 & 0 & 0 \end{pmatrix}$$

We need to find a maximal positive κ such that $A^{(k)} \geq \kappa B^{(k)}$, in the sense of Hermitian matrices, for all k . Such a constant exists if $\text{Ker} A^{(k)} \subset \text{Ker} B^{(k)}$ for all k . An explicit constant κ can be obtained if we can find minimal constants $\lambda^{(k)}$ such that, for some vector $v^{(k)} \notin \text{Ker} A^{(k)}$,

$$A^{(k)} v^{(k)} = \lambda^{(k)} (B^{(k)} - A^{(k)}) v^{(k)}.$$

In that case we would obtain $\kappa = \lambda/(1 + \lambda)$, where $\lambda = \min_k \lambda^{(k)}$. We perform these calculations separately for $k = 0, \pm 1, \pm 2, 3$.

Case $k = 0$: $\text{Ker}(A^{(0)}) = \text{Ker}(B^{(0)}) = \text{span}\{v_0\}$, with $v_0 = (0, 1, 0, -1, 0, 2)$; therefore we add $v_0 \otimes v_0$ to $A^{(0)}$ to make it strictly positive definite and solve

$$0 = \det(v_0 \otimes v_0 + A^{(0)} - \lambda(B^{(0)} - A^{(0)})) = 72(4 - 3\lambda),$$

to obtain that $\lambda^{(0)} = \frac{4}{3}$.

Case $k = \pm 1$: $\text{Ker}(A^{(\pm 1)}) = \text{Ker}(B^{(\pm 1)}) = \text{span}\{v_0\}$, with $v_0 = (\mp 1, \sqrt{3}, \pm\sqrt{3}, -1, \pm 1, \sqrt{3})$; therefore we add $v_0 \otimes v_0$ to $A^{(\pm 1)}$ and solve

$$0 = \det(v_0 \otimes v_0 + A^{(\pm 1)} - \lambda(B^{(\pm 1)} - A^{(\pm 1)})) = 24(24 - 5\lambda),$$

from where we find $\lambda^{(\pm 1)} = \frac{24}{5}$.

Case $k = \pm 2$: In this case $\text{Ker}A^{(\pm 2)} = \text{Ker}B^{(\pm 2)} = \{0\}$; hence we solve

$$0 = \det(A^{(2)} - \lambda(B^{(2)} - A^{(2)})) = 6(2 - 5\lambda),$$

to obtain that $\lambda^{(\pm 2)} = \frac{2}{5}$.

Case $k = 3$: In this case $\text{Ker}A^{(3)} = \text{Ker}B^{(3)} = \{0\}$; hence we solve

$$0 = \det(A^{(3)} - \lambda(B^{(3)} - A^{(3)})) = 4(9 - 11\lambda),$$

to obtain that $\lambda^{(3)} = \frac{9}{11}$.

Conclusion: The smallest of the eigenvalues is given by

$$\lambda = \min_{k=-2, \dots, 3} \lambda^{(k)} = \frac{2}{5},$$

which gives the coercivity constant $\kappa = \frac{\lambda}{1+\lambda} = \frac{2}{7}$. \square

6.6. Sharpness of the stability estimate. To understand whether Theorem 6.2 is sharp, we consider a homogeneous deformation $y_h = y_{\mathbf{B}}$ and a Lennard-Jones or Morse type interaction potential: we assume that there exists $s_{\text{turn}} > 1$ (a turning point) such that

$$\begin{aligned} \varphi'(s) &\leq 0 \text{ for } s \in (0, 1), & \varphi'(s) &\geq 0 \text{ for } s \in (1, +\infty), \\ \varphi''(s) &> 0 \text{ for } s \in (0, s_{\text{turn}}), & \text{and } \varphi''(s) &\leq 0 \text{ for } s \in (s_{\text{turn}}, +\infty). \end{aligned} \quad (6.43)$$

These conditions are satisfied by the original Lennard-Jones potential, and by the Morse potential.

If we also assume that $\mathbb{V} = \emptyset$, then (6.12) is the last approximation that we made, that is, all subsequent calculations are sharp. In particular, for the case $\mathbf{B} = m\mathbb{1}$ our main approximation was to drop the non-negative non-nearest neighbour terms

$$\sum_{b \in \mathcal{B}_c \setminus \mathcal{B}_{\text{nn}}} \frac{\varphi'(|\mathbf{B}r_b|)}{|\mathbf{B}r_b|^3} |\mathbf{B}r_b \times \nabla_b u_h|^2 + \sum_{b \in \mathcal{B}_a \setminus \mathcal{B}_{\text{nn}}} \frac{\varphi'(|\mathbf{B}r_b|)}{|\mathbf{B}r_b|^3} \int_b |\mathbf{B}r_b \times D_b u_h|^2 \text{ db}.$$

Suppose for a moment that the atomistic region is empty then we could have kept the terms in the analysis without any major modifications and would have obtained the coercivity constant

$$\tilde{\gamma} = \min\left(\frac{3}{4}c + \frac{9}{4}\tilde{c}^\perp, \frac{9}{4}c + \frac{3}{4}\tilde{c}^\perp\right), \quad \text{where } \tilde{c}^\perp = \sum_{n=1}^{\infty} \varphi'(m\ell_n)\ell_n.$$

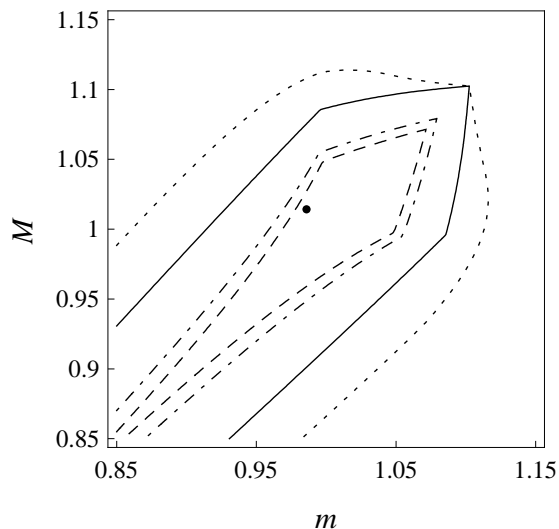


FIGURE 7. Regions of stability in (m, M) parameter space. The dotted line is the boundary of the maximal region in (m, M) space such that $y_{\mathbf{B}}$ is stable in the full atomistic model for all \mathbf{B} with singular values $0 < m \leq M$. The full line is the zero level set of $\gamma(m, M, 0, \emptyset)$. The dot-dashed and the dashed lines are the zero level sets of $\gamma(m, M, 0, 2/7)$ and $\gamma(m, M, 0.02, 2/7)$ respectively, which corresponds to a vacancy defect. The point on the graph corresponds to m and M computed from the computed solution as described in §8.1.

We are interested in the case when $m > 1$ so that \mathbf{B} approaches the region of instability. In that case we have

$$\tilde{\gamma} = \gamma + \frac{3}{4} \sum_{n=2}^{\infty} \varphi'(m\ell_n)\ell_n > \gamma.$$

This shows that our estimate is *not* sharp, even for exact triangular lattices. However, the gap is small in this case.

If, however, \mathbf{B} contains a significant shear component, then our estimates are not particularly sharp as the numerical experiment shown in Figure 7 demonstrates. In this figure we plot the zero level line of γ in (m, M) parameter space for $\kappa \in \{0, 2/7\}$, and for $\Delta \in \{0, 0.02\}$. In particular, the case $\kappa = 2/7, \Delta = 0.02$ corresponds to our numerical experiment in §8.1.

7. A PRIORI ERROR ESTIMATES

Having established consistency and stability of the a/c method introduced in §3, we are now in a position to prove a priori error estimates for the deformation gradient and for the energy. For the statement of the following result recall the definition of $\mathcal{S}_{\mathbf{B},h}(m, M, \Delta)$ from §6.1.3, and the definition of $\Pi_2(y)$ from §4.3.

Below, in §7.1, we discuss the computational complexity predicted by our error estimates, that is, we reformulate them in terms of the number of degrees of freedom.

Theorem 7.1. *Suppose that Assumption A holds. Let $\mathbf{B} \in \mathbb{R}_+^{2 \times 2}$, and let $y_a \in \mathcal{Y}_{\mathbf{B}}$ be a solution of (2.5) and $y_{ac} \in \mathcal{Y}_{\mathbf{B},h}$ a solution of (3.7), such that the following stability assumption holds: there exist $0 < m \leq M$ and $\Delta > 0$ such that $\gamma := \gamma(m, M, \Delta, \kappa(\mathbb{V})) > 0$ (defined in (6.3)) and such that*

$$(1-t)y_{ac} + tI_h y_a \in \mathcal{S}_{\mathbf{B},h}(m, M, \Delta) \quad \forall t \in [0, 1]. \quad (7.1)$$

Then, there exist constants c_1 and c_2 , which depend only on the shape regularity of \mathcal{T}_h , on m , and on $\mu_a(y_a)$, such that

$$\|\nabla \bar{y}_a - \nabla y_{ac}\|_{L^2(\Omega)} \leq \frac{c_1}{\gamma} \inf_{\tilde{y}_a \in \Pi_2(y_a)} \|h \nabla^2 \tilde{y}_a\|_{L^2(\Omega_c)}, \quad \text{and} \quad (7.2)$$

$$|\mathcal{E}_a(y_a) - \mathcal{E}_{ac}(y_{ac})| \leq \frac{c_2}{\gamma^2} \inf_{\tilde{y}_a \in \Pi_2(y_a)} \|h \nabla^2 \tilde{y}_a\|_{L^2(\Omega_c)}^2. \quad (7.3)$$

Remark 7.1 (The Stability Assumption). The only assumption in Theorem 7.1 that we have not justified rigorously is the stability condition (7.1). The assumption is fairly natural as it requires, essentially, that y_{ac} belongs to the basin of stability of the local minimizer y_a .

Nevertheless, one would prefer to make only assumptions on y_a itself and establish the properties for y_{ac} and $I_h y_a$ rigorously. However, short of proving the existence of atomistic and a/c solutions y_a, y_{ac} such that

$$\|\nabla \bar{y}_a - \nabla y_{ac}\|_{L^\infty} + \|\nabla \bar{y}_a - \nabla I_h y_a\|_{L^\infty} \quad \text{is “sufficiently small”}, \quad (7.4)$$

one cannot hope to remove it, except by postulating even stronger requirements, e.g., phrasing (7.4) as an assumption.

A rigorous estimate on $\|\nabla \bar{y}_a - \nabla I_h y_a\|_{L^\infty}$ requires a regularity theory for atomistic systems with defects, and we are currently unaware of any results in this direction.

A rigorous estimate on $\|\nabla \bar{y}_a - \nabla y_{ac}\|_{L^\infty}$ could, in principle, be achieved using the inverse function theorem [24, 17, 21], but requires stability of $\delta^2 \mathcal{E}_{ac}(I_h y_a)$ as an operator from (discrete variants of) $W^{1,\infty}$ to $W^{-1,\infty}$. For the discretized Laplace operator such results are classical for quasiuniform meshes [26], and have recently been extended to locally refined meshes by Demlow *et al* [3]. These results give legitimate hope that assumption (7.1) could be (partially) removed. \square

Proof. 1. Error in the H^1 -norm. Let $e_h = I_h y_a - y_{ac}$, then there exists $\theta_h \in \text{conv}\{I_h y_a, y_{ac}\}$ such that

$$\langle \delta^2 \mathcal{E}_{ac}(\theta_h) e_h, e_h \rangle = \int_0^1 \langle \delta^2 \mathcal{E}_{ac}(y_{ac} + t e_h) e_h, e_h \rangle dt = \langle \delta \mathcal{E}_{ac}(I_h y_a) - \delta \mathcal{E}_{ac}(y_{ac}), e_h \rangle.$$

Using the stability assumption (7.1) to bound $\langle \mathcal{E}_{ac}(\theta_h) e_h, e_h \rangle$ from below, and the fact that $\langle \delta \mathcal{E}_{ac}(y_{ac}), e_h \rangle = 0$, we obtain

$$\gamma \|\nabla e_h\|_{L^2(\Omega)}^2 \leq \langle \delta \mathcal{E}_{ac}(I_h y_a), e_h \rangle.$$

We employ the consistency result, Theorem 5.1, to estimate

$$\gamma \|\nabla e_h\|_{L^2(\Omega)}^2 \leq C^{\text{cons}} \inf_{\tilde{y}_a \in \Pi_2(y_a)} \|h \nabla^2 \tilde{y}\|_{L^2(\Omega_c)} \|\nabla e_h\|_{L^2}, \quad (7.5)$$

where C^{cons} depends on $\mu_a(y_a)$ and $\mu_c(I_h y_a)$.

Employing the interpolation error bounds (4.3) and (4.4) to estimate

$$\begin{aligned} \|\nabla \bar{y}_a - \nabla y_{ac}\|_{L^2} &\leq \|\nabla \bar{y}_a - \nabla I_h y_a\|_{L^2(\Omega)} + \|\nabla e_h\|_{L^2(\Omega)} \\ &\leq \inf_{\tilde{y}_a \in \Pi_2(y_a)} \left[\|\nabla \bar{y}_a - \nabla \tilde{y}_a\|_{L^2(\Omega_c)} + \|\nabla \tilde{y}_a - \nabla I_h y_a\|_{L^2(\Omega_c)} \right] + \|\nabla e_h\|_{L^2(\Omega)} \\ &\leq \inf_{\tilde{y}_a \in \Pi_2(y_a)} \|(\tilde{C}_a + \tilde{C}_h h) \nabla^2 \tilde{y}_a\|_{L^2(\Omega_c)} + \|\nabla e_h\|_{L^2(\Omega)}, \end{aligned}$$

applying (7.5), and noting that $h \geq 1$, we obtain (7.2) with $c_1 = C^{\text{cons}} + \gamma(\tilde{C}_a + \tilde{C}_h)$. This constant depends indeed only on the shape regularity of \mathcal{T}_h , on $\mu_a(y_a)$, and on $\mu_c(I_h y_a) \geq m$.

2. *Error in the energy.* To estimate the error in the energy, $|\mathcal{E}_a(y_a) - \mathcal{E}_{ac}(y_{ac})|$, we first split it into

$$\begin{aligned} |\mathcal{E}_a(y_a) - \mathcal{E}_{ac}(y_{ac})| &\leq |\mathcal{E}_a(y_a) - \mathcal{E}_a(I_h y_a)| + |\mathcal{E}_a(I_h y_a) - \mathcal{E}_{ac}(I_h y_a)| \\ &\quad + |\mathcal{E}_{ac}(I_h y_a) - \mathcal{E}_{ac}(y_{ac})| \\ &=: E_1 + E_2 + E_3, \end{aligned}$$

and estimate the three terms E_j , $j = 1, 2, 3$, separately.

2.1. *The term E_1 .* Since $y_a \in \mathcal{B}$, and $\delta \mathcal{E}_a(y_a) = 0$, we can estimate

$$\begin{aligned} |\mathcal{E}_a(I_h y_a) - \mathcal{E}_a(y_a)| &= \left| \langle \delta \mathcal{E}_a(y_a), I_h y_a - y_a \rangle \right. \\ &\quad \left. + \int_0^1 \langle \delta \mathcal{E}_a((1-t)y_a + tI_h y_a) - \delta \mathcal{E}_a(y_a), I_h y_a - y_a \rangle dt \right| \\ &\leq \int_0^1 \left| \langle \delta \mathcal{E}_a((1-t)y_a + tI_h y_a) - \delta \mathcal{E}_a(y_a), I_h y_a - y_a \rangle \right| dt \end{aligned}$$

For each $t \in [0, 1]$ we use Lemma 5.3 to further estimate

$$\left| \langle \delta \mathcal{E}_a((1-t)y_a + tI_h y_a) - \delta \mathcal{E}_a(y_a), I_h y_a - y_a \rangle \right| \leq t C_L \|\nabla \bar{y}_a - \nabla \overline{I_h y_a}\|_{L^2}^2,$$

where C_L depends on $\mu_a(y_a)$ and $\mu_a(I_h y_a) \geq \min\{\mu_a(y_a), m\}$, and apply 4.6, to obtain

$$\begin{aligned} |\mathcal{E}_a(I_h y_a) - \mathcal{E}_a(y_a)| &\leq \max_{t \in [0, 1]} \left| \langle \delta \mathcal{E}_a((1-t)y_a + tI_h y_a) - \delta \mathcal{E}_a(y_a), I_h y_a - y_a \rangle \right| \\ &\leq C_1 \inf_{\tilde{y}_a \in \Pi_2(y_a)} \|h \nabla^2 \tilde{y}_a\|_{L^2(\Omega_c)}^2, \end{aligned} \quad (7.6)$$

where C_1 depends only on $\mu_a(y_a)$ and on m .

2.2 *The term E_3 .* The term E_3 can be estimated in a similar manner as E_1 . Following closely the proof of the Lipschitz estimate for $\delta \mathcal{E}_a$, Lemma 5.3, one can prove that, if $y_h^{(j)} \in \mathcal{Y}_h$, $j = 1, 2$, then

$$\left| \langle \delta \mathcal{E}_{ac}(y_h^{(1)}) - \delta \mathcal{E}_{ac}(y_h^{(2)}), u_h \rangle \right| \leq C_L \|\nabla y_h^{(1)} - \nabla y_h^{(2)}\|_{L^2(\Omega)} \|\nabla u_h\|_{L^2(\Omega)} \quad \forall u_h \in \mathcal{U}_h,$$

where $C_L = C_L(\min\{\mu_c(y_h^{(1)}), \mu_c(y_h^{(2)})\})$. Repeating the first part of the argument in step 2.1, and using the H^1 -norm error estimate (7.2), we obtain

$$|\mathcal{E}_{ac}(I_h y_a) - \mathcal{E}_{ac}(y_{ac})| \leq C'_3 \|\nabla I_h y_a - \nabla y_{ac}\|_{L^2}^2 \leq C_3 \inf_{\tilde{y}_a \in \Pi_2(y_a)} \|h \nabla^2 \tilde{y}_a\|_{L^2(\Omega_c)}^2, \quad (7.7)$$

where C'_3 and C_3 depend on m and on the shape regularity of \mathcal{T}_h , and C_3 depends also on γ .

2.3. *The term E_2 .* Estimating this term requires a little more work. In Lemma 7.2 below, we prove that

$$|\mathcal{E}_a(I_h y_a) - \mathcal{E}_{ac}(I_h y_a)| \leq C_2 \inf_{\tilde{y}_a \in \Pi_2(y_a)} \|h^{1/2} \nabla^2 \tilde{y}_a\|_{L^2(\Omega_c)}^2, \quad (7.8)$$

where C_2 depends only on $\mu_c(I_h y_a) \geq m$, and on the shape regularity of \mathcal{T}_h .

2.4. *Conclusion.* Combining (7.6), (7.7), and (7.8) yields the energy error estimate (7.3) and concludes the proof of the theorem. \square

Lemma 7.2. *Let $y_h \in \mathcal{Y}_h$; then*

$$|\mathcal{E}_a(y_h) - \mathcal{E}_{ac}(y_h)| \leq C_1^E \|\nabla y_h\|_{L^2(\Omega_c)}^2, \quad (7.9)$$

where $C_1^E = c'_1 \sum_{r \in \mathbb{L}_*} M_2(\mu_c(y_h)|r|)|r|^4$, and c'_1 depends on the shape regularity of \mathcal{T}_h .

Moreover, if $y \in \mathcal{Y}$, and $\mu_c(I_h y) > 0$, then

$$|\mathcal{E}_a(I_h y) - \mathcal{E}_{ac}(I_h y)| \leq C_2^E \inf_{\tilde{y} \in \Pi_2(y)} \|h^{1/2} \nabla^2 \tilde{y}\|_{L^2(\Omega_c)}^2, \quad (7.10)$$

where $C_2^E = c'_2 \sum_{r \in \mathbb{L}_*} M_2(\mu_c(I_h y)|r|)|r|^4$, and c'_2 depends on the shape regularity of \mathcal{T}_h .

Proof. First note that the difference $\mathcal{E}_a(y_h) - \mathcal{E}_{ac}(y_h)$ depends only on continuum bonds:

$$\mathcal{E}_a(y_h) - \mathcal{E}_{ac}(y_h) = \sum_{b \in \mathcal{B}_c} \left\{ \phi(D_b y_h) - \int_b \phi(\nabla_b y_h) db \right\}.$$

For each $b \in \mathcal{B}_c$, we have

$$\begin{aligned} \phi(\nabla_b y_h) &= \phi(D_b y_h) + \phi'(D_b y_h) \cdot (\nabla_b y_h - D_b y_h) \\ &\quad + \int_0^1 \left[\phi'(t \nabla_b y_h + (1-t) D_b y_h) - \phi'(D_b y_h) \right] dt \cdot (\nabla_b y_h - D_b y_h) \end{aligned}$$

Since $\phi'(D_b y_h)$ is a constant on the bond b and since $\int_b (\nabla_b y_h - D_b y_h) db = 0$ (cf. (3.2)), we obtain, using the Lipschitz bound for ϕ' inside the integral over t ,

$$\left| \int_b [\phi(\nabla_b y_h) - \phi(D_b y_h)] db \right| \leq \frac{1}{2} M_{|b|} \int_b |\nabla_b y_h - D_b y_h|^2 db,$$

where $M_{|b|} = M_2(\mu_c(y_h)|b|)$.

Summing over all bonds $b \in \mathcal{B}_c$ yields the estimate

$$|\mathcal{E}_a(y_h) - \mathcal{E}_{ac}(y_h)| \leq \frac{1}{2} \sum_{b \in \mathcal{B}_c} M_{|b|} \int_b |\nabla_b y_h - D_b y_h|^2 db, \quad (7.11)$$

which is precisely the same expression as $E(y_h)^2$ defined in (5.7), with $p = 2$ and $a_b = 1$. Hence, we can use (5.14) and (5.16) to obtain

$$|\mathcal{E}_a(y_h) - \mathcal{E}_{ac}(y_h)| \leq C_1^E \|\nabla y_h\|_{L^2(\mathcal{F}_h^c)}^2,$$

where \mathcal{F}_h^c and $[\nabla y_h]$ was defined in §4.4; with constants $C_1^E = c'_1 \sum_{r \in \mathbb{L}_*} M_2(\mu_c(y_h)|r|)|r|^4$, where c'_1 depends only on the shape regularity of \mathcal{T}_h . This concludes the proof of (7.9).

The estimate (7.10) follows immediately from Lemma 4.4. \square

7.1. Optimal meshes. In this subsection we give an informal discussion of refinement rates of the mesh, in order to obtain error estimates in terms of the number of degrees of freedom. Moreover, this discussion provides heuristics on how to choose atomistic region sizes in relation to finite element meshes. For the sake of generality (and simplicity), we will slightly deviate from the assumptions and results of our analysis. Throughout this section, we will liberally make use of the symbols \lesssim and \approx to indicate bounds up to constants that are independent of the mesh parameters (but may depend on the shape regularity).

Consider a domain Ω of diameter $O(N)$, an atomistic region of diameter $O(K)$ such that $\frac{K}{N} \leq C < 1$ (i.e., the atomistic region does not occupy most of the domain Ω), with a defect in the centre of the atomistic region. We conjecture that (7.2) holds for general $p \in [1, \infty]$, that is,

$$\|\nabla \bar{y}_a - \nabla y_{ac}\|_{L^p(\Omega)} \lesssim \inf_{\tilde{y}_a \in \Pi_2(y_a)} \|h \nabla^2 \tilde{y}_a\|_{L^p(\Omega_c)}. \quad (7.12)$$

The main ingredient to prove (7.12) is a stability estimate for $\delta^2 \mathcal{E}_{ac}(y_h)$ (for certain $y_h \in \mathcal{Y}_h$) as an operator between (discrete variants of) $W^{1,p}$ and $W^{-1,p}$. Such a result would be very technical to establish, however, there is some hope that the techniques recently developed in [3] could be used as a starting point to achieve this.

We assume that, for some “good” interpolant \tilde{y}_a (e.g., the HCT interpolant discussed in Remark 4.1) we have the following decay property:

$$|\nabla^2 \tilde{y}_a(x)| \approx r^{-\beta}, \quad (7.13)$$

where $\beta > 0$, and where r denotes the distance from the defect. For example, it can be observed numerically that $\beta = 2$ for a dislocation [9], and, as observed in our own numerical experiments, $\beta = 3$ for a vacancy.

We consider a finite element mesh \mathcal{T}_h with the mesh size function $h(r) \approx h_K (r/K)^\alpha$, where $h_K \geq 1$ and $\alpha > 0$ are the refinement parameters that we want to optimize. Note that we have shown (7.2) only under the assumption that $h = 1$ on $\partial\Omega_a$, which would require us to choose $h_K \approx 1$. However, for the sake of argument, we might assume that (7.12) still holds for more general h_K (possibly by replacing Ω_c with an enlarged region on the right-hand side of (7.12)). Remarkably, our analysis below shows that $h_K \approx 1$ is in fact a quasi-optimal choice.

In terms of the various parameters introduced above, the conjectured error estimate (7.12) can be rewritten as

$$\|\nabla \bar{y}_a - \nabla y_{ac}\|_{L^p(\Omega)} \lesssim \|h \nabla^2 \tilde{y}_a\|_{L^p(\Omega_c)} \approx \left(\int_K^N (h_K \left(\frac{r}{K}\right)^\alpha r^{-\beta})^p r \, dr \right)^{1/p} =: \text{Err}, \quad (7.14)$$

	§	Parameter Regime	Err	DoF
1.	§7.1.2	$\beta > 1$ and $p > \frac{2}{\beta-1}$	$\text{DoF}^{1/p-\beta/2}$	K^2
2.	§7.1.3	$\beta > 1$ and $p = \frac{2}{\beta-1}$	$\text{DoF}^{-1/2}(\log \frac{N}{K})^{1/2+1/p}$	$K^2 \log \frac{N}{K}$
3.	§7.1.4	$\beta \leq 1$ or $p < \frac{2}{\beta-1}$	$\text{DoF}^{-1/2} N^{1/2+1/p-\beta/2}$	$K^2 \left(\frac{N}{K}\right)^{2-2\alpha}$

TABLE 2. Convergence rates for $\|\nabla \bar{y}_a - \nabla y_{ac}\|_{L^p(\Omega)}$ in terms of degrees of freedom for the optimised size of the atomistic region and finite element mesh. In all cases $\alpha = \beta p / (2+p)$ and $h_K \approx 1$ are quasi-optimal, leaving the atomistic domain size, K , as the remaining free parameter. All quantities are understood as approximate orders of magnitude.

and the number of degrees of freedom approximated by

$$\text{DoF} := K^2 + \int_K^N \frac{1}{h(r)^2} r \, dr = K^2 + \int_K^N \frac{r}{h_K^2 (r/K)^{2\alpha}} dr. \quad (7.15)$$

In the following paragraphs we will obtain heuristic optimal choices for the mesh parameters, α and h_K , in terms of K , p , and β . It turns out that $\alpha = \beta p / (2+p)$ and $h_K \approx 1$ are always quasi-optimal. The remaining results are summarized in Table 2. The most interesting situations, which are $p = 2, \infty$ (corresponding to energy and $W^{1,\infty}$ norms) and $\beta = 2, 3$ (corresponding to dislocations and vacancies, or possibly more general defects with zero Burgers vectors), are covered by the first two rows. In the case $p = 2$ and $\beta = 3$ (vacancy), for which the error estimate (7.12) was rigorously proved, we obtain $\text{Err} \approx \text{DoF}^{-1}$.

7.1.1. *Equidistribution principle.* We begin by applying the error equidistribution principle to obtain the optimal value for α (see [2, Sec. 5] for the case $p = 2$, which is readily generalized).

Consider a vertex q at distance r from the defect, with local mesh size $h(q) \equiv h(r)$. The error contribution of a degree of freedom associated with this vertex can be approximately estimated as

$$|h(r) \nabla^2 \tilde{y}_a|^p h(r)^2 \approx \left(\frac{r}{K}\right)^{2\alpha} \left(h_K \left(\frac{r}{K}\right)^\alpha r^{-\beta}\right)^p h_K^2 = r^{\alpha(2+p)-\beta p} K^{-\alpha(2+p)} h_K^{p+2}.$$

From the equidistribution principle, this quantity should not depend on r , i.e., $\alpha(2+p) - \beta p = 0$, from where we find that $\alpha = \frac{p}{2+p} \beta$.

We now consider three cases: $\alpha > 1$, $\alpha = 1$, and $\alpha < 1$. If $\beta > 1$ then these three cases correspond, respectively, to $p > \frac{2}{\beta-1}$, $p = \frac{2}{\beta-1}$, and $p < \frac{2}{\beta-1}$. If $\beta \leq 1$ then $\alpha < 1$ always holds.

7.1.2. *Case 1: $\alpha > 1 \Leftrightarrow (\beta > 1 \text{ and } p > \frac{2}{\beta-1})$.* In this case, since $2 - 2\alpha < 0$, the approximate number of degrees of freedom is given by

$$\text{DoF} \approx K^2 + \frac{N^{2-2\alpha} - K^{2-2\alpha}}{h_K^2(2-2\alpha)} \approx K^2 + h_K^{-2} K^2 \approx K^2.$$

The error can be estimated as

$$\begin{aligned} \text{Err} &= \frac{1}{p(\beta-\alpha)-2} h_K K^{2/p-\beta} \left(1 - \left(\frac{K}{N}\right)^{p(\beta-\alpha)-2}\right)^{1/p} \\ &\approx h_K K^{2/p-\beta} \approx h_K \text{DoF}^{1/p-\beta/2}, \end{aligned} \quad (7.16)$$

Since the estimate for DoF does not depend on h_K , the optimal choice for h_K is $h_K \approx 1$, and the resulting convergence rate is therefore $\text{Err} \approx \text{DoF}^{1/p-\beta/2}$.

Remark 7.2. In the present case one can show directly (without using the equidistribution principle) that $h_K \approx 1$ and any α such that $1 < \alpha < \beta - \frac{2}{p}$, including $\alpha = \frac{p}{p+2} \beta$, are quasi-optimal, i.e., the error for this choice differs from the error for the best choice by at most a constant factor. This constant, however, tends to infinity as α tends to 1 or to $\beta - \frac{2}{p}$. \square

Remark 7.3. Dropping the error equidistribution assumption and allowing $\alpha = 1$, while still assuming $p > 2/(\beta - 1)$, yields

$$\text{Err} \approx \text{DoF}^{1/p-\beta/2} \left(\log \frac{N}{K}\right)^{\beta/2-1/p}, \quad (7.17)$$

which is clearly suboptimal in comparison with (7.16), but may be acceptable for relatively small systems. For instance, in the numerical experiments shown in §8 we used $4 \leq K \leq 64$, $N = 128$, $\beta = 3$, and $p = 2$, in which case the error estimate is at most 4 times larger than for the optimal mesh.

The advantage of the choice $\alpha = 1$ is that it is relatively easy to construct such a mesh: e.g., for a hexagonal region one can consider a mesh \mathcal{T}_h consisting of hexagonal layers (i.e., hexagonal rings), each of the 6 sides of the layer is refined M times, so that the typical size of a triangle at distance r is $h_T \approx \frac{r}{M}$; see Figure 10(a). The condition $h_K \approx 1$ corresponds to $M \approx K$. \square

7.1.3. *Case 2: $\alpha = 1 \Leftrightarrow (\beta > 1 \text{ and } p = \frac{2}{\beta-1})$.* In this case, $h(r) \approx rh_K/K$, and hence the error and the number of degrees of freedom can be estimated as

$$\begin{aligned} \text{Err} &\approx h_K K^{-1} \left(\log \frac{N}{K}\right)^{1/p}, \quad \text{and} \\ \text{DoF} &\approx K^2 + \log \frac{N}{K} h_K^{-2} K^2. \end{aligned}$$

For fixed Err, we wish to choose K and h_K to minimize DoF. Upon solving this constrained minimization problem in two variables (a slightly tedious but straightforward computation), one obtains for the optimal choices of K and h_K that $K \text{Err} \approx \left(\log \frac{N}{K}\right)^{1/p}$, and hence $h_K \approx 1$. Inserting these into the above expression for DoF one obtains

$$\text{Err} \approx \text{DoF}^{-1/2} \left(\log \frac{N}{K}\right)^{1/2+1/p} \quad \text{and} \quad \text{DoF} \approx K^2 \log \frac{N}{K}.$$

7.1.4. *Case 3: $\alpha < 1 \Leftrightarrow (\beta \leq 1 \text{ or } p < \frac{2}{\beta-1})$.* In this case we obtain the following estimates on Err and DoF:

$$\begin{aligned} \text{Err} &\approx h_K K^{-p\beta/(2+p)} N^{2/p-2\beta/(2+p)} = h_K K^{-\alpha} N^{2(1-\alpha)/p}, \quad \text{and} \\ \text{DoF} &\approx K^2 + h_K^{-2} K^{2p\beta/(2+p)} N^{2-2p\beta/(2+p)} = K^2 + h_K^{-2} K^{2\alpha} N^{2-2\alpha}. \end{aligned}$$

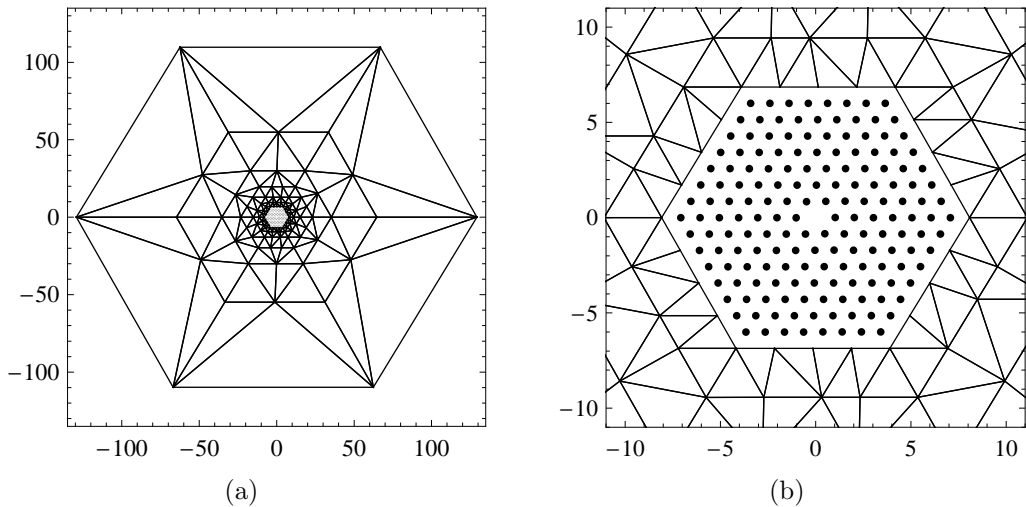


FIGURE 8. Illustration of the region and the algebraically refined mesh for $K = 8$, $h_K = 2$, and $\alpha = 3/2$.

Solving again the constrained optimization problem of minimizing DoF subject to keeping Err fixed, we obtain $K\text{Err} \approx K^{1-\alpha} N^{(1-\alpha)/p}$, which yields once again $h_K \approx 1$,

$$\text{Err} \approx \text{DoF}^{-1/2} N^{1/2+1/p-\beta/2}, \quad \text{and} \quad \text{DoF} \approx K^2 \left(\frac{N}{K}\right)^{2-2\alpha}.$$

8. NUMERICAL EXAMPLES

We conducted several numerical experiments to confirm the convergence rates obtained in §7.1, and to experimentally verify stability of the a/c method near bifurcation points, where our stability analysis does not apply.

In all tests, the effective region of periodicity was a hexagon centered at the origin with each side of the length $N = 128$, as illustrated in Fig. 8. A defect was placed near the origin. One can show that such a hexagonal region can be embedded into a larger periodic cell $\mathbf{A}_6(0, 3N]^2$, thus reducing the hexagonal symmetry to the square symmetry as was assumed in §2–7.

The atomistic region formed a smaller hexagon also centered at the origin whose side contained K atoms, as illustrated in Fig. 8(b) for $K = 8$. In the continuum region, either an algebraically refined mesh with $|T| \approx h_K(r/K)^{3/2}$ (where r is the distance from $T \in \mathcal{T}_h$ to the defect) or a radial mesh $|T| \approx h_K(r/K)$ was constructed (see Fig. 8 for an example of the algebraically refined mesh). The parameter $\alpha = \frac{3}{2}$ is an optimal parameter for $\beta = 3$ and $p = 2$ (*cf.* Table 2). The a/c interface thus formed a hexagon each side of which was subdivided into intervals with length h_K , $1 \leq h_K \leq K$ (the illustration on Fig. 8 is for $h_K = 2$).

8.1. Vacancy. We consider an example with a single vacancy defect. The macroscopic strain \mathbf{B} is chosen as

$$\mathbf{B} = \begin{pmatrix} 1.01 & 0.01 \\ 0 & 0.99 \end{pmatrix}.$$

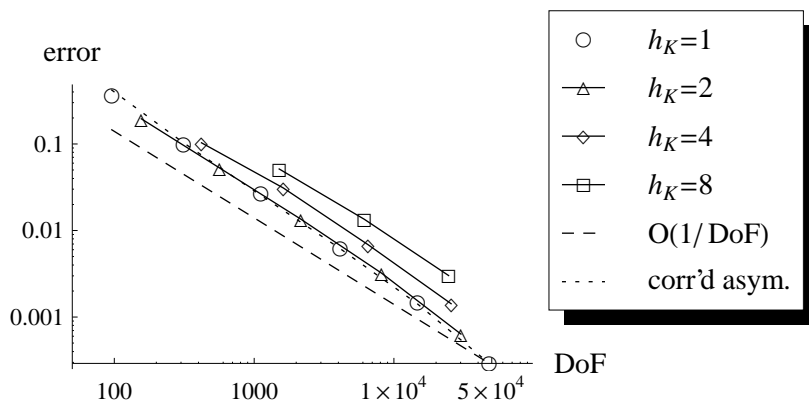


FIGURE 9. Error of the computed solutions as a function of the number of degrees of freedom (DoF) for various choices of h_K . It is seen that the choice $h_K \in \{1, 2\}$ is optimal. Moreover, a first-order convergence, $\text{Err} \approx \text{DoF}^{-1}$, is clearly observed. This is also predicted in the estimate (7.16), which is plotted with a dotted line.

A nonlinear conjugate gradient solver with linesearch [29] was used to find a stable equilibrium of the atomistic system. A simple Laplace preconditioner was used to accelerate convergence. The atoms were interacting with the Lennard-Jones potential with the cut-off distance 3.1, measured in the reference hexagonal configuration.

In Figure 9 we plot the relative error, $\frac{\|\nabla \bar{y}_a - \nabla y_{ac}\|_{L^2(\Omega)}}{\|\nabla \bar{y}_a - \nabla y_B\|_{L^2(\Omega)}}$ against the number of degrees of freedom (DoF). We observe first order convergence, for the optimal choices $h_K = 1$ or $h_K = 2$, which is in agreement with predictions made in §7.1. What is remarkable, is that the error estimate (7.16) gives an excellent approximation to the magnitude of the actual error (compare the solid and the dotted graphs in Figure 9). This indicates that the error estimates obtained in the present paper are qualitatively accurate.

It is also interesting to compare the algebraically refined mesh with $\alpha = \frac{3}{2}$ and the radial mesh with $\alpha = 1$. The error for these two meshes is plotted in Figure 10. We observe that there is only a negligible difference in the error. This is in correspondence with the estimate (7.17): the effect of the term $\log \frac{N}{K}$ can only be observed only for a large ratio N/K .

8.2. Collapsed Cavity. The second test case is a collapsed cavity defect, as considered in [27]. This defect is formed by removing eight atoms and applying a macroscopic compression to force the cavity to collapse and form two edge dislocations (see Figure 11(a) and [27] for a detailed test case description). Since they have opposite Burgers' vectors we obtain again $\beta = 3$ for the analysis in §7.1.

The results, presented in Figure 11(b) are similar to the single vacancy case, the main difference being that one requires larger K to represent the defect and that for the fixed (K, h_K) the error is higher than for the single vacancy case due to a slightly “stronger” defect.

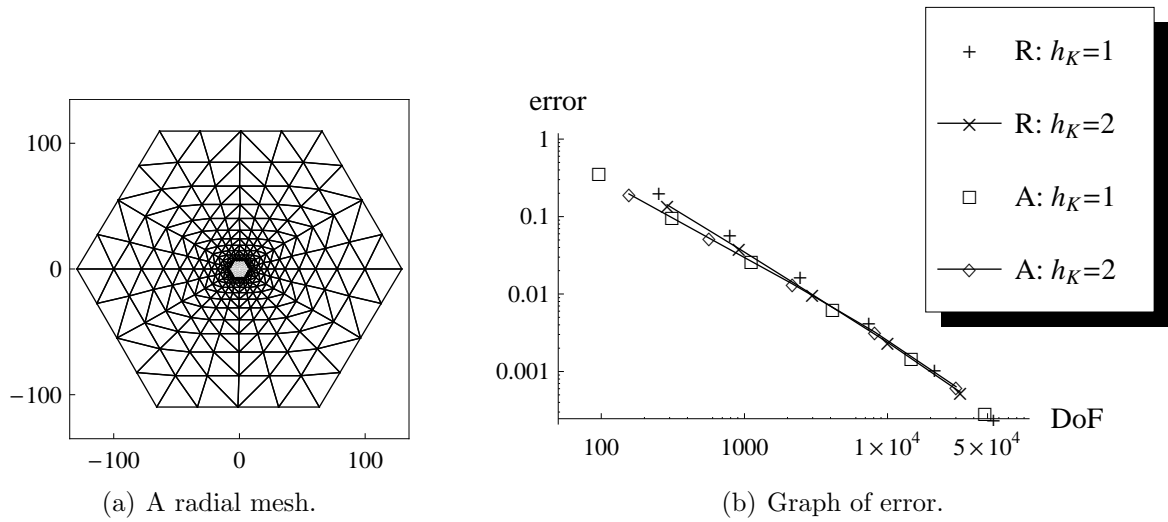


FIGURE 10. Error of the computed solutions as a function of the number of degrees of freedom (DoF) for the algebraically refined mesh with $|T| \approx h_K \left(\frac{r}{K}\right)^{3/2}$ (marked “A” in the legend) and the radial mesh (see the illustration on the left) with $|T| \approx h_K \left(\frac{r}{K}\right)$ (marked “R” in the legend), for $h_K \in \{1, 2\}$. No essential difference in results between these two meshes is observed. A more pronounced difference may appear for larger (or infinite) domains.

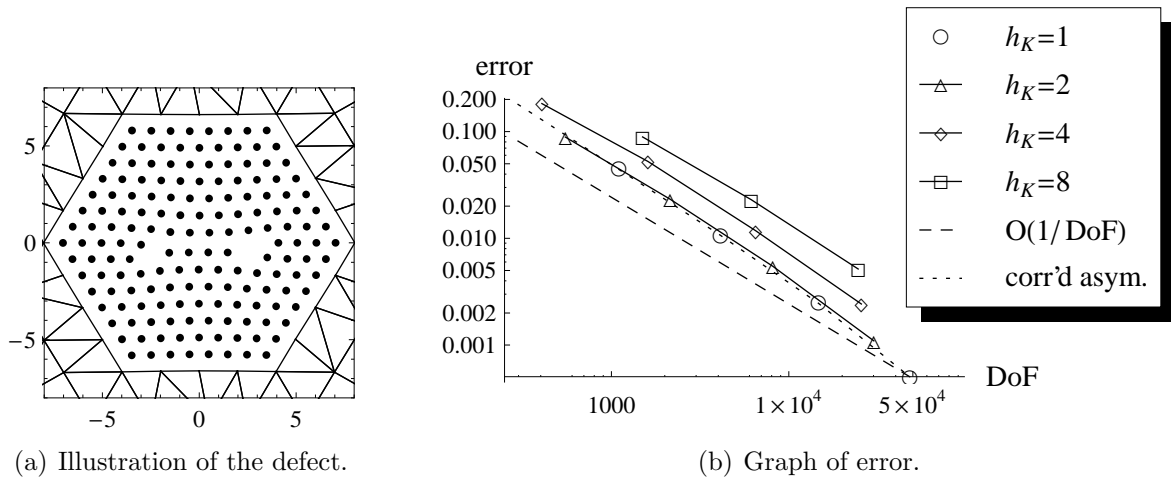


FIGURE 11. Error of the computed solutions for the collapsed cavity test as a function of the number of degrees of freedom (DoF) for various choices of h_K . As in the single vacancy test, we observe (1) the choice $h_K \in \{1, 2\}$ are optimal, (2) a first-order convergence in DoF, and (3) a remarkable correspondence between the actual error and the estimate (7.16), plotted with dotted line.

K	DoF	t_{ac}, t_a	a	b
4	288	0.06104434		
8	912	0.05962851	2.15	3.57
16	2976	0.05950837	2.19	3.73
32	9984	0.05949904	2.53	4.42
64	32256	0.05949861	2.57	4.36
exact	105338	0.05949859		

TABLE 3. Results of the stability test described in §8.3. $K = 4, 8, \dots, 64$ and $h_K = 2$ are the mesh parameters, DoF is the number of degrees of freedom, t_{ac}, t_a are the computed critical parameters, a, b are estimated convergence rates: $|t_{ac} - t_a| \approx \text{DoF}^a$, and $|t_{ac} - t_a| \approx K^b$.

8.3. Stability Test for a Vacancy. In addition to investigating the error in the a/c method, in terms of the number of degrees of freedom, we also conducted a series of numerical experiments to explore the stability regions of the a/c coupling (3.4).

Our first test case was similar to the one in §8.1, the only difference being that the macroscopic strain now depends on a parameter t :

$$\mathbf{B} = \begin{pmatrix} 1 & 0 \\ 0 & 1 + t \end{pmatrix}.$$

The parameter t is gradually increased from 0. For each value of t the atomistic and a/c solutions are computed using Newton's method taking the previous critical point as the initial guess. In each step, the lowest eigenvalue of $\delta^2 \mathcal{E}_a$ (respectively, $\delta^2 \mathcal{E}_{ac}$) (ignoring the two zero eigenvalues corresponding to translations) is used to determine whether the computed solution is a stable equilibrium, and thus determine the critical parameter t_a (respectively, t_{ac}). Only radial meshes were used.

The results of the experiment are displayed in Table 3. We observe at least a quadratic convergence rate $|t_a - t_{ac}| \lesssim \text{DoF}^{-2}$, and in particular, that the a/c method is stable up to this bifurcation point. The quadratic convergence rate might be attributed to the well-known superconvergence of eigenvalues [31].

8.4. Stability Test for a Bravais Lattice. Our second stability test is conducted with a two parameter family of the macroscopic strains

$$\mathbf{B} = \begin{pmatrix} 1 + s & 0.1 \\ 0 & 1 + t \end{pmatrix} \quad (8.1)$$

for a lattice with no defects. In the (s, t) -plane we compared two regions of stability: the region of the stability of the atomistic model (as $N \rightarrow \infty$; cf. [11]), and the region of stability of the a/c method, for $K = 16$ and $h_K = 2$. The results are shown in Figure 12. We observe that the stability region of the a/c method contains the stability region for the atomistic model, but that they are comparable up to numerical errors.

We believe that the minor visual difference between the two regions is caused by a finite size of the domain and the discretization of the continuum region. It would

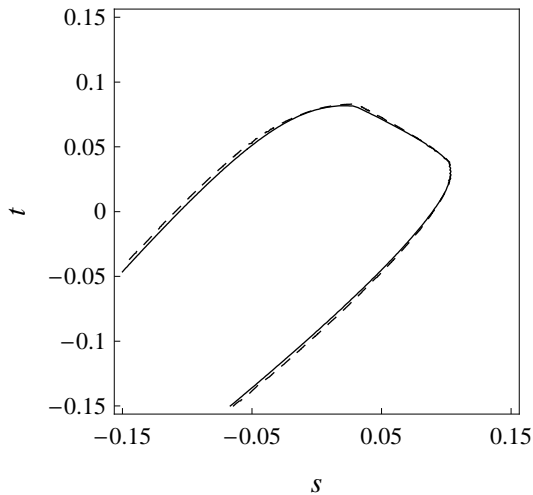


FIGURE 12. Stability regions of the atomistic model (solid line) and the a/c method for $K = 16$ and $M = 8$ (dashed line). The axis variables, s and t , are the parameters for the macroscopic strain (8.1). One can observe that the stability region of the a/c method contains the stability region for the atomistic model, and that the discrepancy is “small”.

require extensive calculations to verify that the stability region of the a/c method indeed converges to the stability region of the atomistic model as $\text{DoF} \rightarrow \infty$.

CONCLUSION

We have presented a comprehensive *a priori* error analysis of a practical energy based atomistic/continuum coupling method recently proposed in [27], admitting simple lattice defects in the domain. The method (and the analysis) are valid in two dimensions, for pair-potential interactions.

The main theoretical question left open in our analysis is whether the a/c method is stable up to bifurcation points. This is a question first posed in [5] as a fundamental step in understanding a/c methods. Our numerical experiments in §8.3 and §8.4 indicate that the error in the stability regions between the atomistic model and the a/c method is indeed “small”, however, establishing such a result rigorously appears to be challenging.

Among the other interesting questions motivated by our analysis are: (1) Rigorously establishing the stability assumption (7.1), for example, following the discussion in Remark 7.1. (2) Developing a regularity theory for crystal defects, to make the analysis in §7.1 rigorous. In particular, this would allow for optimal *a priori* mesh refinement and remove the need for mesh adaptivity. (3) Extending the analysis to other classes of defects. While treating impurities should be straightforward with the present techniques, other defects with zero Burgers vector such as interstitials, or dislocation dipoles, require a more advanced account of stability. An extension to dislocations would in addition require a more general consistency analysis as dislocations do not have an underlying reference configuration, which is a Bravais lattice.

APPENDIX A. PROOFS OF SOME AUXILIARY RESULTS

Proof of Lemma 2.2. 1. Proof of (2.1): The first result is motivated by the observation that the quadratic form

$$a[r] = \sum_{j=1}^6 |\mathbf{G}\mathbf{Q}_6^j r|^2$$

has hexagonal symmetry, that is, $a[\mathbf{Q}_6 r] = a[r]$ for all $r \in \mathbb{R}^2$. Suppose that a is represented by the symmetric matrix $\mathbf{A} \in \mathbb{R}^{2 \times 2}$, $a[r] = r^\top \mathbf{A} r$, then

$$\mathbf{Q}_6^\top \mathbf{A} \mathbf{Q}_6 = \mathbf{A}.$$

By equating the entries in this matrix one obtains that \mathbf{A} must in fact be a multiple of the identity. In particular, this implies that $a[r] = a[e_1]$, for $|r| = 1$, and a direct computation yields (2.1).

2. Proof of (2.2): The second result is motivated by the observation that the map $\mathbf{G} \mapsto \sum_{j=1}^6 [(\mathbf{Q}_6^j r)^\top \mathbf{G} (\mathbf{Q}_6^j r)]^2$ defines a fourth-order tensor with hexagonal symmetry, and the usual major and minor symmetries. It is well-known that such a tensor is isotropic and must therefore take the form given in (2.2) (though with still undermined Lamé parameters). Having observed this, it is more convenient however, to prove the result by a direct algebraic computation.

Clearly the expression on the left-hand side of (2.2) depends only on \mathbf{G}^{sym} , hence we assume without loss of generality that $\mathbf{G} = \mathbf{G}^{\text{sym}}$.

Let \mathbf{R} be a rotation matrix such that $r = \mathbf{R}e_1$, where $e_1 = (1, 0)$, then

$$q[r] := \sum_{j=1}^6 [(\mathbf{Q}_6^j r)^\top \mathbf{G} (\mathbf{Q}_6^j r)]^2 = \sum_{j=1}^6 [(\mathbf{Q}_6^j e_1)^\top (\mathbf{R}^\top \mathbf{G} \mathbf{R}) (\mathbf{Q}_6^j e_1)]^2.$$

Noting that $\mathbf{Q}_6^j e_1 = (\cos \frac{\pi j}{3}, \sin \frac{\pi j}{3})$, that $\mathbf{Q}_6^{j+3} = -\mathbf{Q}_6^j$, and that $\mathbf{R}^\top \mathbf{G} \mathbf{R}$ is symmetric, i.e.,

$$\mathbf{R}^\top \mathbf{G} \mathbf{R} = \begin{pmatrix} 2a & 2c \\ 2c & 2d \end{pmatrix},$$

for some real numbers a, c, d , we can explicitly compute

$$\begin{aligned} q[r] &= 2 \sum_{j=1}^3 \left(2a \cos^2 \frac{\pi j}{3} + 4c \cos \frac{\pi j}{3} \sin \frac{\pi j}{3} + 2d \sin^2 \frac{\pi j}{3} \right)^2 \\ &= 2 \sum_{j=1}^3 \left((a+d) + (a-d) \cos \frac{2\pi j}{3} + 2c \sin \frac{2\pi j}{3} \right)^2. \end{aligned}$$

After expanding the squares and simplifying the sum we obtain

$$\begin{aligned} q[r] &= 3(a+d)^2 + 6a^2 + 6d^2 + 12c^2 \\ &= \frac{3}{4} |\text{tr}(\mathbf{R}^\top \mathbf{G} \mathbf{R})|^2 + \frac{3}{2} |\mathbf{R}^\top \mathbf{G} \mathbf{R}|^2 = \frac{3}{4} |\text{tr} \mathbf{G}|^2 + \frac{3}{2} |\mathbf{G}|^2. \end{aligned} \quad \square$$

Proof of Theorem 3.3. For each $b \in \mathcal{B}_c$ we have $\chi_{\Omega_c^\#} = 1$ on the entire segment b , and hence we obtain

$$\sum_{b \in \mathcal{B}_c} \int_b \phi(\nabla_b y_h) \, db = \sum_{b \in \mathcal{B}_c} \int_b \chi_{\Omega_c^\#} \phi(\nabla_b y_h) \, db.$$

Recall from §2.2.4 that \mathbb{B} denotes the set of all bonds between any two lattice sites, including vacancies. In particular, $\mathcal{B}_c \subset \mathbb{B}$, and hence,

$$\sum_{b \in \mathcal{B}_c} \int_b \phi(\nabla_b y_h) \, db = \sum_{b \in \mathbb{B}} \int_b \chi_{\Omega_c^\#} \phi(\nabla_b y_h) \, db - \sum_{b \in \mathbb{B} \setminus \mathcal{B}_c} \int_b \chi_{\Omega_c^\#} \phi(\nabla_b y_h) \, db. \quad (\text{A.1})$$

Note that, since we assumed that the continuum region contains no vacancies the second group contributes only to the energy in a neighbourhood of the atomistic/continuum interface.

We first focus on the first term on the right-hand side of (A.1). Using the additivity of the characteristic functions, and the fact that $\nabla_r y_h = (\nabla y_h|_T) r$ in each element T (including the element edges that are parallel to r) we have

$$\begin{aligned} \sum_{b \in \mathbb{B}} \int_b \chi_{\Omega_c^\#} \phi(\nabla_b y_h) \, db &= \sum_{T \in \mathcal{T}_h^c} \sum_{b \in \mathbb{B}} \int_b \chi_{T^\#} \phi((\nabla y_h|_T) r_b) \, db \\ &= \sum_{T \in \mathcal{T}_h^c} \sum_{r \in \mathbb{L}_*} \phi((\nabla y_h|_T) r) \left[\sum_{x \in \mathbb{L}} \int_x^{x+r} \chi_{T^\#} \, db \right]. \end{aligned}$$

We can now apply the periodic bond-density lemma, and insert the definition of the Cauchy–Born stored energy density, to obtain

$$\begin{aligned} \sum_{b \in \mathbb{B}} \int_b \chi_{\Omega_c^\#} \phi(\nabla_b y_h) \, db &= \sum_{T \in \mathcal{T}_h^c} \frac{1}{\det \mathbf{A}_6} |T| \sum_{r \in \mathbb{L}_*} \phi((\nabla y_h|_T) r) \\ &= \sum_{T \in \mathcal{T}_h^c} |T| W(\nabla y_h|_T) = \int_{\Omega_c} W(\nabla y_h) \, dV. \end{aligned} \quad (\text{A.2})$$

The stated decomposition of \mathcal{E}_{ac} is obtained by combining (A.2) and (A.1). \square

Proof of Lemma 4.2. To prove this result we employ the bond density lemma. Assume, in addition, that $p < \infty$. Since all norms involved are effectively weighted ℓ^p -norms, one can obtain the case $p = \infty$ as the limit $p \nearrow \infty$.

If $p \leq 2$, set $C_1 := \sqrt{\frac{2}{3}}$; if $p > 2$, set $C_1 = \sqrt{\frac{2}{3}} 3^{(p-2)/(2p)}$. With that definition, and using (2.1), we get

$$|\mathbf{G}|_2 = \sqrt{\frac{2}{3}} \left(\sum_{j=1}^3 |\mathbf{G}a_j|^2 \right)^{1/2} \leq C_1 \left(\sum_{j=1}^3 |\mathbf{G}a_j|_2^p \right)^{1/p} \quad \forall \mathbf{G} \in \mathbb{R}^{2 \times 2}$$

In particular, we have

$$\|\nabla \bar{y}_h\|_{L^p(\Omega)}^p = \|\|\nabla \bar{y}_h\|\|_{L^p(\Omega)}^p \leq C_1^p \sum_{j=1}^3 \int_{\Omega} |\nabla_{a_j} \bar{y}_h|^p \, dV. \quad (\text{A.3})$$

Fix some $j \in \{0, 1, 2\}$; then, using the periodic bond density lemma, and the fact that $\{\chi_{\tau^\#} : \tau \in \mathcal{T}_a\}$ is a partition of unity for \mathbb{R}^2 , we have

$$\begin{aligned} \int_{\Omega} |\nabla_{a_j} \bar{y}_h|^p \, dV &= \sum_{\tau \in \mathcal{T}_a} |\tau| |\nabla_{a_j} \bar{y}_h|_{\tau}|^p = \sum_{\tau \in \mathcal{T}_a} |\nabla_{a_j} \bar{y}_h|_{\tau}|^p \sum_{x \in \mathbb{L}} \int_x^{x+a_j} \chi_{\tau^\#} \, db \\ &= \sum_{x \in \mathbb{L}} \sum_{\tau \in \mathcal{T}_a} \int_x^{x+a_j} |\nabla_{a_j} \bar{y}_h|^p \chi_{\tau^\#} \, db = \sum_{x \in \mathbb{L}} \int_x^{x+a_j} |\nabla_{a_j} \bar{y}_h|^p \, db. \end{aligned} \quad (\text{A.4})$$

We have also used the fact that $\nabla_{a_j} \bar{y}_h$ is continuous across edges that have direction a_j .

Due to the specific choice of the triangulation \mathcal{T}_a it follows that $\nabla_{a_j} \bar{y}_h$ is constant along each bond $(x, x + a_j)$, and hence

$$\int_x^{x+a_j} |\nabla_{a_j} \bar{y}_h|^p \, db = |D_{a_j} \bar{y}_h|^p = |D_{a_j} y_h|^p = \left| \int_x^{x+a_j} \nabla_{a_j} y_h \, db \right|^p \leq \int_x^{x+a_j} |\nabla_{a_j} y_h|^p \, db,$$

where we employed Jensen's inequality in the last step.

Inserting this estimate into (A.4), and reversing the argument in (A.4), we obtain

$$\begin{aligned} \int_{\Omega} |\nabla_{a_j} \bar{y}_h|^p \, dV &\leq \sum_{x \in \mathbb{L}} \int_x^{x+a_j} |\nabla_{a_j} y_h|^p \, db \\ &= \sum_{T \in \mathcal{T}_h} \sum_{x \in \mathbb{L}} \int_x^{x+a_j} |\nabla_{a_j} y_h|^p \chi_{T^\#} \, db \\ &= \sum_{T \in \mathcal{T}_h} |T| |\nabla_{a_j} y_h|_T|^p = \|\nabla_{a_j} y_h\|_{L^p(\Omega)}^p. \end{aligned}$$

Inserting this estimate back into (A.3), we deduce that

$$\|\nabla \bar{y}_h\|_{L^p(\Omega)}^p \leq C_1^p \int_{\Omega} \sum_{j=1}^3 |\nabla_{a_j} y_h|^p \, dV.$$

Let $C_2 = \sqrt{\frac{3}{2}}$ if $p > 2$, and $C_2 = \sqrt{\frac{3}{2}} 3^{(2-p)/(2p)}$ if $p \leq 2$, then

$$\left(\sum_{j=1}^3 |\mathbf{G} a_j|^p \right)^{1/p} \leq C_2 |\mathbf{G}|_2 \quad \forall \mathbf{G} \in \mathbb{R}^{2 \times 2}.$$

This gives the stated estimate,

$$\|\nabla \bar{y}_h\|_{L^p(\Omega)} \leq C_1 C_2 \|\nabla y_h\|_{L^p(\Omega)}$$

with $C_1 C_2 = \max(3^{(p-2)/(2p)}, 3^{(2-p)/(2p)}) \leq \sqrt{3}$. \square

A technical ingredient in the proof of Lemma 4.4 and Lemma 4.5 is a trace inequality for piecewise constant functions. In its proof we use the following well-known trace identity (contained, for example, in the proof of Lemma 2 in [23]).

Lemma A.1. *Let f be a face of a non-degenerate simplex $T \subset \mathbb{R}^d$, q_f the corner of T not contained in f , and $|f|$ the $(d-1)$ -dimensional area of f ; then*

$$\frac{|T|}{|f|} \int_f w \, ds = \int_T w \, dV + \frac{1}{2} \int_T (x - q_f) \cdot \nabla w \, dV \quad \forall w \in W^{1,1}(T). \quad (\text{A.5})$$

Proof of Lemma 4.4. Let $y_h = I_h y$ and $\tilde{y} \in \Pi_2(y)$. Since $\tilde{y} \in C^1(\mathbb{R}^d)$, we have the following estimate,

$$h_f |[\nabla y_h]_f| = \left| \int_f [\nabla(y_h - \tilde{y})] ds \right| \leq \left| \int_f \nabla(y_h - \tilde{y})^+ ds \right| + \left| \int_f \nabla(y_h - \tilde{y})^- ds \right|.$$

We deduce from (A.5), choosing $w = \nabla(y_h - \tilde{y})$ and $T = T_\pm$, that

$$\frac{|T_\pm|}{h_f} \left| \int_f \nabla(y_h - \tilde{y})^\pm ds \right| \leq \|\nabla y_h - \nabla \tilde{y}\|_{L^1(T_\pm)} + \frac{1}{2} h_{T_\pm} \|\nabla^2 \tilde{y}\|_{L^1(T_\pm)}.$$

Note, moreover, that $|T_\pm|/h_f \geq \frac{1}{C'_f} h_T$, where C'_f depends only on the shape regularity of T_\pm .

Recalling that $y_h = I_h y$, we can use Lemma (4.3) to deduce that

$$\frac{h_{T_\pm}}{C'_f} \left| \int_f \nabla(y_h - \tilde{y})^\pm ds \right| \leq (\tilde{C}_h + \frac{1}{2}) h_{T_\pm} \|\nabla^2 \tilde{y}\|_{L^1(T_\pm)},$$

which immediately yields (4.6) for $p = 1$:

$$\|[\nabla y_h]_f\|_{L^1(f)} \leq C'_f (\tilde{C}_h + \frac{1}{2}) \|\nabla^2 \tilde{y}\|_{L^1(T_+ \cup T_-)}. \quad (\text{A.6})$$

Using similar calculations it is also easy to prove the estimate for $p = \infty$:

$$|[\nabla y_h]_f| \leq 2\tilde{C}_h \|h \nabla^2 \tilde{y}\|_{L^\infty(T_+ \cup T_-)}.$$

Applying the Riesz–Thorin interpolation theorem, we obtain (4.6) for all p . (Alternatively, one could derive this by applying a Hölder inequality to (A.6); however, this would lead to a worse constant for $p > 1$.)

The estimate (4.7) is an immediate consequence of (4.6). \square

The following lemma will be used in the proof of Lemma 4.5:

Lemma A.2. *Let $f \in \mathcal{F}_a$, $f \subset \tau \in \mathcal{T}_a$ and let $w : \tau \rightarrow \mathbb{R}^k$ be piecewise constant with respect to the mesh \mathcal{T}_h ; then*

$$|\tau| \left| \int_f w ds \right| \leq \|w\|_{L^1(\tau)} + \frac{1}{2} \| [w] \|_{L^1(\mathcal{F}_h^\# \cap \text{int}(\tau))}.$$

Proof. Assume, first, that $w_\varepsilon \in W^{1,1}(\tau)^k$, then, noting that $\text{length}(f) = 1$, (A.5) implies

$$|\tau| \left| \int_f w_\varepsilon ds \right| \leq \int_\tau |w_\varepsilon| dV + \frac{1}{2} \int_\tau |\nabla w_\varepsilon| dV.$$

Since $W^{1,1}(\tau)^k$ is dense in $\text{BV}(\text{int}(\tau))^k$ (which contains all piecewise constant functions w.r.t. \mathcal{T}_h) in the strict topology [8, Sec. 5.2.2], it follows that

$$|\tau| \left| \int_f w ds \right| \leq \int_\tau |w| dV + \frac{1}{2} |D'w|(\text{int}(\tau))$$

as well, where $|D'w|$ denotes the total variation measure of w . Using integration by parts it is straightforward to show that

$$|D'w|(\text{int}(\tau)) := \sup_{\substack{\psi \in C_0^1(\tau)^{k \times 2} \\ |\psi| \leq 1}} \int_\tau w \cdot \text{div} \psi dV \leq \| [w] \|_{L^1(\mathcal{F}_h^\# \cap \text{int}(\tau))}. \quad \square$$

Proof of Lemma 4.5. Fix an edge $f \in \mathcal{F}_a$, $f \subset \tau$, such that $f = (q, q + a_j)$, then, using Lemma A.2, we have

$$\begin{aligned} |(\nabla \bar{y}_h|_\tau)_{a_j}| &= |D_{a_j} y_h(q)| = \left| \int_f \nabla y_h a_j \, ds \right| \\ &\leq |\tau|^{-1} \left[\|\nabla y_h a_j\|_{L^1(\tau)} + \frac{1}{2} \|\nabla y_h a_j\|_{L^1(\mathcal{F}_h^\# \cap \text{int}(\tau))} \right]. \end{aligned}$$

There exists a constant C_3 , depending only on the shape regularity of \mathcal{T}_h , such that $\text{length}(\mathcal{F}_h^\# \cap \text{int}(\tau)) \leq C_3$; hence, Hölder's inequality yields

$$|(\nabla \bar{y}_h|_\tau)_{a_j}| \leq |\tau|^{1/p'-1} \|\nabla y_h a_j\|_{L^p(\tau)} + \frac{1}{2} C_3^{1/p'} |\tau|^{-1} \|\nabla y_h a_j\|_{L^p(\mathcal{F}_h^\# \cap \text{int}(\tau))}.$$

Summing over $j = 1, 2, 3$, applying Lemma 2.2, (2.1), and noting that all constants can be bounded independently of p , we obtain the result.

We remark that, for $p = 2$, a careful computation yields the inequality

$$\|\nabla \bar{y}_h\|_{L^2(\tau)}^2 \leq 2 \|\nabla y_h\|_{L^2(\tau)}^2 + \frac{2}{3^{1/4}} C_3 \|\nabla y_h\|_{L^2(\mathcal{F}_h^\# \cap \text{int}(\tau))}^2. \quad \square$$

APPENDIX B. A SIMPLIFIED CONSISTENCY RESULT

In this appendix, we present an alternative consistency error estimate, which yields weaker results, but requires fewer technical tools. Further simplifications (e.g., removing the need to extend deformations and displacements to vacancy sites) can be achieved if one assumes that ϕ has a finite cut-off radius, and that all ‘‘active’’ bonds $b \in \mathcal{B}_a$ are resolved exactly (by giving \mathcal{T}_h full atomistic resolution in a sufficiently large neighbourhood of Ω_a).

Theorem B.1. *Suppose that Assumption A holds. Let $y \in \mathcal{Y}$ such that $\mu := \min\{\mu_a(y), \mu_c(I_h y), \mu_c(\bar{y})\} > 0$; then, for all $\tilde{y} \in \Pi_2(y)$,*

$$\begin{aligned} \|\delta \mathcal{E}_{\text{ac}}(I_h y) - \delta \mathcal{E}_a(y)\|_{W_h^{-1,p}} &\leq C^{\text{coarse}} \left(\sum_{T \in \mathcal{T}_h} |T| (h_T \|\nabla^2 \tilde{y}\|_{L^\infty(T)})^p \right)^{1/p} \\ &\quad + C^{\text{model}} \left(\sum_{\substack{\tau \in \mathcal{T}_a \\ \tau \subset \Omega_c}} \sum_{r \in \mathbb{L}^*} K_{|r|} \|\nabla^2 \tilde{y}\|_{L^\infty(\omega_{\tau,r})}^p \right)^{1/p}. \end{aligned}$$

where $C^{\text{coarse}} = C_1 \sum_{r \in \mathbb{L}^*} M_2(\mu r) |r|^2$ with C_1 depending only on the shape regularity of \mathcal{T}_h , $K_r = M_2(\mu |r|) |r|^3$, $C^{\text{model}} = (5/2)^{1/p} (\sum_{r \in \mathbb{L}^*} K_r)^{1/p'}$, and the neighbourhoods $\omega_{\tau,r} \subset \Omega_c$ are defined as follows:

$$\omega_{\tau,r} := \text{conv} \left(\bigcup \{b \in \mathcal{B}_c : r_b = r \text{ and } \text{length}(b \cap \tau) > 0\} \right). \quad (\text{B.1})$$

Proof. 1. Alternative splitting. Fix $y \in \mathcal{Y}$, $\tilde{y} \in \Pi_2(y)$, and recall the definition of \bar{y} from §4.2. This time, we split the consistency error differently:

$$\begin{aligned} \langle \delta \mathcal{E}_{\text{ac}}(I_h y) - \delta \mathcal{E}_a(y), u_h \rangle &= \langle \delta \mathcal{E}_{\text{ac}}(I_h y) - \delta \mathcal{E}_{\text{ac}}(\bar{y}), u_h \rangle + \langle \delta \mathcal{E}_{\text{ac}}(\bar{y}) - \delta \mathcal{E}_a(y), u_h \rangle \\ &=: E^{\text{coarse}} + E^{\text{model}}, \end{aligned}$$

where $\delta \mathcal{E}_{\text{ac}}(\bar{y})$ is defined through the bond integral formula (3.4).

2. *Coarsening error.* The coarsening contribution to the consistency error is defined as follows:

$$\begin{aligned} E^{\text{coarse}} &= \langle \delta \mathcal{E}_{\text{ac}}(I_h y) - \delta \mathcal{E}_{\text{ac}}(\bar{y}), u_h \rangle \\ &= \sum_{b \in \mathcal{B}_a} [\phi'(D_b I_h y) - \phi'(D_b \bar{y})] \cdot D_b u_h + \sum_{b \in \mathcal{B}_c} \int_b [\phi'(\nabla_b I_h y) - \phi'(\nabla_b \bar{y})] \cdot \nabla_b u_h \, \text{db}. \end{aligned}$$

With only minor modifications of the proof of Lemma 5.3, we can prove that

$$E^{\text{coarse}} \leq \left(\sum_{b \in \mathcal{B}} M'_{|b|} |b|^{-p} \int_b \chi_{\Omega_c^\#} |\nabla_b I_h y - \nabla_b \bar{y}|^p \, \text{db} \right)^{1/p} C_L^{1/p'} \|\nabla u_h\|_{L^{p'}(\Omega)}, \quad (\text{B.2})$$

where $C_L = C_L(\mu) = \sum_{r \in \mathbb{L}_*} M_2(\mu|r|)|r|^2$. We can avoid the technical results in §4.5, by estimating the interpolation error directly in (B.2).

Let the norm $\|\cdot\|_{\mathcal{B}}$ be defined by

$$\|w\|_{\mathcal{B}} := \left(\sum_{b \in \mathcal{B}} M'_{|b|} |b|^{-p} \int_b \chi_{\Omega_c^\#} |\nabla_b w|^p \, \text{db} \right)^{1/p},$$

and let $\tilde{y} \in \Pi_2(y)$, then

$$\|I_h y - \bar{y}\|_{\mathcal{B}} \leq \|I_h y - \tilde{y}\|_{\mathcal{B}} + \|\tilde{y} - \bar{y}\|_{\mathcal{B}}.$$

We apply the interpolation error estimate, Lemma 4.3, for $p = \infty$, and the bond density lemma, to bound

$$\begin{aligned} \|I_h y - \tilde{y}\|_{\mathcal{B}}^p &\leq \sum_{T \in \mathcal{T}_h} \left(\sum_{r \in \mathbb{L}_*} M'_{|r|} \right) \left(\tilde{C}_h h_T \|\nabla^2 \tilde{y}\|_{L^\infty(T)}^p \right) \sum_{x \in \mathbb{L}^\#} \int_x^{x+r} \chi_{T^\#} \, \text{db} \\ &= C_L(\mu) \tilde{C}_h \sum_{T \in \mathcal{T}_h} |T| (h_T \|\nabla^2 \tilde{y}\|_{L^\infty(T)})^p. \end{aligned} \quad (\text{B.3})$$

By the same argument, using (4.4) instead of (4.3), we also obtain

$$\|\tilde{y} - \bar{y}\|_{\mathcal{B}}^p \leq \frac{3}{2} C_L(\mu) \sum_{\tau \in \mathcal{T}_a} |\tau| \|\nabla^2 \tilde{y}\|_{L^\infty(\tau)}^p, \quad (\text{B.4})$$

where we have also used the fact, which is easy to establish, that $\tilde{C}_a \leq 3/2$ for $p = \infty$.

The bound (B.3) gives the first term in the consistency error estimate. We will not combine (B.4) with the coarsening error, but instead combine it with the modelling error.

3. *Modelling error.* The modelling error contribution is defined by

$$E^{\text{model}} = \langle \delta \mathcal{E}_{\text{ac}}(\bar{y}) - \delta \mathcal{E}_a(y), u_h \rangle = \sum_{b \in \mathcal{B}_c} \int_b [\phi'(\nabla_b \bar{y}) - \phi'(D_b y)] \cdot \nabla_b u_h \, \text{db}, \quad (\text{B.5})$$

where we used (3.2), and the fact that the bonds treated atomistically cancel. Applying the local Lipschitz estimate to ϕ' , Hölder's inequality, and the bond density lemma, we

bound (B.5) above by

$$\begin{aligned} E^{\text{model}} &\leq \sum_{b \in \mathcal{B}_c} M'_{|b|} \int_b (|b|^{-1-1/p'} |\nabla_b \bar{y} - D_b y|) (|b|^{-1+1/p'} |\nabla_b u_h|) \, db \\ &\leq \left(\sum_{b \in \mathcal{B}_c} M'_{|b|} |b|^{-2p+1} \int_b |\nabla_b \bar{y} - D_b y|^p \, db \right)^{1/p} C_1^{1/p'} \|\nabla u_h\|_{L^{p'}}, \end{aligned} \quad (\text{B.6})$$

where $C_1 = \sum_{r \in \mathbb{L}^*} M_2(\mu|r|)|r|^3$.

We now split the first group over elements. To that end, we use the definition of $\omega_{\tau,r}$ given in (B.1), and estimate

$$\begin{aligned} \int_b \chi_{\tau\#} |\nabla_b \bar{y} - D_b y|^p \, db &= \int_b \chi_{\tau\#} \left| \nabla_{r_b} \bar{y} - \int_b \nabla_{r_b} \tilde{y} \, db \right|^p \, db \\ &\leq \|\nabla_{r_b}^2 \tilde{y}\|_{L^\infty(\omega_{\tau,r_b})}^p \leq |b|^{2p} \|\nabla^2 \tilde{y}\|_{L^\infty(\omega_{\tau,r_b})}^p. \end{aligned}$$

In addition, we note that, since $D_b y = \nabla_b \bar{y}$ for all $b \in \mathcal{B}_{\text{nn}}$, all nearest-neighbour terms vanish. Hence, we obtain

$$\sum_{b \in \mathcal{B}_c} M'_{|b|} |b|^{-2p+1} \int_b |\nabla_b \bar{y} - D_b y|^p \, db \leq \sum_{\substack{\tau \in \mathcal{T}_a \\ \tau \subset \Omega_c}} |\tau| \sum_{r \in \mathbb{L}^* \setminus \mathbb{L}_{\text{nn}}} M_2(\mu|r|)|r|^3 \|\nabla^2 \tilde{y}\|_{L^\infty(\omega_{\tau,r})}^p.$$

Combining this estimate with (B.4), we arrive at

$$\begin{aligned} E^{\text{model}} + \|\tilde{y} - \bar{y}\|_{\mathcal{B}} C_L^{1/p'} \|\nabla u_h\|_{L^{p'}} \\ \leq \left(\frac{5}{2}\right)^{1/p} C_L^{1/p'} \left(\sum_{\substack{\tau \in \mathcal{T}_a \\ \tau \subset \Omega_c}} \sum_{r \in \mathbb{L}^*} M_2(\mu|r|)|r|^3 \|\nabla^2 \tilde{y}\|_{L^\infty(\omega_{\tau,r})}^p \right)^{1/p} \|\nabla u_h\|_{L^{p'}}. \end{aligned}$$

This yields the second term in the consistency error estimate. \square

REFERENCES

- [1] P. G. Ciarlet. *The finite element method for elliptic problems*, volume 40 of *Classics in Applied Mathematics*. Society for Industrial and Applied Mathematics (SIAM), Philadelphia, PA, 2002. Reprint of the 1978 original.
- [2] L. Demkowicz, Ph. Devloo, and J. T. Oden. On an h -type mesh-refinement strategy based on minimization of interpolation errors. *Comput. Methods Appl. Mech. Engrg.*, 53(1):67–89, 1985.
- [3] A. Demlow, D. Leykekhman, A. H. Schatz, and L. B. Wahlbin. Best approximation property in the W_∞^1 norm on graded meshes. Preprint.
- [4] M. Dobson and M. Luskin. An optimal order error analysis of the one-dimensional quasicontinuum approximation. *SIAM Journal on Numerical Analysis*, 47(4):2455–2475, 2009.
- [5] M. Dobson, M. Luskin, and C. Ortner. Accuracy of quasicontinuum approximations near instabilities. *J. Mech. Phys. Solids*, 58(10):1741–1757, 2010.
- [6] M. Dobson, M. Luskin, and C. Ortner. Stability, instability, and error of the force-based quasicontinuum approximation. *Arch. Ration. Mech. Anal.*, 197(1):179–202, 2010.
- [7] W. E, J. Lu, and J. Z. Yang. Uniform accuracy of the quasicontinuum method. *Phys. Rev. B*, 74(21):214115, 2006.
- [8] L. C. Evans and R. F. Gariepy. *Measure theory and fine properties of functions*. Studies in Advanced Mathematics. CRC Press, Boca Raton, FL, 1992.
- [9] F. C. Frank and J. H. van der Merwe. One-dimensional dislocations. I. static theory. *Proc. R. Soc. London*, A198:205–216, 1949.

- [10] M. Giaquinta. *Introduction to regularity theory for nonlinear elliptic systems*. Lectures in Mathematics ETH Zürich. Birkhäuser Verlag, Basel, 1993.
- [11] T. Hudson and C. Ortner. Linear stability of atomistic energies and their Cauchy–Born approximations. OxMOS Preprint No. 31/2010.
- [12] M. Iyer and V. Gavini. A field theoretic approach to the quasi-continuum method. to appear in *J. Mech. Phys. Solids*.
- [13] P. A. Klein and J. A. Zimmerman. Coupled atomistic-continuum simulations using arbitrary overlapping domains. *J. Comput. Phys.*, 213(1):86–116, 2006.
- [14] S. Kohlhoff and S. Schmauder. A new method for coupled elastic-atomistic modelling. In V. Vitek and D. J. Srolovitz, editors, *Atomistic Simulation of Materials: Beyond Pair Potentials*, pages 411–418. Plenum Press, New York, 1989.
- [15] X. H. Li and M. Luskin. A generalized quasi-nonlocal atomistic-to-continuum coupling method with finite range interaction. arXiv:1007.2336.
- [16] J. Lu and P. Ming. Convergence of a force-based hybrid method for atomistic and continuum models in three dimension. arXiv:1102.2523.
- [17] C. Makridakis, C. Ortner, and E. Süli. A priori error analysis of two force-based atomistic/continuum hybrid models of a periodic chain. OxMOS Report No. 28/2010.
- [18] R. Miller and E. Tadmor. A unified framework and performance benchmark of fourteen multiscale atomistic/continuum coupling methods. *Modelling Simul. Mater. Sci. Eng.*, 17, 2009.
- [19] P. Ming and J. Z. Yang. Analysis of a one-dimensional nonlocal quasi-continuum method. *Multiscale Modeling & Simulation*, 7(4):1838–1875, 2009.
- [20] M. Ortiz, R. Phillips, and E. B. Tadmor. Quasicontinuum analysis of defects in solids. *Philosophical Magazine A*, 73(6):1529–1563, 1996.
- [21] C. Ortner. A priori and a posteriori analysis of the quasi-nonlocal quasicontinuum method in 1D. arXiv.org:0911.0671v1, to appear in *Math. Comp.*
- [22] C. Ortner. The role of the patch test in 2D atomistic-to-continuum coupling methods. arXiv:1101.5256v2.
- [23] C. Ortner and D. Praetorius. On the convergence of adaptive nonconforming finite element methods for a class of convex variational problems. *SIAM J. Numer. Anal.*, 49(1):346–367, 2011.
- [24] C. Ortner and E. Süli. Analysis of a quasicontinuum method in one dimension. *M2AN Math. Model. Numer. Anal.*, 42(1):57–91, 2008.
- [25] C. Ortner and H. Wang. Coarse graining in energy-based quasicontinuum methods. OxMOS Report No. 30/2010, to appear in *Math. Models Methods Appl. Sc.*
- [26] R. Rannacher and R. Scott. Some optimal error estimates for piecewise linear finite element approximations. *Math. Comp.*, 38(158):437–445, 1982.
- [27] A. V. Shapeev. Consistent energy-based atomistic/continuum coupling for two-body potential: 1D and 2D case. arXiv:1010.0512, to appear in *SIAM MMS*.
- [28] V. B. Shenoy, R. Miller, E. B. Tadmor, D. Rodney, R. Phillips, and M. Ortiz. An adaptive finite element approach to atomic-scale mechanics—the quasicontinuum method. *J. Mech. Phys. Solids*, 47(3):611–642, 1999.
- [29] J. R. Shewchuk. An introduction to the conjugate gradient method without the agonizing pain, 1994. Available from <http://www.cs.cmu.edu/~quake-papers/painless-conjugate-gradient.pdf>.
- [30] T. Shimokawa, J. J. Mortensen, J. Schiotz, and K. W. Jacobsen. Matching conditions in the quasicontinuum method: Removal of the error introduced at the interface between the coarse-grained and fully atomistic region. *Phys. Rev. B*, 69(21):214104, 2004.
- [31] G. Strang and G. Fix. *An Analysis of the Finite Element Method*. Wellesley-Cambridge Press, 2008.
- [32] B. Van Koten, Z. H. Li, M. Luskin, and C. Ortner. A computational and theoretical investigation of the accuracy of quasicontinuum methods. arXiv:1012.6031.
- [33] S. P. Xiao and T. Belytschko. A bridging domain method for coupling continua with molecular dynamics. *Comput. Methods Appl. Mech. Engrg.*, 193(17-20):1645–1669, 2004.

C. ORTNER, MATHEMATICAL INSTITUTE, 24-29 ST GILES', OXFORD OX1 3LB, UK
E-mail address: `ortner@maths.ox.ac.uk`

A. V. SHAPEEV, SECTION OF MATHEMATICS, SWISS FEDERAL INSTITUTE OF TECHNOLOGY (EPFL),
STATION 8, CH-1015, LAUSANNE, SWITZERLAND
E-mail address: `alexander.shapeev@epfl.ch`